REALTIDE

This project has received funding from the European Union's Horizon 2020 research and innovation programme under Grant Agreement No 727689

Document Title:
D2.2 – Next Generation Flow Measurements and Flow Classification

Document No:
RLT-WP2-2-PDL-0000-04

Status Code	Description
A	Accepted
B	Issued for Acceptance
C	Issued for Review
D	Information Only Approval not required
E	Cancelled

Rev No	Status	Revision Description	Prepared By / Date	Reviewed By / Date	Approved By / Date
004	B	Issued for acceptance	B Sellar, C Old, P McCallum		Stéphane Paboeuf 18/10/2021
003	C	Issued Draft	Chris Old, Peter McCallum 14/10/2021	Brian Sellar 15/10/2021	
002	D	Working Draft	Chris Old, Brian Sellar, Peter McCallum, Nayef Zigrat, Marilou Jordain de Thieulloy, Mairi Dorward 12/10/2021		
001	D	Working Draft	Brian Sellar - 24/09/2021		
00	D	Document Preparation	Chris Old, Brian Sellar, Mairi Dorward, David Crooks, Andrew Price		
00	D	Document Creation	Chris Old - 19/03/2019		

European Commission
H2020 Programme for Research & Innovation

Advanced monitoring, simulation and control of tidal devices in unsteady, highly turbulent realistic tide environments

Grant Agreement number: 727689

Project Acronym: RealTide

Project Title: Advanced monitoring, simulation and control of tidal devices in unsteady, highly turbulent realistic tide environments

Deliverable 2.2
Next Generation Flow Measurements and Flow Classification
WP 2
Realistic Tidal Environment

WP Leader: The University of Edinburgh

Dissemination level: Public

Report describing an advanced methodology for data acquisition and analysis of flow measurements in tidal sites, their classification and related metrics.

Sensitivity analysis will be performed on post-processing stages and comparisons of results to those derived from datasets acquired at other tidal sites (European-waters) will be included.

Recommendations for future resource characterisations will be provided.

Summary: This report forms Deliverable 2.2 and details the work of Task 2.2 within WP2 of RealTide. It provides the description of the work carried out on the development and implementation of a multi-component resource characterisation methodology. The methodology includes in-situ and hydrodynamic modelling and includes the use of re-analyses of existing datasets as well as the generation of new data sets at both a commercial tidal energy site, the Fromveur Strait, and the European Marine Energy Centre's tidal energy test site. The report builds on specification works that are reported in RealTide Deliverable D2.1 - Deployment and Instrument Specification for Advanced Flow Characterisation.

Objective:
1 - Specifically target the collection of "missing-piece" high-resolution (spatio-temporal) field data through
a) an identification of key gaps in already secured data, and
b) use of in-development analysis techniques.
2 - A dedicated trial of a UEDIN's next-generation velocimetry sensor system (first assembled and optimised in the laboratory at the FloWave facility) will be used to calibrate/validate off-the-shelf instrumentation commonly used by the industry.

Table of Contents

List of Figures

List of Tables

Abbreviations & Definitions

ADCP	Acoustic Doppler Current Profiler
ADV	Acoustic Doppler Velocimeter
BEMT	Blade Element Momentum Theory
BV	Bureau Veritas
C-ADP	Convergent-beam acoustic Doppler profiler
CANDHIS	Centre d'Archivage National de Données de Houle In Situ
CFD	Computational Fluid Dynamics
CRS	Coordinate Reference System
CTOH	Center for Topographic studies of the Ocean and Hydrosphere
D	Deliverable
D10	Sabella D10 Tidal Energy Converter
D-ADP	Divergent-beam acoustic Doppler profiler
EMEC	European Marine Energy Centre
EMODnet	European Marine Observation and Data Network
GA	Grant Agreement
HO	HydrOcean
IEC	International Electrotechnical Commission
IFREMER	Institut français de recherche pour l'exploitation de la mer
MONITOR	Multi-model investigation of tidal energy converter reliability
MRE	Marine Renewable Energy
MSL	Mean Sea Level
OSU	Oregon State University
OTIS	Tidal Inversion Software
QGIS	Quantum Geographical Information System
ReDAPT	Reliable Data Acquisition Platform for Tidal
SAB	Sabella
SBD	Legacy name for single-beam Doppler profilers
SB-ADP	Single-Beam acoustic Doppler profiler
SEM	Synthetic Eddy Method
SHOM	Le service Hydrographique et Océanographique de la Marine
SR	Sample Rate
TEC	Tidal Energy Converter
TKE	Turbulent Kinetic Energy
OTS	Off-the-shelf
UEDIN	The University of Edinburgh
UTC	Universal Time Coordinated
UTM	Universal Transverse Mercator
WP	Work Package

Nomenclature

Symbol	Term	Units
u, v, w	Velocity in the streamwise, transverse and vertical direction where streamwise is positive in the direction of flow and vertical is positive pointing upwards from the "sea-bed".	m/s
$\bar{u}, \bar{v}, \bar{w}$	Spatial or temporal averaged u, v, w (see Reynolds decomposition)	m/s
u', v', w'	Velocity perturbations of u, v, w (see Reynolds decomposition)	m/s
ε	Water surface elevation	m
τ_{rotor}	Rotor Torque	Nm
T_{rotor}	Rotor Thrust	N
m_U	Blade-root bending moment, in the u direction	Nm
ω_{rotRPM}	Rotational speed	RPM
F_X	Force in Z direction	N
F_Y	Force in Y direction	N
F_Z	Force in Z direction	N
M_X	Moment around X direction (roll)	Nm
M_Y	Moment around Y direction (pitch)	Nm
M_Z	Moment around Z direction (yaw)	Nm
X	Streamwise flow direction (positive towards TEC/away from inlet boundary condition). Right-handed coordinate system. (see Figure 1)	m
Y	Transverse flow direction. Right-handed coordinate system. (see Figure 1)	m
Z	Vertical flow direction. Positive from seabed upwards. Right-handed coordinate system. (see Figure 1)	m
E_{Geo}	East direction. Oceanographic coordinate system	Lat/Lon & UTM
N_{Geo}	North direction. Oceanographic coordinate system	Lat/Lon & UTM
U_{Geo}	Up direction. Oceanographic coordinate system	m
X_T	Right-handed coordinate system, aligned with Axial direction of the TEC (see Figure 1)	m
Y_T	Transverse flow direction. Right-handed coordinate system. (see Figure 1)	m
Z_T	Vertical flow direction. Positive from seabed upwards. Right-handed coordinate system. (see Figure 1)	m
H_{m0}	Significant wave height	m
T_p	Peak wave period (spectral peak)	S
θ_1	Wave direction (at peak frequency)	◦ (ang. degrees)
θ_2	Wave direction (mean)	◦ (ang. degrees)
I_x, I_y, I_z	Turbulence Intensity in the X,Y,Z direction	%
$I_{x\text{-nc}}, I_{y\text{-nc}}, I_{z\text{-nc}}$	Turbulence Intensity in the X,Y,Z direction with noise correction applied	%
$L_{u\text{-}x}$	Lengthscale component: the change of u in the streamwise direction	m
$L_{v\text{-}x}$	Lengthscale component: the change of v in the streamwise direction	m
$L_{w\text{-}x}$	Lengthscale component: the change of w in the streamwise direction	m
$L_{u\text{-}y}$	Lengthscale component: the change of u in the lateral direction	m
$L_{v\text{-}y}$	Lengthscale component: the change of v in the lateral direction	m
$L_{w\text{-}y}$	Lengthscale component: the change of w in the lateral direction	m
$L_{u\text{-}z}$	Lengthscale component: the change of u in the vertical direction	m
$L_{v\text{-}z}$	Lengthscale component: the change of v in the vertical direction	m
$L_{w\text{-}z}$	Lengthscale component: the change of w in the vertical direction	m

References

[1] RealTide Technical Report, "RLT-WP2-1-PDL-000-03: Deployment and Instrument Specification for Advanced Flow Characterisation," 2019, url: https://realtide.eu/realtide-project-deliverables.

[2] RealTide Technical Report, "RLT-WP2-3-PDL-001-03: Advanced Monitoring, Simulation and Control of Tidal Devices in Unsteady, Highly Turbulent Realistic Tide Environments," 2021, url: https://realtide.eu/realtide-project-deliverables.

[3] J. T. F. Zimmerman, "Topographic generation of residual circulation by oscillatory (tidal) currents," *Geophysical & Astrophysical Fluid Dynamics,* vol. 11, no. 1, pp. 35-47, 1978, doi:10.1080/03091927808242650.

[4] I. Robinson, "Tidal vorticity and residual circulation," *Deep Sea Research Part A. Oceanographic Research Papers,* vol. 28, no. 3, pp. 195-212, 1981, doi:10.1016/0198-0149(81)90062-5.

[5] R. Martinez, G. S. Payne and T. Bruce, "The effects of oblique waves and currents on the loadings and performance of tidal turbines," *Ocean Engineering,* vol. 164, pp. 55-64, 2018, doi:10.1016/j.oceaneng.2018.05.057.

[6] S. Draycott, B. Sellar, T. Davey, D. Noble, V. Venugopal and D. Ingram, "Capture and simulation of the ocean environment for offshore renewable energy," *Renewable and Sustainable Energy Reviews,* vol. 104, pp. 15-29, 2019, doi:10.1016/j.rser.2019.01.011.

[7] C. P. Old and R. Vennell, "Acoustic Doppler current profiler measurements of the velocity field of an ebb tidal jet," *Journal of Geophysical Research: Oceans,* vol. 106, no. C4, pp. 7037-7049, 2001, doi:10.1029/1999JC000144.

[8] F. Nicolau del Roure, S. A. Socolofsky and K.-A. Chang, "Structure and evolution of tidal starting jet vortices at idealized barotropic inlets," *Journal of Geophysical Research: Oceans,* vol. 114, no. C5, 2009, doi:10.1029/2008JC004997.

[9] P. Mycek, B. Gaurier, G. Germain, G. Pinon and E. Rivoalen, "Experimental study of the turbulence intensity effects on marine current turbines behaviour. Part I: One single turbine," *Renewable Energy,* vol. 66, pp. 729-746, 2014, doi:10.1016/j.renene.2013.12.036.

[10] T. Blackmore, L. E. Myers and A. S. Bahaj, "Effects of turbulence on tidal turbines: Implications to performance, blade loads, and condition monitoring," *International Journal of Marine Energy,* vol. 14, 2016, doi:10.1016/j.ijome.2016.04.017.

[11] G. Payne, T. Stallard, H. R. Mullings and R. Martinez, "Experimental investigation into unsteady loads on horizontal axis tidal turbines," in *In: Proceedings of European Wave and Tidal Energy Conference (EWTEC-2017)*, 2017.

[12] S. Draycott, J. Steynor, A. Nambiar, B. Sellar and V. Venugopal, "Experimental assessment of tidal turbine loading from irregular waves over a tidal cycle," *Journal of Ocean Engineering and Marine Energy,* vol. 5, no. 2, pp. 173-187, 2019, doi:10.1007/s40722-019-00136-9.

[13] S. Draycott, A. Nambiar, B. Sellar, T. Davey and V. Venugopal, "Assessing extreme loads on a tidal turbine using focused wave groups in energetic currents," *Renewable Energy,* vol. 135, pp. 1013-1024, 2019, doi:10.1016/j.renene.2018.12.075.

[14] S. Draycott, G. Payne, J. Steynor, A. Nambiar, B. Sellar and V. Venugopal, "An experimental investigation into non-linear wave loading on horizontal axis tidal turbines," *Journal of Fluids and Structures,* vol. 84, pp. 199-27, 2019, doi:10.1016/j.jfluidstructs.2018.11.004.

[15] L. Mackie, P. S. Evans, M. J. Harrold, T. O`Doherty, M. D. Piggott and A. Angeloudis, "Modelling an energetic tidal strait: investigating implications of common numerical configuration choices," *Applied Ocean Research,* vol. 108, no. January, p. 102494, 2021, doi:10.1016/j.apor.2020.102494.

[16] N. Guillou and J. Thiébot, "The impact of seabed rock roughness on tidal stream power extraction," *Energy,* vol. 112, no. C, pp. 762-773, 2016, doi:10.1016/j.energy.2016.06.053.

[17] B. Gaurier, S. Ordonez-Sanchez, J. V. Facq, G. Germain, C. Johnstone, R. Martinez, F. Salvatore, I. Santic, T. Davey, C. Old and B. G. Sellar, "MaRINET2 tidal energy round robin tests-performance comparison of a horizontal axis turbine subjected to combined wave and current conditions," *Journal of Marine Science and Engineering,* vol. 8, no. 6, 2020, doi:10.3390/JMSE8060463.

[18] M. Dorward, "PhD Thesis: Enabling Tools for the Development of Marine Renewable Energy," 2020, doi:10.7488/era/969, url: https://era.ed.ac.uk/handle/1842/37691.

[19] B. Sellar, "Metocean Data Set from the ReDAPT Tidal Project: Batch 1, Part 1, 2011-2014 [dataset]," 2016, url: https://datashare.ed.ac.uk/handle/10283/2329, doi:10.7488/ds/1686.

[20] B. Sellar, "Metocean Data Set from the ReDAPT Tidal Project: Batch 1, Part 2, 2011-2014 [dataset]," 2017, url: https://datashare.ed.ac.uk/handle/10283/2330, doi:10.7488/ds/1687.

[21] Technical Standard, "IEC TS 62600-200:2013 - Marine energy - Wave, tidal and other water current converters - Part 200: Electricity producing tidal energy converters - Power performance assessment," 2013.

[22] D. Woodruff, J. Haxel, J. Vavrinec, S. Southard, S. Zimmerman and K. Hall, "Sequim Bay Underwater UXO Prototype Demonstration Site: Field Operations Summary, 2020 (PNNL-30930)," *Pacific Northwest National Laboratory, United States Department Of Energy,* 2021, url: https://www.osti.gov/servlets/purl/1784318.

[23] S. Harding, M. Dorward, B. Sellar and M. Richmond, "Field validation of an actuated convergent-beam acoustic Doppler profiler for high resolution flow mapping," *Measurement Science and Technology,* 2021, doi:10.1088/1361-6501/abd5ef.

[24] M. Jourdain de Thieulloy, M. Dorward, C. Old, R. Gabl, T. Davey, D. M. Ingram and B. G. Sellar, "On the use of a single beam acoustic current profiler for multi-point velocity measurement in a wave and current basin," *Sensors (Switzerland),* vol. 20, no. 14, 2020, doi:10.3390/s20143881.

[25] M. Jourdain de Thieulloy, M. Dorward, C. Old, R. Gabl, T. Davey, D. M. Ingram and B. G. Sellar, "Single-beam acoustic doppler profiler and co-located acoustic doppler velocimeter flow velocity data," *Data,* vol. 5, no. 3, 2020, doi:10.3390/data5030061.

[26] M. Dorward, B. Sellar, C. Old and P. R. Thies, "Currents, Waves and Turbulence Measurement: A view from multiple Industrial-Academic Projects in Tidal Stream Energy," in *Institute of Electrical and Electronics Engineers (IEEE)*, 2019, doi:10.1109/CWTM43797.2019.8955294.

[27] Integrated Ocean Observing System (IOOS), "Manual for Real-Time Quality Control of Stream Flow Observations (Qartod) v2.1," no. July, 2019 (July), doi: 10.25923/sqe9-e310, url: https://repository.oceanbestpractices.org/handle/11329/1004.

[28] AODN, "IMOS Toolbox," 2021 (v2.6.13), url: https://github.com/aodn/imos-toolbox.

[29] M. Hidas, R. Proctor, N. Atkins, J. Atkinson, L. Besnard, P. Blain, P. Bohm, J. Burgess, K. Finney, D. Fruehauf, G. Galibert, X. Hoenner, J. Hope, C. Jones, S. Mancini, B. Pasquer, D. Nahodil, K. Reid and K. Tattersall, "Information infrastructure for Australia's Integrated Marine Observing System," *Earth Science Informatics,* vol. 9, no. 4, pp. 525-534, 2016, doi:10.1007/s12145-016-0266-2.

[30] RealTide, "Grant agreement ID: 727689 – RealTide Consortium & European Commission," 2017 (December), url: https://cordis.europa.eu/project/id/727689.

[31] RealTide, "Consortium Agreement (Rev.3, FINAL) – RealTide Consortium," 2017 (November).

[32] TiME Technical Report, "MRCF-TiME-KS9b (v1.1): Turbulence: Best Practices for the Tidal Industry. Part 2: Data Processing and Characterisation," 2015.

[33] TiME Technical Report, "MRCF-TiME-KS10 (v1.1): Turbulence: Best Practices for the Tidal Industry. Part 3: Turbulence and Turbulent Effects in Turbine Array Engineering," 2015.

[34] TiME Technical Report, "MRCF-TiME-KS9a (v1.1): Turbulence: Best Practices for the Tidal Industry. Part 1: Measurement of Turbulent Flows," 2015.

[35] W. J. Emery and R. E. Thomson, Data Analysis Methods in Physical Oceanography, 3rd Ed., Elsevier, 2014.

[36] ReDAPT Technical Report, "MD1.5 (v0.5): CFD Simulation of Turbulence at a Tidal Stream Site Based on Field Measurements.," 2013, url: http://redapt.eng.ed.ac.uk/?p=library_redapt _reports.

[37] D. Pugh and P. Woodworth, Sea-Level Science, Understanding Tides, Surges, Tsunamis and Mean Sea-Level Changes: Chapter 4 - Tidal analysis and prediction, Cambridge University Press, 2014, doi:10.1017/CBO9781139235778.007.

[38] M. Piano, S. Neill, M. Lewis, P. Robins, M. Hashemi, A. Davies, S. Ward and M. Roberts, "Tidal stream resource assessment uncertainty due to flow asymmetry and turbine yaw misalignment," *Renewable Energy,* vol. 114, no. B, pp. 1363-1375, 2017, 10.1016/j.renene.2017.05.023.

[39] C. Pattiaratchi, A. James and M. Collins, "Island wakes and headland eddies: A comparison between remotely sensed data and laboratory experiments," *Journal of Geophysical Research: Oceans,* vol. 92, no. C1, p. 783– 794, 1987, doi:10.1029/JC092iC01p00783.

[40] R. P. Signell and W. R. Geyer, "Transient eddy formation around headlands," *Journal of Geophysical Research: Oceans,* vol. 96, no. C2, pp. 2561-2575, 1991, doi:10.1029/90JC02029.

[41] P. Russell and R. Vennell, "High-resolution observations of secondary circulation and tidally synchronized upwelling around a coastal headland," *Journal of Geophysical Research: Oceans,* vol. 122, no. 2, pp. 890-913, 2017, doi:10.1002/2016JC012117.

[42] L. White and E. Wolanski, "Flow separation and vertical motions in a tidal flow interacting with a shallow-water island," *Estuarine, Coastal and Shelf Science,* vol. 77, no. 3, pp. 457-466, 2008, doi:10.1016/j.ecss.2007.10.003.

[43] P. M. Branson, M. Ghisalberti, G. N. Ivey and E. J. Hopfinger, "Cylinder wakes in shallow oscillatory flow: the coastal island wake problem," *Journal of Fluid Mechanics,* vol. 874, p. 158–184, 2019, doi:10.1017/jfm.2019.441.

[44] M. Thiébaut, J. F. Filipot, C. Maisondieu, G. Damblans, R. Duarte, E. Droniou, N. Chaplain and S. Guillou, "A comprehensive assessment of turbulence at a tidal-stream energy site influenced by wind-generated ocean waves," *Energy,* vol. 191, 2020, doi:10.1016/j.energy.2019.116550.

[45] L. Furgerot, A. Sentchev, P. Bailly Du Bois, G. Lopez, M. Morillon, E. Poizot, Y. Méar and A. C. Bennis, "One year of measurements in Alderney Race: Preliminary results from database analysis: In situ measurements in Alderney Race," *Philosophical Transactions of the Royal Society A: Mathematical, Physical and Engineering Sciences,* vol. 378, 2020, doi:10.1098/rsta.2019.0625.

[46] L. Perez, R. Cossu, A. Grinham and I. Penesis, "Evaluation of wave-turbulence decomposition methods applied to experimental wave and grid-generated turbulence data," *Ocean Engineering,* vol. 218, no. May, p. 108186, 2020, doi:10.1016/j.oceaneng.2020.108186.

[47] M. Togneri, I. Masters and I. Fairley, "Wave-turbulence separation at a tidal energy site with empirical orthogonal function analysis," *Ocean Engineering,* vol. 237, no. July, p. 109523, 2021, doi:10.1016/j.oceaneng.2021.109523.

[48] Technical Standard, "IEC TS 62600-2:2019 - Marine energy - Wave, tidal and other water current converters - Part 2: Marine energy systems - Design requirements," 2019.

[49] Technical Standard, "IEC TS 62600-201:2015 - Marine energy - Wave, tidal and other water current converters - Part 201: Tidal energy resource assessment and characterization," 2015.

[50] Technical Standard (DNV), "DNVGL-ST-0164: Tidal Turbines," 2015, url: https://rules.dnv.com/docs/pdf/DNV/ST/2015-10/DNVGL-ST-0164.pdf.

[51] Recommended Practice (DNVGL), "DNV-RP-C205: Environmental conditions and environmental loads".

[52] Guidance Note (Burea Veritas), "NI 603 DT R01 E: Current and Tidal Turbines," 2015, url: https://erules.veristar.com/dy/data/bv/pdf/603-NI_2015-05.pdf.

[53] Bureau Veritas, "Rules for the Classification of Offshore Units: PART B – Structural Safety," 2016, url: https://erules.veristar.com/dy/data/bv/pdf/445-NR_PartB_2016-12.pdf.

[54] P. Marsh, I. Penesis, J. R. Nader, C. Couzi and R. Cossu, "Assessment of tidal current resources in Clarence Strait, Australia including turbine extraction effects," *Renewable Energy,* vol. 179, pp. 150-162, 2021, doi:10.1016/j.renene.2021.07.007.

[55] M. Guerra, A. E. Hay, R. Karsten, G. Trowse and R. A. Cheel, "Turbulent flow mapping in a high-flow tidal channel using mobile acoustic Doppler current profilers," *Renewable Energy,* vol. 177, pp. 759-772, 2021, doi:10.1016/j.renene.2021.05.133.

[56] R. Cossu, I. Penesis, J. R. Nader, P. Marsh, L. Perez, C. Couzi, A. Grinham and P. Osman, "Tidal energy site characterisation in a large tidal channel in Banks Strait, Tasmania, Australia," *Renewable Energy,* vol. 177, pp. 859-870, 2021, doi:10.1016/j.renene.2021.05.111.

[57] P. Mercier, M. Thiébaut, S. Guillou, C. Maisondieu, E. Poizot, A. Pieterse, J. Thiébot, J. F. Filipot and M. Grondeau, "Turbulence measurements: An assessment of Acoustic Doppler Current Profiler accuracy in rough environment," *Ocean Engineering,* vol. 226, no. March, p. 108819, 2021, doi:10.1016/j.oceaneng.2021.108819.

[58] M. Thiébaut, J. F. Filipot, C. Maisondieu, G. Damblans, R. Duarte, E. Droniou and S. Guillou, "Assessing the turbulent kinetic energy budget in an energetic tidal flow from measurements of coupled ADCPs: TKE budget in an energetic tidal flow," *Philosophical Transactions of the Royal Society A: Mathematical, Physical and Engineering Sciences,* vol. 378, 2020, doi:10.1098/rsta.2019.0496.

[59] A. Sentchev, T. D. Nguyen, L. Furgerot and P. Bailly Du Bois, "Underway velocity measurements in the Alderney Race: Towards a three-dimensional representation of tidal motions: Underway velocity measurements," *Philosophical Transactions of the Royal Society A: Mathematical, Physical and Engineering Sciences,* vol. 378, 2020, doi:10.1098/rsta.2019.0491.

[60] M. Thiébaut, J. F. Filipot, C. Maisondieu, G. Damblans, C. Jochum, L. F. Kilcher and S. Guillou, "Characterization of the vertical evolution of the three-dimensional turbulence for fatigue design of tidal turbines: 3D turbulence for fatigue design of TEC," *Philosophical Transactions of the Royal Society A: Mathematical, Physical and Engineering Sciences,* vol. 10.1098/rsta.2019.0495, 2020, doi:10.1098/rsta.2019.0495.

[61] D. Zhang, X. Liu, M. Tan, P. Qian and Y. Si, "Flow field impact assessment of a tidal farm in the Putuo-Hulu Channel," *Ocean Engineering,* vol. 208, no. February, p. 107359, 2020, doi:10.1016/j.oceaneng.2020.107359.

[62] U. Rathnayake, M. Folley, S. D. Gunawardane and C. Frost, "Investigation of the error of mean representative current velocity based on the method of bins for tidal turbines using ADP data," *Journal of Marine Science and Engineering,* vol. 8, no. 6, 2020, doi:10.3390/JMSE8060390.

[63] J. Thiébot, N. Guillou, S. Guillou, A. Good and M. Lewis, "Wake field study of tidal turbines under realistic flow conditions," *Renewable Energy,* vol. 151, pp. 1196-1208, 2020, doi:10.1016/j.renene.2019.11.129.

[64] C. Greenwood, A. Vogler and V. Venugopal, "On the variation of turbulence in a high-velocity tidal channel," *Energies,* vol. 12, no. 4, 2019, doi:10.3390/en12040672.

[65] J. Imamura, K. Takagi and S. Nagaya, "Engineering analysis of turbulent flow measurements near Kuchinoshima Island," *Journal of Marine Science and Technology (Japan),* vol. 24, no. 2, pp. 329-337, 2019, doi:10.1007/s00773-018-0573-z.

[66] M. Thiébaut, A. Sentchev and P. B. du Bois, "Merging velocity measurements and modeling to improve understanding of tidal stream resource in Alderney Race," *Energy,* vol. 178, pp. 460-470, 2019, doi:10.1016/j.energy.2019.04.171.

[67] B. Sellar, S. Harding and M. Richmond, "High-resolution velocimetry in energetic tidal currents using a convergent-beam acoustic Doppler profiler," *Measurement Science and Technology,* vol. 26, p. 085801, 2015, doi:10.1088/0957-0233/26/8/085801.

[68] A. E. Hay, L. Zedel, S. Nylund, R. Craig and J. Culina, "The Vectron," in *2015 IEEE/OES Eleveth Current, Waves and Turbulence Measurement (CWTM)*, 2015, doi:10.1109/CWTM.2015.7098130.

[69] B. Sellar, G. Wakelam, D. R. J. Sutherland, D. M. Ingram and V. Venugopal, "Characterisation of tidal flows at the European Marine Energy Centre in the absence of ocean waves," *Energies,* vol. 11, no. 1, 2018, doi:10.3390/en11010176.

[70] D. G. Goring and V. I. Nikora, "Despiking Acoustic Doppler Velocimeter Data," *Journal of Hydraulic Engineering,* vol. 128, no. 1, pp. 117-126, 2002, doi:10.1061/(asce)0733-9429(2002)128:1(117).

[71] N. Mori, T. Suzuki and S. Kakuno, "Noise of Acoustic Doppler Velocimeter Data in Bubbly Flows," *Journal of Engineering Mechanics,* vol. 133, no. 1, pp. 122-125, 2007, doi:10.1061/(asce)0733-9399(2007)133:1(122).

[72] N. Mori, "Despiking," *MATLAB Central File Exchange,* 2021, url: https://uk.mathworks.com /matlabcentral/fileexchange/15361-despiking, Accessed 2021-10-13.

[73] Nortek AS, "Manual: Principles of Operation, 55|100|250|500|1000kHz (N3015-025)," 2021.

[74] Nortek AS, "Manual: Signature Integration, 55|100|250|500|1000kHz (N3015-007)," 2021.

[75] Teledyne RD Instruments, "Manual: Acoustic Doppler Current Profiler Principles of Operation: A Practical Primer (P/N 951-6069-00)," 2011.

[76] Teledyne RD Instruments, "Manual: Backscatter Estimation Using Broadband Acoustic Doppler Current Profilers (Application Note - FSA-031)," 2017 (July).

[77] Teledyne RD Instruments, "Manual: Waves Primer: Wave Measurement and the TRDI ADCP Waves Array Technique (P/N 957-6279-00)," 2017 (July).

[78] Teledyne RD Instruments, "Manual: Workhorse Sentinel, Mariner, Long Ranger, and Quarter Master Commands and Output Data Format (P/N 957-6156-00)," 2018.

[79] Teledyne RD Instruments, "Manual: Workhorse Sentinel, Monitor, & Mariner Operation Manual (P/N 957-6150-00)," 2018.

[80] J. J. Williams and L. S. Esteves, "Guidance on Setup, Calibration, and Validation of Hydrodynamic, Wave, and Sediment Models for Shelf Seas and Estuaries," *Advances in Civil Engineering,* p. 5251902, 2017, doi:10.1155/2017/5251902.

[81] F. Birol, N. Fuller, F. Lyard, M. Cancet, F. Niño, C. Delebecque, S. Fleury, F. Toublanc, A. Melet, M. Saraceno and F. Léger, "Coastal applications from nadir altimetry: Example of the X-TRACK regional products," *Advances in Space Research,* vol. 59, no. 4, pp. 936-953, 2017, doi:10.1016/j.asr.2016.11.005.

[82] B. Veritas, Bureau Veritas, August 2021. [Online]. Available: https://www.cps.bureauveritas.com/newsroom/bureau-veritas-becomes-first-openchain-certifier-great-china-region.

[83] Y. Lu and R. G. Lueck, "Using a Broadband ADCP in a Tidal Channel. Part I: Mean Flow and Shear," *Journal of Atmospheric and Oceanic Technology,* vol. 16, no. 11, p. 1556–1567, 1999, doi:10.1175/1520-0426(1999)016<1556:UABAIA>2.0.CO;2.

[84] Y. Lu and R. G. Lueck, "Using a broadband ADCP in a tidal channel. Part II: Turbulence," *Journal of Atmospheric and Oceanic Technology,* vol. 16, no. 11, p. 1568–1579, 1999, doi:10.1175/1520-0426(1999)016<1568:UABAIA>2.0.CO;2.

[85] J. Thomson, B. Polagye, V. Durgesh and M. C. Richmond, "Measurements of turbulence at two tidal energy sites in puget sound, WA," *IEEE Journal of Oceanic Engineering,* vol. 37, no. 3, pp. 363-374, 2012, doi:10.1109/JOE.2012.2191656.

[86] I. Milne, R. Sharma, R. Flay and S. Bickerton, "Characteristics of the turbulence in the flow at a tidal stream power site," *Philosophical transactions. Series A, Mathematical, Physical, and Engineering Sciences,* vol. 371, p. 20120196, 2013, doi:10.1098/rsta.2012.0196.

[87] B. Polagye and J. Thomson, "Tidal energy resource characterization: methodology and field study in Admiralty Inlet, Puget Sound, WA (USA)," *Proceedings of the Institution of Mechanical Engineers, Part A: Journal of Power and Energy,* vol. 227, no. 3, pp. 352-367, 2013, doi:10.1177/0957650912470081.

[88] L. Goddijn-Murphy, D. K. Woolf and M. C. Easton, "Current Patterns in the Inner Sound (Pentland Firth) from Underway ADCP Data," *Journal of Atmospheric and Oceanic Technology,* vol. 30, no. 1, pp. 96-111, 2013, doi:10.1175/JTECH-D-11-00223.1.

[89] B. Gunawan, V. Neary and J. Colby, "Tidal energy site resource assessment in the East River tidal strait, near Roosevelt Island, New York, New York," *Renewable Energy,* vol. 71, pp. 509-517, 2014, doi:10.1016/j.renene.2014.06.002.

[90] P. Jeffcoate, R. Starzmann, B. Elsäßer, S. Scholl and S. Bischoff, "Field Measurements of a Full Scale Tidal Turbine," *International Journal of Marine Energy,* vol. 12, 2015, doi:10.1016/j.ijome.2015.04.002.

[91] K. McCaffrey, B. Fox-Kemper, P. Hamlington and J. Thomson, "Characterization of Turbulence Anisotropy, Coherence, and Intermittency at a Prospective Tidal Energy Site: Observational Data Analysis," *Renewable Energy,* vol. 76, pp. 441-453, 2015, doi:10.1016/j.renene.2014.11.063.

[92] M. Lewis, S. Neill, P. Robins, M. R. Hashemi and S. Ward, "Characteristics of the velocity profile at tidal-stream energy sites," *Renewable Energy,* vol. 114, 2017, doi:10.1016/j.renene.2017.03.096.

[93] M. Togneri, M. Lewis, S. Neill and I. Masters, "Comparison of ADCP observations and 3D model simulations of turbulence at a tidal energy site," *Renewable Energy,* vol. 114, 2017, doi:10.1016/j.renene.2017.03.061.

[94] S. Harding, L. Kilcher and J. Thomson, "Turbulence Measurements from Compliant Moorings. Part I: Motion Characterization," *Journal of Atmospheric and Oceanic Technology,* vol. 34, no. 6, pp. 1235-1247, 2017, doi:10.1175/JTECH-D-16-0189.1.

[95] L. F. Kilcher, J. Thomson, S. Harding and S. Nylund, "Turbulence Measurements from Compliant Moorings. Part II: Motion Correction," *Journal of Atmospheric and Oceanic Technology,* vol. 34, no. 6, pp. 1249-1266, 2017, doi:10.1175/JTECH-D-16-0213.1.

[96] M. Guerra and J. Thomson, "Turbulence measurements from 5-beam acoustic doppler current profilers," *Journal of Atmospheric and Oceanic Technology,* vol. 34, 2017, doi:10.1175/JTECH-D-16-0148.1.

[97] E. Boudière, C. Maisondieu, F. Ardhuin, M. Accensi, L. Pineau-Guillou and J. Lepesqueur, "A Suitable Metocean Hindcast Database for the Design of Marine Energy Converters," *International Journal for Marine Energy,* Vols. 3-4, pp. e40-e52, 2013, doi:10.1016/J.IJOME.2013.11.010.

Distribution List

This Document is a RealTide Public Document and is classified as a Public Report.

1 EXECUTIVE SUMMARY

This report forms Deliverable 2.2 and details the work of Task 2.2 within WP2 of RealTide. It provides the description of the work carried out on the development and implementation of a multi-component resource characterisation methodology. The methodology includes in-situ sensing and hydrodynamic modelling and includes the use of re-analyses of existing datasets as well as the generation of new data sets at both a commercial tidal energy site, the Fromveur Strait, and the European Marine Energy Centre's tidal energy test site.

1.1 Context within the RealTide project

This report builds on specification works reported in RealTide Deliverable D2.1 - "Deployment and Instrument Specification for Advanced Flow Characterisation" [1]. The follow-on report, D2.3 – "Advanced Monitoring, Simulation and Control of Tidal Devices in Unsteady, Highly Turbulent Realistic Tide Environments" [2] completes work-package two reporting and details RealTide-produced extensive datasets that have been collated, coordinated, archived and assimilated into the new RealTide Database.

D2.1 Deployment and Instrument Specification for Advanced Flow Characterisation [1], includes:

- The motivations behind tidal energy site measurement campaign.
- The flow conditions including waves, currents and turbulence that a campaign seeks to capture and key drivers of these conditions.
- Identified off-the-shelf sensors from candidate technologies and recommendations for their configuration and placement.
- Outlines of engineering design and interfacing of a turbine and seabed-mounted sensor package including actuated convergent-beam acoustic Doppler profiling, targeting the capture of 3D turbulence measurements at multiple positions upstream from the TEC rotor plane.

D2.2 Next Generation Flow Measurements and Flow Classification, includes:

- The implementation of the RealTide field measurement campaign
- The reprocessing and re-analyses of identified open data from a highly energetic and industrially-relevant tidal channel
- The execution of 3D site modelling following methodology designed to be transportable to other sites of interest, including preliminary testing of the methodology at an open-data site.
- Lessons-learned and recommendations from the activities

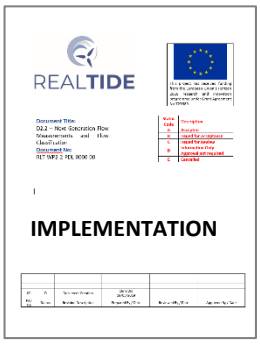

D2.3 Environmental Conditions Database [2]

- The structure and implementation of the extensible database for long-term and reliable access to new data and re-analysis datasets associated with the RealTide project.
- The detailed design of the generalised database schema for integrating in-situ field measurements, as well as tank test data, machine and sensor data, and numerical modelling outputs.
- The design and deployment of a prototype web service for moderated public access to tidal data, including description of front and back-end design, and full user experience cycle.

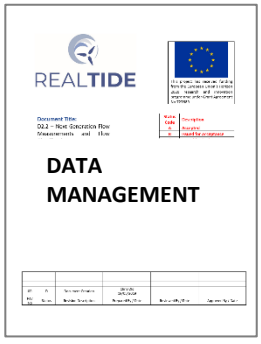

1.2 Objectives

Work Package 2 of the RealTide project has the following objectives:

1. Specifically target the collection of "missing-piece" high-resolution (spatio-temporal) field data through:
   1.1. an identification of key gaps in already secured data, and
   1.2. use of in-development analysis techniques.
2. A dedicated trial of a UEDIN's next-generation velocimetry sensor system (first assembled and optimised in the laboratory at the FloWave facility) will be used to calibrate/validate off-the-shelf instrumentation commonly used by the industry.

1.3 Highlights

- **Site Characterisation:** Evidence from a previous tidal energy project suggested that spatial variation levels in constricted channels would present major uncertainties in energy yield and device loading. This insight has been investigated, substantiated and progressed quantification.

- **Regional Modelling:** A fully open-source and open-data regional modelling solution has been designed and implemented that provides highly-relevant spatial information for use in tidal energy application and the lessons-learned are already feeding new projects in this area.

- **Data Processing and Data Management:** Previous projects highlighted the sensitivity of analyses to the temporal averaging window and type of detrending. RealTide demonstrates that the deconstruction of tidal signals based on physical processes, such as tidal signal and dynamic response, is an improved pre-processing step to the extraction of key parameters. Furthermore, RealTide will make valuable collated and post-processed datasets publicly available on the new data access platform, available at **www.tidalenergydata.org**

- **Measurement:** A comprehensive multi sensor system including novel and advanced configurations capable of more accurately capturing turbulence was designed and implemented based on and around a commercial prototype tidal turbine. Whilst the turbine was twice recovered early due to operational issues the remaining seabed-installed systems captured highly valuable bed-to-surface datasets of duration up to 220 days and exceeding current standards.

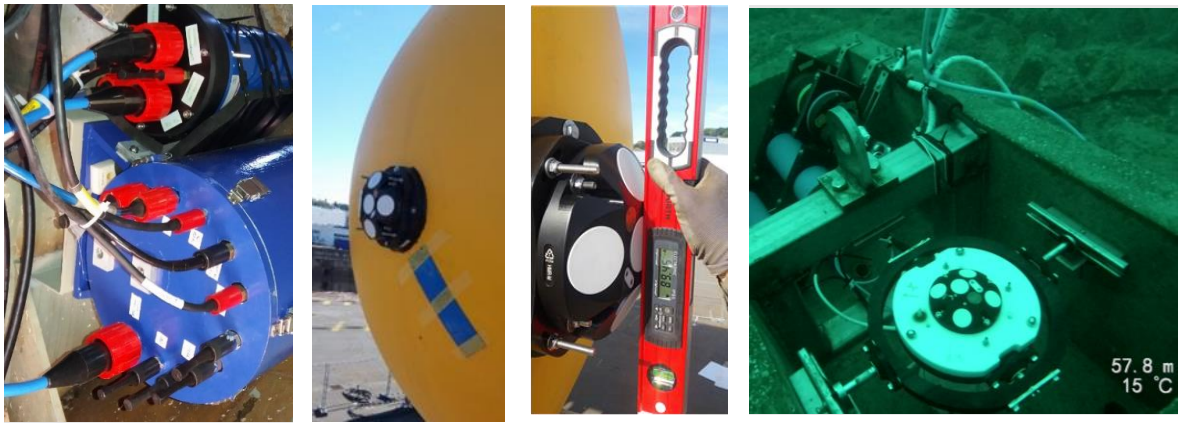

Figure 1-1: RealTide in-situ measurement campaigns: (left) First TEC deployment implementation, (middle) Second TEC deployment, and (right) diver footage of a seabed-mounted sensor implementation.

1.4 The Challenge of Tidal Energy Resource Characterisation

The physical phenomenon of tides, waves, weather, bathymetry and topology, and their interactions, lead to highly energetic velocity fields at tidal energy sites that are also highly spatially variable. Velocity fields exhibit large (with respect to turbine loading and power production) variation in three dimensions i.e., from seabed to surface and across and along channel directions. The following processes have been identified as key challenges:

- **Tidal forcing and harmonics:** Tidal forcing and flow interactions at tidal energy extraction sites are complex and often result in the generation of non-tidal processes [3, 4] which has implications for the estimation related parameters.

- **Flow Directionality:** This is important when determining the siting of different types of TECs. Deviation from rectilinear flow will have a significant effect on power output for TECs which cannot yaw their rotor plane [5], effectively reducing available power. Methods for mapping this across a site provides information of value to site developers and tidal array designers.

- **Intra-channel eddies:** These produce large spatially and temporally local flow modifications, as observed in the Fall of Warness, Orkney [6]. The challenges are interpreting their impact on single point *in situ* measurements, reproducing these structures in regional scale numerical simulations, and determining their potential impact on turbine loading and performance.

- **Extra-channel eddies:** The extra-channel eddies are formed by flow separation at channel exit region, and are represented by a tidal jet structure that form a pair of counter-rotating eddies [7, 8]. The representation of persistent structures in regional scale simulations is current research. The misrepresentation of these processes may impact site characterisation predictions.

- **Turbulent fluctuations:** These are multi-scale and spatially varying. Turbine designers require turbulence metrics to optimise design for reliability. Turbine power output has been shown to be directly linked to the level (TI) and nature (length-scale) of the turbulence [9, 10, 11]. Improved methods for calculating and presenting site turbulence data are required.

- **Surface gravity waves:** Waves have been shown to impact turbine performance and loading, and present stability issues for floating devices [6, 12, 13, 14]. The degree to which waves will affect the power output will be device and site-specific. Methods for capturing wave statistics from standard site measurements, and for quantifying their impact on flow are required.

- **Local bathymetry and topography:** Seabed shape and roughness plays a significant role in the generation of the complex non-tidal fluid dynamic structures, and in controlling the vertical profile. Bathymetric data used to define regional model boundaries define how well these processes represented [15]. The impact of the resolution of both the bathymetric data the model mesh needs to be determined.

- **Variable bottom friction:** This is related to spatial variations in seabed substrate type and the corresponding roughness. It has been shown [16, 15] that the inclusion of a spatially varying map of bottom friction significantly improves the accuracy of numerical models. Methods for generating bottom friction maps are required.

1.5 Holistic Approach to Data

As briefly summarised (and discussed in further detail in this report) there are many challenges associated with tidal site characterisation. Therefore, data acquisition and subsequent analyses within RealTide was conducted holistically considering a range of tools that can be exploited to increase machine reliability and lower system cost. In addition, specific project partner needs were identified through internal activities and captured in internal reports. This led to the specification for a combined measurement-modelling-reprocessing set of activities. Figure 1-2 illustrates the overall methodology and includes graphical representations of generated project outputs directly linked to WP2.

The programme of activities can be broadly grouped into three categories: TEC-mounted systems exploiting the availability of the Sabella D10 tidal energy converter (TEC); seabed mounted systems; and a dedicated advanced turbulence sensor platform. In reality, due to the nature of marine-based work centred on prototype technologies operating in highly-dynamic sites there were near-continuous developments, upgrades, adjusted plans and implemented mitigations to issues in implementation - mainly targeting improved resilience of systems or exploiting arising opportunities. In addition, between categories of work there were multiple cross-overs e.g., elements of advanced turbulence sensing can be achieved via the installation of a 5-Beam horizontally mounted acoustic Doppler Current profiler (ADCP) onto the D10 TEC as the opportunity arose. Examples of work within these categories can be seen in **Error! Reference source not found.** and progress made is summarised in Table 1-2.

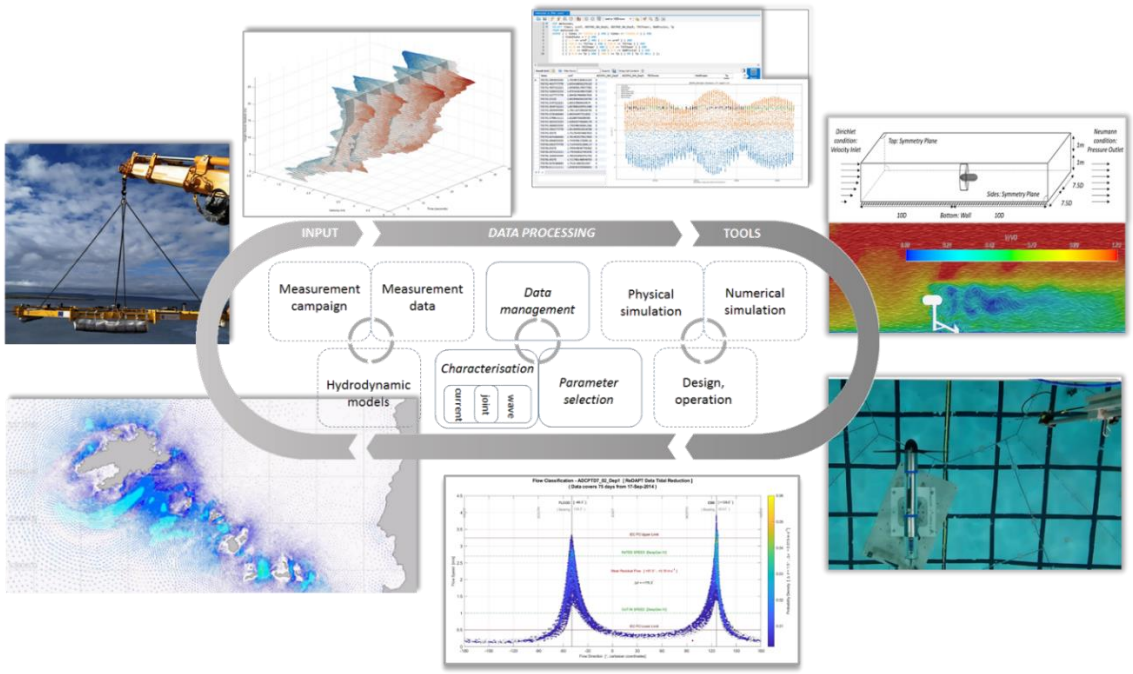

Figure 1-2: The RealTide Holistic Approach. Clockwise from bottom left: RealTide developed 3D models of a commercial tidal energy site; Field work completed in France and the UK, Captured data processed and visualised - showing strong influence of ocean waves; screenshot of the WP2 Database architecture; outputs of WP3's CFD modelling using WP2 inputs, FloWave tests of an instrumented scale TEC and proximal and essential flow-measuring sensor [17]; and site characterisation techniques (central image courtesy of [18]).

1.6 Combined Multi-Site in-Situ Sensing and Hydrodynamic Modelling

1.6.1 Multi-site In-situ Measurement

Data acquisition including in-situ measurement and targeted re-analyses were conducted on data acquired at two highly dynamic tidal channel locations, one in north west France and one in Scotland, UK, as shown in the maps of Figure 1-4. Table 1-1 below summarises the key datasets produced.

Table 1-1. Key datasets of RealTide WP2

Fall of Warness, EMEC - Tidal Energy Test Site, Orkney, UK
RE-ANALYSIS Four targeted datasets acquired during the ReDAPT tidal project [19, 20] were analysed. These data sets were identified based on relevant IEC/TS standards and use-cases, specifically to: - probe spatial variation at scales of the order of 3-5 rotor diameters. - develop model-data comparison analyses for regions suspected of featuring large-scale eddies. - create benchmark datasets for the sector e.g., inline streamwise ambient flow analyses to assist with IEC 62600-200 Power Performance Assessment [21] Datasets have been re-packaged with updated meta-data - and Quality Control (QC) applied - and released for public download via RealTide data platform (see RealTide Technical Report D2.3). Together they represent over 130 days of open data with each set featuring dual instruments deployed contemporaneously to IEC 62600-200 specifications. **NEW DATA** The recently (Sep. 2021) recovered prototype sensor platform, the C-ADP MkIII, has produced data from an important region of the EMEC tidal test site (deployment area of the Orbital tidal turbine). - The analysis of a baseline/benchmark system, a 500kHz 5-Beam ADCP operating for 40 days, has been prioritized due to the complexity of the C-ADP multi-beam system. First-round analysis shows that the mooring frame was extremely stable on the seabed and acquired data shows significant penetration of wave-activity throughout the water column. - C-ADP: whilst post-deployment analysis and data-extraction continues, data and reporting outputs from the phased development of the C-ADP, up to the full-scale trial at EMEC, are publicly available [22, 23, 24, 25, 26]**.**
Fromveur Strait, north west France
RE-ANALYSIS Two ADCP datasets collected prior to the RealTide project commencement were provided by Sabella to UEDIN. These data were presumed corrupted, however, new processing scripts were developed and used to fully extract the measurement records. These internal commercial datasets have been used to inform design work by Sabella and to develop the modelling methodology of WP2 (for model calibration/validation). **NEW DATA** The RealTide-specified measurement campaign was successfully implemented and met and exceeded requirements of the relevant IEC/TS standard. This has produced data that: - far exceeds previously available knowledge in terms of spatio-temporal resolution and duration. - has been post-processed, captures robust meta-data and has newly developed QC applied. - represents 67 days of data where two co-located instruments are available for analysis. - in the case of one instrument provide over 220 days of uninterrupted data covering winter months and capturing flows from seabed to sea-surface. - will enable (with the permission of the data owner) multiple future analyses

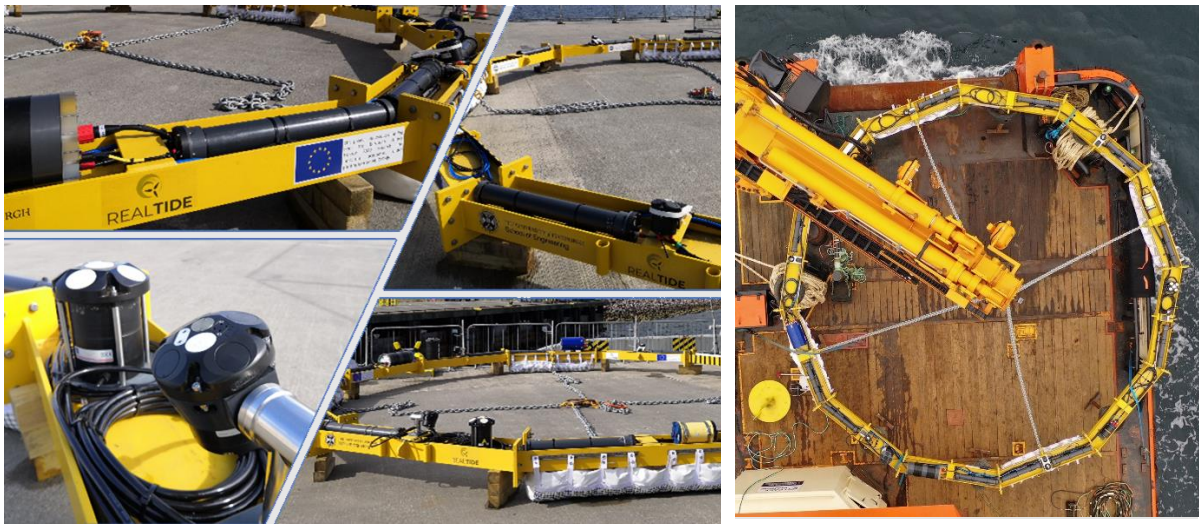

Figure 1-3: RealTide Advanced Turbulence Sensor multi-sensor system assembled and awaiting deployment (left and middle) and being deployed (right) in August-September 2021 at the EMEC tidal energy test site, Fall of Warness, Orkney.

1.6.2 Multi-site Hydrodynamic Modelling

A set of 3D non-hydrostatic Telemac models – chosen to meet the specification of D2.1 - were created and run for time periods covering periods of acquired *in situ* data. Models were developed for two sites: (1) Fromveur Strait, North West France, and (2) the Falls or Warness, Orkney, UK. Fromveur Strait was modelled to address questions raised by Sabella, to support the interpretation of *in situ* measurement made during the project, and to provide data for CDF modelling work. There are restrictions, for reasons of commercial sensitivity, on the use of data from the Fromveur model as per the RealTide agreement. The Falls of Warness was modelled to complement the legacy (and re-analysed as part of WP2) ReDAPT data and to address questions about levels of horizontal spatial variability in the flow across the site.

These two locations represent different types of tidal energy sites, with different model design requirements. Fromveur Strait is part of a complex headland structure with an extended area of dynamical influence. For this reason models with a range of high-resolution coverage were construct to assess the importance of capturing far-field processes when designing models for site assessment and characterisation. The Falls of Warness is a channel within an Island archipelago feed by a network of side channels and containing small islands. The model design methodologies developed for the Fromveur Strait models were transferred and applied to develop the Falls of Warness models.

Open Data: Importantly, the Falls of Warness model data generated are open-access and are integrated into the database developed in task D2.3 of this work package. The Falls of Warness model data were used to develop a generalised flow classification diagram that can be applied to observed and modelled data. This has identified possible methods for modifying model validation against *in situ* data from high-energy tidal sites, which will be followed up in the new FASTWATER project. The model data were used to develop methods for mapping key flow metrics to determine how these could be used to support site development decision making processes.

A methodology has been developed for producing stable model constructs in the OpenTelemac system. It has been shown that spatially varying bottom friction significantly improves model accuracy and stability. Methods were developed to generate maps of bottom friction coefficients from archived maps of substrate class data.

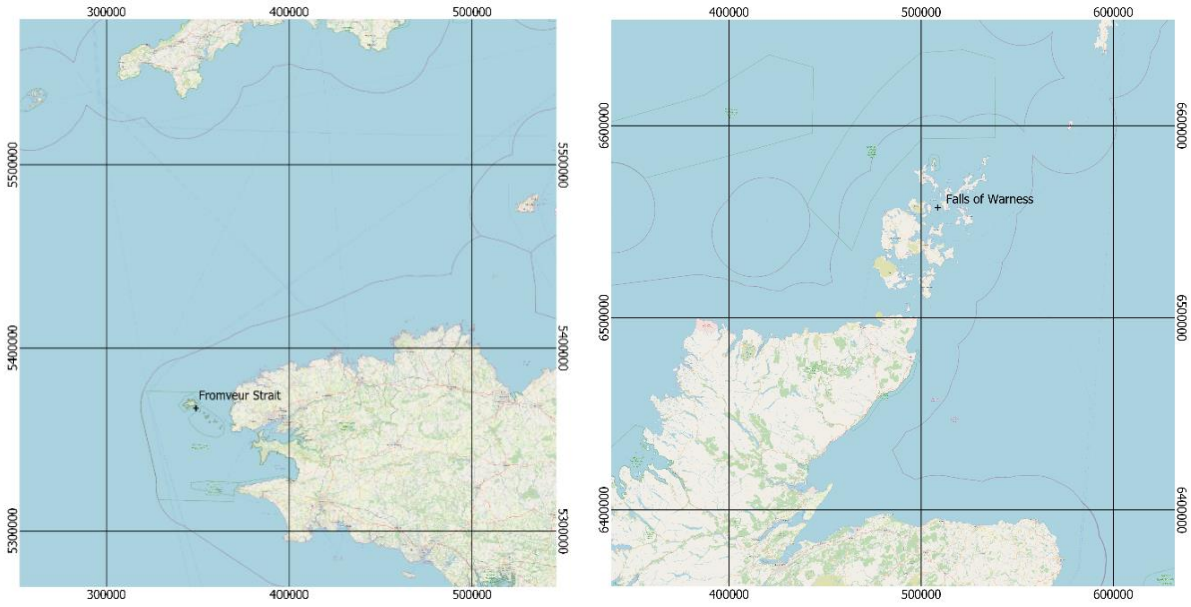

Fromveur Strait, North West France

Falls of Warness, Orkney, UK

Figure 1-4 Maps showing the two regions of interest within RealTide WP2. (left) Fromveur Strait, France and (right) Fall of Warness, Orkney, UK

1.6.3 Data Processing and Software Tools

Previous projects highlighted the sensitivity of analyses to the temporal averaging window and type of detrending. Methods developed in RealTide have demonstrated that the deconstruction of measured or predicted time series of data base on physical processes, such as tidal signal, weather, and dynamic response, is a more effective method of pre-processing the data prior to the extraction of key parameters. This is useful for the extraction of turbulence metrics from high-frequency velocity data, extracting wave parameters from high-frequency pressure sensor data, and for quantifying non-tidal dynamical response of the fluid to the various forcing processes.

In association with the development of the regional models, a suite of software tools have been developed to support data extraction, the calculation of advanced site parameters (e.g. vorticity, circulation, Courant number, etc.), post-processing tools to support flow classification methods. Tools for generating maps of spatially varying bottom friction for a range of coefficients that OpenTelemac accepts (e.g. Manning, Chezy, Nikuradse, etc.) have been developed. The tools will be made available as open-source code following final cleaning and documenting. These will be hosted using the infrastructure developed as part of WP2 Data Management work. For further information see RealTide D2.3 [2] and www.tidalenergydata.org

Following a literature review based on the use of acoustic Doppler Current Profilers (ADCP) in the offshore renewable energy (ORE) sector and oceanographic use more broadly Quality Control (QC) using various methods and thresholds was implemented on acquired data sets. The processes are reported and have been applied to datasets that have been made available to the public via the RealTide programme [27, 28, 29].

1.6.4 Summary of the RealTide WP2 Implementation

A summary of the phased elements of the work is provided in Table 1-2 and is described in further detail in Section 3 of the report.

Table 1-2: The RealTide In-Situ Activities: Summary of TEC-mounted, Seabed-mounted and Advanced Turbulence Sensing (see Section 3 for further information).

System & Features	Completion Status				
	Electrical Mechanical Comms &	Implemented	Tested	Deployed	DATA ACQUIRED
TEC Deployment 1 • Implemented the specification developed in RealTide D2.1 • Iterative system design reviews of key sensors and sub-systems • Procurement and integration of off-the-shelf (OTS) components and extensive custom engineering (mechanical and electrical) • Extensive electrical, controller and IT design tying in with D10 systems • Detailed 3rd-party structural analysis prior to retrofitted tasks • Multiple sensors installed ready for D10 deployment	Yes	Yes	Yes (partial testing with TEC systems possible)	Yes	None - before unplanned TEC recovery
TEC Deployment 2 • Full redesign to exploit re-designed D10 aux. electrical system • "bypass" system to de-couple seabed / D10 mounted systems • Improved fusing, redundancy, resilience and miniaturization • All systems fully tested and functioning over TEC infrastructure	Yes	Yes	Yes (extensive)	Yes	Limited - before unplanned TEC recovery
Seabed-Mounted system • Diver removable sensors and battery packs • Hybrid power: either by D10 or by battery via diver connected cable • Pre-installed cables • Smart and robust re-routing of power and comms to D10 control • Stable, flexible and capable mooring systems	Yes	Yes	N/A	Yes	Yes (extensive)
Convergent Acoustic Doppler Profilometry (Advanced Sensing)					
• Design of System and control software	Yes	Yes	Yes	Yes	Yes
• High-resolution sensor unit performance tests	Yes	Yes	Yes	Yes	Yes
• C-ADP in controlled environment tests	Yes	Yes	Yes	Yes	Yes
• C-ADP with novel actuation capability: scaled test in USA	Yes	Yes	Yes	Yes	Yes
• Full-Scale Tests – TEC D10 – Connected Tests	Yes	Yes	No	No	No
• Full-Scale Tests – Autonomous Actuated 3D at EMEC	Yes	Yes	Yes	Yes	TBC

1.7 Key Outputs

Key outputs across five activity themes are summarised in Table Table 1-3. Further detail is provided in Section 8 of the report.

Table 1-3. Five Activity Themes: Summary of Key Outputs

DATA ANALYSES	
-Wave-Current Processed Datasets	Output flow conditions to inform the CFD activities of WP3, Tank-Testing activities of WP3 and BEMT model development activities of WP1
-Spatial Variation Studies	Published via re-processing two previously unavailable datasets covering 70 days+ of contemporaneous measurement allowing studies of spatial variation at TEC-relevant scales.
-Power Performance	Published via re-processing two previously unavailable datasets covering 40 days of contemporaneous measurement allowing study of power performance assessment methodologies
REGIONAL MODELLING	
- Design	Methodology developed to capture key flow features of tidal energy sites using open modelling tools that can be replicated at other sites.
- Execution	Demonstrated the importance of key model design steps to tidal energy applications through demonstrating the affect of varying implementation on output parameters e.g., energy yield and spatial variability.
- Tools	Generated methods for readily extracting data from large 4D vector fields to allow tidal-energy information generation.
DATA TOOLS	
- Data Handling	Developed multiple tools for the handling of complex 4D heterogenous datasets across physically sensed and modelled datasets.
-Data Processing	Developed multiple tools for the processing of complex 4D heterogenous datasets across physically sensed and modelled datasets.
-Quality Control	Implemented & reported a QC methodology for re-analysed and new datasets.
SENSORS AND SENSOR SYSTEMS	
-Sub-System	Designed and implemented multiple sub-systems to improve capability and capacity of subsea sensing for tidal energy applications.
-Autonomous	Developed and implemented functioning autonomous controllers based on low-power embedded computing fit-for-purpose for subsea deployment
-Hard-Wired/Remote	Developed and implemented multiple electrical and mechanical systems for resilient connection of mixed-type sensors to the internet via TEC-integration.
Marine Operations	Successfully demonstrated instrument package deployment via ROV, diver and vessel-crane-only techniques.
DATABASE AND DATA ACCESS	
-Database Design	Design of stable and scale-able environmental data database for WP2 (and transferred to WP1 for Reliability Database) internally tested using experience and datasets generated in WP2. Due for release Q4 2021. www.tidalenergydata.org
-File I/O and Interface	File handling, data extraction and standardisation processed developed as well as a front end web-app methodology
DATA CLASSES	***In-Situ , Regional Modelling, Physical Testing (Numerical Simulation pending)***
-Public Website	Launched www.tidalenergydata.org to generate impact via data access to pre-packaged datasets and searchable access to data in the RealTide database.
-Datasets	Multiple datasets published (see Section 4 and Section 8).

1.8 Lessons Learned (Summary)

A selection of key lessons learned are summarised below across the five activity themes as presented in Section 1.7 *Key Outputs*, namely: Data Analysis, Regional Modelling, Data Tools, Sensors and Sensor Systems, and Database and Data Access. Further lessons learned across these themes are provided in Section 8 of the report.

DATA ANALYSES

A. When capturing and comparing model and in-situ results, e.g., for model calibration / validation the specific the final use-case of the analysis should be considered, where turbine geometry and location in the water column will play a significant role in the interpretation of the results. For example, large differences in velocity agreement at the seabed may or may not be relevant to exploiting the model data at a particular hub-height.
B. The inclusion of non-tidal components e.g., waves and large eddies in measurements strongly affects turbulence analysis, specifically estimates of Turbulence Intensity and in spectral analyses.
C. Signal detrending: Methods developed in RealTide have demonstrated that the deconstruction of measured or predicted time series of data base on physical processes, such as tidal signal, weather, and dynamic response, is a more effective method of pre-processing the data prior to the extraction of key parameters.

REGIONAL MODELLING

A. IEC guidance on model development guidelines acknowledged that large-scale flow structures need to be considered, but do not provide any further detail. There are recommended mesh resolutions within the region of interest depending on the end-use of the model data, but no discussion of the extent this region should cover. It was decided that this was a fundamental and highest-priority question that needed to be addressed before advancing to the full wave modelling. The subsequent analyses on this aspect affected time and resource constraints which meant that proposed wave modelling work could not be addressed in the project time frame.
B. 3-D non-hydrostatic models are required to capture the complex flow structures, such as coherent eddies and secondary circulations, and to accurately estimate available power for a range of turbine designs and installation methods and locations.
C. 2-way wave-current modelling with open-source tools is difficult and computationally expensive and requires further development work to bridge the expertise gap and to reduce barriers to exploitation of these tools by tidal energy developers.

DATA TOOLS

A. Lack of transparent and user-friendly tools / limited uptake of tools that are available hinders post-processing of data and is a barrier to researcher and developer participation.
B. There is a need for robust and systematic QC procedures tailored for high-energy tidal channels.
C. The prevalence of non-tidal processes integrated in site measurements reduces the reliability of Turbulence Intensity estimates and necessitates standardized post-processing.

SENSORS AND SENSOR SYSTEMS

A. Further work is required on the quantification of the consequences and increase in uncertainty of sampling flow-fields using D-ADP devices in extremely high energy sites where levels of spatial variation of flow scales comparable to the acoustic beam separation distances in horizontal and vertical directions is large and temporally varying. Alternate configurations remain promising in terms of being able to capture at reduced uncertainty in characterisation of 3D turbulent flows.
B. For cabled solutions hybrid and robustly switchable power systems incorporating battery back-up power are implementable using small low-power components and are valuable investment.
C. It is challenging and time consuming – but not impossible – to execute interfaced engineering works remotely where travel restrictions are in place with sufficient levels of time and *enthusiasm*.

DATABASE AND DATA ACCESS (see RealTide Technical Report D2.3 for further information)

A. Provisioning external public access to an organisation's internal IT systems comes with technical and security risks. Long-term, a pooled and dedicated service provider should be engaged with.
B. Re-analysis legacy data is time consuming. It is much better to capture the data correct "first time around" including all necessary meta-data.
C. Designing data campaigns with the final database of data in mind leads to the establishment of good practice.

1.9 Next Steps

RealTide outputs will be further explored and progressed as part of internal research and ongoing collaborative projects. These include further data archival and data publishing to increase impact of the captured data together with post-processing tools to accelerate the extraction of meaningful information. The modeling work continues in internal projects as well as new funded projects with the overarching aim of removing barriers to model use for making informed decisions in tidal energy.

Data archival and publishing: In addition to those datasets already in the RealTide D2.3 data platform demonstrator, it is planned to re-analyze, QC, convert, archive and publish all UEDIN-held site measurement datasets, pertinent tank-testing results and arising modelling outputs from new projects including the SuperGen ORE Hub funded project, FASTWATER. Already identified CFD and BEMT will be prepared and transferred to the database. Permissions, where required, have already been granted.

Data post-processing: Efforts will continue via internal research and through collaborations established during RealTide. Efforts will seek to extract further site parameters including turbulence metrics and wave statistics which will be captured in academic publications as well, as being archived and published to the database. Efforts will continue on Data QC processes as the consolidated database forms an excellent basis to develop and assess robust thresholds – which currently processed outputs are sensitive to.

Further data capture campaigns: In parallel to processing any retrieved data from the C-ADP MkIII prototype recovered at the end of the RealTide project, opportunities are being explored to exploit the gained ground on hardware and software related to advanced sensing, including options to redeploy seabed and TEC-mounted measurement systems to continue progress in providing better and fit-for-purpose site characterisation.

Advanced open modelling: In separate work further model methodological development will be conducted exploiting the RealTide winter 2019 Fromveur Strait datasets. This will be used directly by the site developer and by the wider sector through incorporating the methodology the UK FASTWATER project, where the RealTide modelling methodology will be taken-on, exploited, standardized and made more accessible to the wider community. These stable and flow-capturing base models can form the platform for wave-current coupling – which is scheduled to be conducted in 2022.

Long-term legacy: Evidence from related and data-focused industrial-academic research shows that if acquired project data and knowledge can be curated appropriately, new research and industrial opportunities and routes to impact will arise. By widening participation in the analyses of the captured data further gains should be made in improving reliability and lowering costs of tidal energy. RealTide, by implementing an integrated data management plan and data platform via www.tidalenergydata.org improves the chances of these works and outputs generating long term impacts.

1.10 WP2-Related Further Information

The following outputs have resulted from activities conducted in whole or in part from RealTide WP2. Multiple follow-on publications are in preparation.

Ingram, David M., Sellar, Brian G. Sellar, Old, Chris, Davey, Tom, Gabl, Roman, Jordan, Laura-Beth, Nourisson, Ophelie, and Paboeuf, Stephane. 2021. *"Experimental measurement of the loads on tidal turbines using conditions derived from field measurements ".* The 14th European Wave and Tidal Energy Conference (*EWTEC 2021*).

Dorward, Mairi, Brian Sellar, Chris Old, and Philipp R. Thies. 2019. "Currents, Waves and Turbulence Measurement: A View from Multiple Industrial-Academic Projects in Tidal Stream Energy." In *Institute of Electrical and Electronics Engineers (IEEE)*. https://doi.org/doi:10.1109/CWTM43797.2019.8955294.

Harding, Samuel, Brian G. Sellar, and Mairi Dorward. 2019. "Implications of Asymmetric Beam Geometry for Convergent Acoustic Doppler Profilers." In *In IEEE/OES Twelfth Current, Waves and Turbulence Measurement (CWTM 2019)*. https://doi.org/10.1109/ CWTM43797.2019.8955290.

Harding, Samuel, Mairi Dorward, Brian Sellar, and Marshall Richmond. 2021. "Field Validation of an Actuated Convergent-Beam Acoustic Doppler Profiler for High Resolution Flow Mapping." *Measurement Science and Technology* 32 (4). https://doi.org/10.1088/1361-6501/abd5ef.

Jourdain de Thieulloy, Marilou, Mairi Dorward, Chris Old, Roman Gabl, Thomas Davey, David M. Ingram, and Brian G. Sellar. 2020. "On the Use of a Single Beam Acoustic Current Profiler for Multi-Point Velocity Measurement in a Wave and Current Basin." *Sensors (Switzerland)* 20 (14): 1–21. https://doi.org/10.3390/s20143881.

Jourdain de Thieulloy, Marilou, Mairi Dorward, Chris Old, Roman Gabl, Thomas Davey, David M. Ingram, and Brian G. Sellar. 2020. "Single-Beam Acoustic Doppler Profiler and Co-Located Acoustic Doppler Velocimeter Flow Velocity Data." *Data* 5 (3): 1–11.

Gaurier, Benoît, Stephanie Ordonez-Sanchez, Jean Valéry Facq, Grégory Germain, Cameron Johnstone, Rodrigo Martinez, Francesco Salvatore, et al. 2020. "MaRINET2 Tidal Energy Round Robin Tests-Performance Comparison of a Horizontal Axis Turbine Subjected to Combined Wave and Current Conditions." *Journal of Marine Science and Engineering* 8 (6). https://doi.org/10.3390/JMSE8060463.

RealTide. 2018. "Technical Report (Internal): Deliverable 1.5 - Increased Reliability of Tidal Rotors (RLT-WP1-5-PDL-000-01)."

RealTide. 2018. "Technical Report: Deliverable 3.4 - Inter-Comparison of BEMT, Blade-Resolved CFD, and BEMT-CFD Hybrid Models of Scale Turbines (RLT-WP3-4-PDL-000-01)." https://realtide.eu/realtide-project-deliverables.

RealTide. 2019. "Technical Report: Deliverable 2.1 - Deployment and Instrument Specification for Advanced Flow Characterisation (RLT-WP2-1-PDL-000-03)." https://realtide.eu/realtide-project-deliverables.

RealTide. 2021. "Technical Report: Deliverable 3.5 - Synthetic Load Spectra and Time Series of Tidal Turbines (RLT-WP3-5-PDL-001-02)." https://realtide.eu/realtide-project-deliverables.

RealTide. 2021. "Technical Report: Deliverable 2.3 - Environmental Conditions Database: Collation, Demonstration and Dissemination (RLT-WP2-3-PDL-001-03)." https://realtide.eu /realtide-project-deliverables.

2 INTRODUCTION

The purpose of this Work Package Task was to target data and knowledge gaps identified in existing high-resolution field data [30, 31]. This work builds on data processing algorithms, data capture methodologies, and advanced measurement hardware proto-typed in previous projects. A key data gap is the limited amount of information available on the spatial variability of key processes across tidal energy sites, and a clear understanding of how this variability affects the parameter extraction, data capture and site development. Investigation into the identified data and knowledge gaps was carried out using a combination of re-analysis of legacy data, hydrodynamic tidal modelling, and targeted data capture using standard and bespoke instrumentation. New methods for presenting and interpreting these data were investigated. Dataset generated from this work package will be included in the database created in Task 2.3 of this work package, providing searchable open-source data that link together information relevant to the development of the tidal energy sector. This document puts the problems identified into context and describes the approach taken to address the questions to be answered.

2.1 Report Layout

The document has three core sections covering:

1. Data capture and processing (Sections 3 & Section 4)
2. Regional scale hydrodynamic modelling (Section 5)
3. Flow classification methods and sensitivity analysis (Sections 6 & 7)

The document closes with a summary of outputs, discussion of lessons learned and recommendations to the sector based on the findings.

2.2 Objectives

The work package task objectives, based on the Grant Agreement [31], are:

1. Specifically target the collection of “missing-piece” high-resolution (spatio-temporal) field data through:
    a. an identification of key gaps in already secured data, and
    b. use of in-development analysis techniques.

2. A dedicated trial of a UEDIN’s next-generation velocimetry sensor system (first assembled and optimised in the laboratory at the FloWave facility) will be used to calibrate/validate off-the-shelf instrumentation commonly used by the industry.

3. Development of hydrodynamic modelling methodologies targeted at providing information that cannot easily be captured through site measurement, but are identified as relevant to the sector.

2.3 Background

Characterisation of a tidal site - informing resource assessment, site selection, turbine design, turbine siting and subsequent operations and maintenance activity – is a key element in the development of any site. Information sources for site characterisation include *in situ* measurements, remotely sensed data, output from numerical models, local knowledge, historical records, *etc.* At the most basic level site characterisation includes the available resource, the local topography, the local wave environment, and site accessibility. Characterisation will come from a mixture of observations and regional model output. These two data sources are complimentary: the data collected provide detailed localised observations of the real environment that can be used to calibrate and validate regional

numerical models; the flow structures identified by the regional models can be used to inform the optimal siting for instrument deployments to aid in site characterisation.

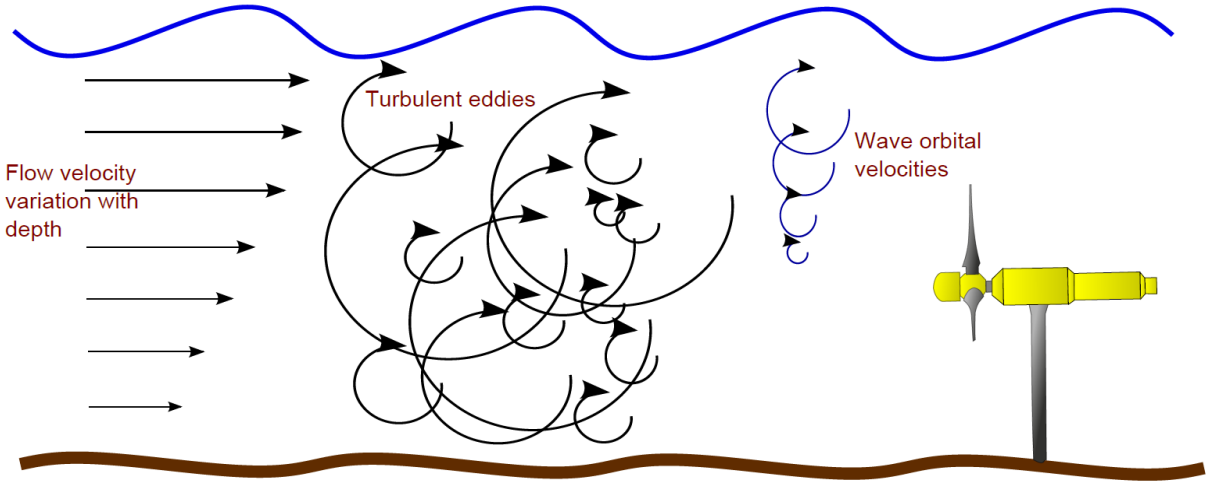

Figure 2-1: The unsteady characteristics of incident flow on a tidal turbine

To support site and turbine developers, the *in situ* observations and model constructs need to be integrated with information collected from operating turbines to allow the attribution of turbine response to the observed system state [32, 33]. This is an iterative process based on feedback between the processes and users of the data as illustrated in [6] and in Figure 1-2. The *in situ* measurements and regional modelling need to capture a range of processes on various spatial and temporal time scales [32, 34, 35], with some of the key processes shown in Figure 2-2. The characterisation data generated are converted to parameters that are used in engineering design tools [36, 32, 33]. Figure 1-3 illustrates the input of these parameters into fluid-structure and electro-mechanical sub-system modelling. Findings from engineering development will identify new parameters that are required. Complementary to this, new marine measurement techniques will capture new parameters allowing different modelling methods to be used for design.

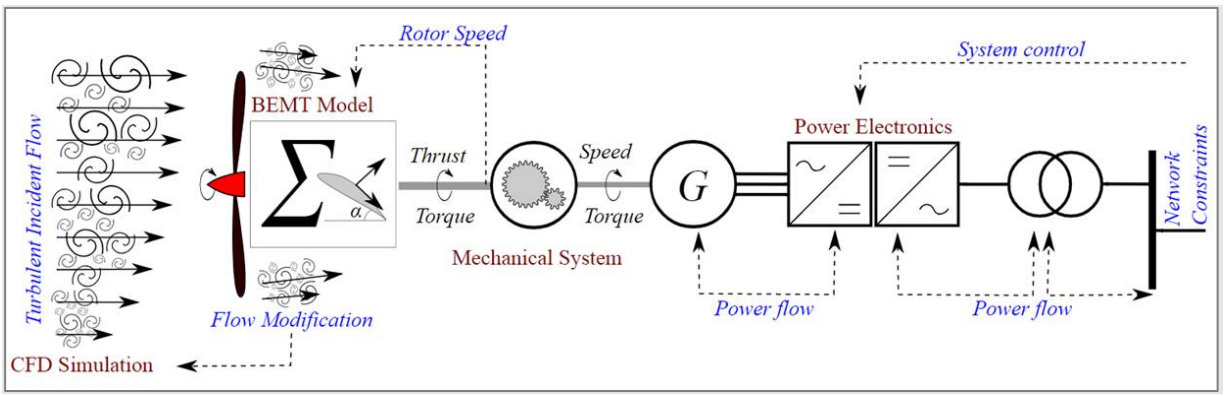

Figure 2-2: RealTide Tide-to-wire model: overview schematic

2.3.1 The Challenge of Tidal Energy Resource Characterisation

The principle roles of site measurement are to provide an assessment of the available energy resource, quantify the levels of spatial and temporal variability in fluid flow across a site, and to assess the potential impact of flow variability on the reliability and survivability of a turbine located within the site. The physical phenomenon of tides, waves, weather, bathymetry and topology, and their interactions, lead to highly energetic velocity fields at tidal energy sites that are also highly spatially variable. Velocity fields exhibit large (with respect to turbine loading and power production) variation in three dimensions *i.e.*, from seabed to surface and across and along channel directions. The processes identified as requiring further investigation are described below.

Tidal forcing and harmonics are generated by the combined gravitational forcing of the sun-earth-moon system and the interaction of the resulting tidally driven flow with the local topography [37]. Tidal oscillation periods range from a few hours (harmonics of fundamental forcing periods) out to 18 years (the orbital nutation period). The dominant forcing period is 12.42 hours, the lunar forcing period. Tidal forcing and flow interactions at tidal energy extraction sites are complex and often result in the generation of non-tidal processes [3, 4]. The impact of these non-tidal processes on MRE relevant parameter and the implications for their estimation based on a tidal reduction of observed data needs to be assessed.

Flow Directionality is important when determining the siting of different types of TECs. Tidal energy extraction sites are typically associated with flow constriction which generates the increased local flow speeds from which energy is extracted. This constriction often results in a shift from simple rectilinear flow [38, 5], i.e. the flood tide peak flow direction is not in line with the ebb tidal peak flow direction. Deviation from rectilinear flow will have a significant effect on power output for TECs which cannot yaw their rotor plane [5], effectively reducing available power. It is important to quantify this effect, to properly account for the reduced energy extraction for devices which cannot yaw, or the expected motions for those that can. Methods for mapping this effect across a site will provide information of value to site developers and tidal array designers.

Intra-channel eddies produce large spatially and temporally local flow modifications, as has been captured in datasets collected at the southern extent of the Fall of Warness, Orkney [6]. The processes that generate intra-channel eddies are headland eddies [39, 40, 41] and island wakes [39, 42, 43]. The challenges are interpreting their impact on single point *in situ* measurements, reproducing these structures in regional scale numerical simulations, and determining their potential impact on turbine loading and performance.

Extra-channel eddies impart future in-channel flow deviation and variability by changing large-scale flow dynamics. The extra-channel eddies are formed by flow separation at channel exit region, and are represented by a tidal jet structure that form a pair of counter-rotating eddies [7, 8]. The large-scale structures formed are seen to persist in satellite imagery and this process varies between spring and neap tides. The full impact of the presence and re-entrainment of these structures on local and regional scale dynamics is less well known. The representation of these persistent structures in regional scale simulations is current research. The misrepresentation of these processes may have impacts on site characterisation based on modelled data.

Turbulent fluctuations are multi-scale and spatially varying. Turbine designers require turbulence metrics to optimise design for reliability. Turbine power output has been shown to be directly linked to the level (TI) and nature (length-scale) of the turbulence [9, 10, 11]. However, there is no unique TI or length scale across a site, so a range of values need to be provided for a site. There is also a distinction between the large-scale coherent structures the are generated by fluid shear and flow

separation processes, which are non-tidal fluctuations with length scale similar to the rotor diameter or smaller. These are not part of the turbulence cascade that is described by the statistical turbulence models, but are the energy contain scales that extract energy from the tidal flow.

Surface gravity waves have been shown to impact turbine performance and loading, and are a source of stability issues for floating devices [6, 12, 13, 14, 44, 45, 46, 47]. The degree to which waves will affect the power output will therefore be highly device and site-specific. The relative direction between waves and tidal currents (i.e. following or opposing) is important, as this leads to both amplitude and frequency modulation of the wave. Analysis shows that some sites appear to have large amplitude waves during periods of low mid-depth current speed, whereas other sites feature larger amplitude waves during peak flows where wave-current interactions are amplified. The relative phasing of these systems is important for operation as it effects design load cases and for operations and maintenance (O&M) as it will strongly affect site access / weather windows.

Local bathymetry and topography plays a significant role in the generation of the complex non-tidal fluid dynamic structures, and in controlling the vertical shear-layer structures. The length scales of spatial variation are from the order 0.5m to 100's of metres. In regions of high-tidal flow there is generally very little fine sediment, and the underlying bed rock is often exposed. Depending on the type of rock and geological processes the seabed has be modified by, there will be a range of structures and depressions the will impact the flow boundary layer structure and eddy shedding processes. The impact of bathymetric structures on the down-stream flow needs to be understood when interpreting in situ flow measurements and estimating variability in flow structures. Bathymetric data used to define the hard boundary for regional models influences how well these processes are captured [15]. The impact of the resolution of both the bathymetric data the model mesh resolution needs to be determined.

Variable bottom friction is related to spatial variations in seabed substrate type and the corresponding roughness. Bottom friction is one of the controlling boundary conditions required for regional scale hydrodynamic modelling. Typically, a constant global values is used when constructing regional models, but it has been shown [16, 15] that the inclusion of a spatially varying map of bottom friction significantly improves the accuracy of numerical models.

2.3.2 Relevant Standards and Guidance Documents

Standards and guidance documents were used to inform the measurement campaign specification, as produced in RealTide Technical Report D2.1. These are summarized below in Table 2-1. Specific attention was given to:

- IEC/TS 62600-200:2013 Marine Energy – *Wave, tidal and other water current converters – Part 200: Electricity producing tidal energy converters – Power performance assessment*
- *IEC/TS 62600-2:2019 Marine energy – Wave, tidal and other water current converters –Part 2: Marine energy systems – Design requirements*
- *IEC/TS 62600-201:2015 Marine energy – Wave, tidal and other water current converters –Part 201: Tidal energy resource assessment & characterisation.*

The results of the implementation are reported in Section 3 and Section 4.

Table 2-1: Overview of industrial standards and guidance containing flow measurement requirements applicable to tidal stream energy [26]

Standards (inc. Guidance and Recommended Practice)	Stated Purpose	Comment
Standard (IEC) **IEC/TS 62600-200:2013** [21] Marine Energy – Wave, tidal and other water current converters – **Part 200**: Electricity producing tidal energy converters – Power performance assessment.	Systematic methodology for evaluating power performance of tidal current energy converters producing electricity for utility scale & localised grids.	Defines: - TEC rated power - Rated water velocity - Power curve production - Results reporting.
Standard (IEC) **IEC/TS 62600-2:2019** [48] Marine energy – Wave, tidal and other water current converters – **Part 2**: Marine energy systems – Design requirements	Primary design criteria to ensure engineering integrity throughout the design life of marine energy converters such as wave & tidal.	- Site-specific environmental loads. - Safety factors - External load cases (extreme, normal) - Failure probability & consequence - Redundancy
Standard (IEC) **IEC/TS 62600-201:2015** [49] Marine energy – Wave, tidal and other water current converters – **Part 201**: Tidal energy resource assessment & characterisation.	System for analysing & reporting theoretical tidal current energy resource in oceanic areas.	Staged approach to calculation of resource assessment with increasing detail from feasibility to design. Outlines data collection for calibration & validation of hydrodynamic models.
Standard (DNVGL) **DNVGL-ST-0164 (2015)** [50] Tidal turbines	Principles, technical requirements & guidance for design, construction & in-service inspection of tidal turbines.	- Requirements for site characterisation. - Limit state approach to design. - Design loads & return periods. - Load effects analysis.
Recommended Practice (DNVGL) **DNVGL-RP-C205** [51] Environmental conditions and environmental loads	- Guidance for modelling analysis & prediction of environmental conditions. - Guidance for calculating environmental loads acting on structures.	- Specific to wind, wave, current loading on a range of structures. - Outlines metrics, their statistical derivation & load calculation methodology.
Guidance Note (BV) **NI 603 DT R01 E** [52] Current and Tidal Turbines	Requirements for Current and Tidal Turbines installed on the seabed with regards to assessment and certification by Bureau Veritas.	- Environmental data specification. - Design loads & load cases. - Load conditions & limits applied.
Rules (BV) **NR 445.B1 DT R05 E** [53] Rules for the Classification of Offshore Units: **Part B** – Structural safety (Environmental conditions-loadings)	Requirements for offshore units relating to design, operational & environmental conditions data.	Outlines wind, wave, current, water-depth metrics & their derivation in relation to structural design.

2.4 Approach

Multi-site - commercial and open: RealTide WP2 activities sought to capture information on multiple physical processes at multiple sites: both commercial development sites i.e., the Fromveur Strait and the tidal energy test site operated by the European Marine Energy Centre at the Fall of Warness, Orkney, UK. The locations of these energetic channels can be seen in Figure 1-4. Relevant physical processes are discussed in the RealTide Technical Report D2.1 [1] which provides summary information and further reading.

Processes and physical drivers: In summary, measuring, modelling and characterising tidal channels for tidal energy applications should take account of the following processes:

- Hydrodynamics
- Tidal Resource
- Large-scale Flow Structures
- Turbulence
- Wave Environment
- Combined Wave-Current Environment
- Seabed Shape and Composition
- Bathymetry
- Seabed Composition
- Wind Field & Atmospheric Surface Pressure

However, the application area – namely improving reliability of tidal energy - must be considered at all times i.e., what is the impact of these processed on the tidal energy generation system. For example, specifying a single value for turbulence e.g., Turbulence Intensity, may be meaningless if the hub-height and rotor diameter of the specific machine are not factored. This is also important when quantifying levels of agreement between different data sources, where large differences may be generated from regions of the domain that do not play an important role in a particular machine's performance or loading.

2.4.1 Flow Classification

The intention is to look at ways to provide a form of flow classification mapping that can be used to provide a more detailed picture of the a site, thereby enhancing the information content available to site developers. At a most basic level this represents the core tidal variations, i.e. ebb/flood and neap/spring variations in the tidal flow. However there are other interacting physical processes that interact with the tidal flow producing non-tidal signals that can significant alter the underlying tidal energy. The 3-D structure of the flow also needs to be considered when estimating available energy. The most well define of these is the variation in the velocity with depth, or velocity profile. This results from the interaction of the flow with the seabed through friction; the effectively goes to zero at the hard boundary interface. Less well defined are the horizontal flow structures that result from flow separation processes, the complex non-linear wave current interactions. Both of these processes have a significant impact on turbine power production, fatigue, and reliability.

2.4.2 Targeted Parameters

An internal project report, RealTide deliverable D1.5, identified the state of the art in tidal flow characterization at project commencement. RealTide deliverable D2.1 gives a detailed review of site characterization methods and the parameters that need to be quantified from data. In D2.1 the key processes that need to be resolved and their corresponding implications for the design of a

measurement campaign are highlighted. Based on experience and knowledge gained from legacy projects and scientific findings in the literature, the various turbulence parameters and the spatio-temporal variability across a site were identified as being the most poorly define flow characteristics. These have implications for turbine design and performance, and turbine placement and tidal array farm design. The separation of wave-current interactions for more accurate estimates of the turbulence parameters was also highlighted as requiring further development. A record of arising literature was maintained, which is summarized in Table 2-4.

Table 2-2: Identified parameters that informed the specification of the measurement and/or modelling campaign and in particular the specification of the Advanced Turbulence Sensor (C-ADP)

Method	Parameter Name	Symbol	Description
1a) Synthetic eddy method (SEM) - RST	Turbulent length scale	$L_i \; with \; i \in [1,3]$	Representative length scales of the turbulent structures in the flow
	Reynolds stresses tensor values	$\overline{\overline{\boldsymbol{R}}} = \begin{pmatrix} R_{uu} & R_{vu} & R_{wu} \\ R_{uv} & R_{vv} & R_{wv} \\ R_{uw} & R_{vw} & R_{ww} \end{pmatrix}$ $with \; R_{ij} = R_{ji}$	Tensor containing multiple information on the flow turbulence such as: • Turbulence intensity • Anisotropy • Interaction between three directions
1b) Synthetic eddy method (SEM) - TI	Turbulent length scale	$L_i \; with \; i \in [1,3]$	Representative length scales of the turbulent structures in the flow
	Turbulence intensity profile or mean value	$I_{turb}(x,y,z) \;\; or \;\; I_{turb}$	Global description of the turbulence in the domain
	Anisotropy coefficients (if available)	$(\sigma_u, \sigma_v, \sigma_w)$	Precision quantifying the anisotropy of turbulence in the flow
2) Turbulent spectrum discretization	Turbulent power spectrum	$[S_u(f), S_v(f), \; S_w(f)]$	Turbulent power spectrum expression established for the turbulent model considered
	Turbulent length scales	$L_i \; with \; i \in [1,3]$	Representative length scales of the turbulent structures in the flow
	Turbulent intensity profiles **OR** standard deviations of velocity profiles	$I_{turb,u}, I_{turb,v}, I_{turb,w}$ **OR** $(\sigma^2(u), \sigma^2(v), \sigma^2(w))$	Description of the turbulent aspect of the flow in the three directions over the domain
	Coherency functions	$Coh_{i,j} \; with \; i,j \in \; [1,3]^2$	Description of the interaction with the turbulent domain depending based on the position
	Coherency decay numbers associated to the coherency functions	$c_{i,j}^{d} \;\; with \; i,j \in \; [1,3]^2$	Characteristic coherency decay value used in coherency functions

Table 2-3: Key measurements and subsequent analyses required in various applications by the sector

	Parameter	Requirements and key considerations	Parameter Usage by the Tidal Industry
Tidal Flow	**Velocity profile**	• Three coordinate components of mean flow. • Multiple neap spring cycles. • Extreme tides. • Vertical profile structure and temporal Variation. • Capture scale and frequency of horizontal eddy structures. • Boundary layer detail for drag coefficients.	• Available energy. • Flow variability. • Hub-height flow. • Input to CFD, tide-to-wire models, tank testing. • fatigue studies. • Validation of regional • models.
	Turbulence Power Spectrum	• High-frequency velocity data. • Low noise base. • Identification of quasi-stationary periods.	Input to CFD, tide-to-wire models.
	Turbulence Intensity	• If assume isotropy can use single sensor. • If anisotropic need all velocity components. • Capture gusts, bursts, etc.	Input to CFD, tide-to-wire models, tank-testing, fatigue studies.
	Turbulence Length Scales	• Spectra for each velocity component. • Sufficient frequency range to fit von Karman. • Low noise base	Input to CFD, tide-to-wire models.
	Reynold's Stress Tensor	• Minimum of 6 independent velocity measurements (7-beam instrument). • High-frequency data. • Low noise base.	Input to CFD, tide-to-wire models.
	Turbulence Anisotropy	• Recovered from spectra. • Recovered from Reynolds Stress Tensor.	Input to CFD, tide-to-wire models.
	Coherency	Synchronous velocity measurement at multiple locations.	Input to CFD, tide-to-wire models.
Waves	**Free Surface Elevation**	• Mean sea level datum. • Astronomical extremes. • Weather-driven extremes. • High-frequency data to capture waves. • Sensor sensitivity to resolve waves.	• Validation of regional models. • Event attribution. • Input to tank testing.
	• 2D Wave Spectra for TEC and instrument locations. • Wave Statistics elsewhere: Significant Wave Height, Peak Wave Period, Peak Wave Direction.	• Required for a range of storms. • Swell + wind wave conditions. • Required for system state (wave-current-turbulence) classification.	• Input to CFD, tide-to-wire models & fatigue studies. • Validation of regional models.
Meteorology	**Wind speed**	• Horizontal velocity components. • Measurement height 10m. • Data from multiple locations across site. • Measurements site must be unobstructed. • Accurate timestamping	Input to regional models Data post processing.
	Surface Pressure	• Multiple locations across site. • Capture weather system passage.	Input to regional models Data post-processing.
Machine (and External Devices)	Type A: Operational System State of Machine Power, Rotor Parked vs Rotor Moving, Turbine Pitch, Roll and Yaw (if relevant to device). Presence of on-station vessels, ROVS.	Required to be synchronous with environmental conditions and available to project partners to allow full use of environmental data.	• Essential for separation of ambient vs flow conditions that are due to the presence and/or operation of the TEC machine. • Required to ascertain sensor orientation of any TEC installed sensors.
	Type B: Electro-Mechanical System State of Machine Rotor: position, RPM, thrust, torque. Blade Pitch, Strain gauges, Vibrations.	Required to be synchronous with environmental conditions to allow fluid-structure interaction studies.	• Validation of BEMT, CFD and tank-testing engineering tools. • Structure loading. • Input to reliability / fatigue studies.

2.4.3 Measurement Campaign Specification

RealTide deliverable D2.1 outlines a proposed data collection campaign for the Fromveur Strait using a combination of bed-mounted, TEC-mounted and bespoke instruments to capture data to support the quantification of the identified target parameters and to improve flow classification, as shown below [1].

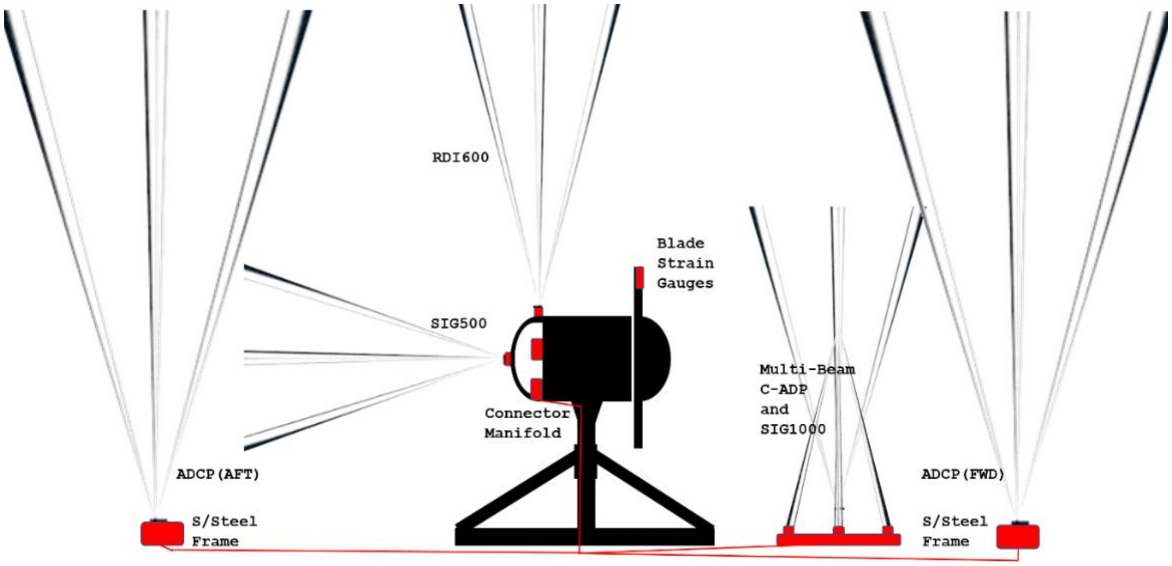

Figure 2-3. Measurement campaign specification (as per D2.1) showing targeted measurement regions and indicative locations and orientations of various instruments, primarily acoustic Doppler profilers.

2.4.4 Role of Modelling.

Tidal energy extraction sites are inherently high-flow regions where marine operations are severely restricted. This imposes limitations on instrument deployment and recovery operations, and increased costs due to the risks. For these reasons it is generally not possible to capture sufficient information on the spatial variability of the tidal flow across a site. Regional modelling complements the site measurements by allowing a more cost-effective and low-risk approach to site characterization. However, all model constructs require good quality site measurements to perform calibration and validation of the model. A well design model can be used to inform where best to make field measurements across a site, by identifying regions where the instruments are likely to perform best within their operating limits. The spatio-temporal data generated by a numerical model provide site classification metrics that cannot be easily derived from field measurements, and can be used to design different site measurement methodologies based on an improved understanding of a sites fluid dynamics.

2.4.5 Parameter Sensitivity.

Parameter values used in engineering design and site characterization are derived from *in situ* measurements and numerical predictions. The accuracy of an estimated parameter values may depend on a range of factors. The uncertainty of in parameter estimate may be more sensitive some of the dependent factors compared with others. Factors the affect *in situ* data are the level of quality assurance, stability of the deployed instrument, capture of sensor drift, quality control of the data extracted, and the accuracy of the algorithms used to extract parameters from the data. Factors affecting the prediction of parameters from hydrodynamic numerical simulations are design of model domain, mesh resolution, time step and level of convergence, 2-D versus 3-D, hydrostatic versus non-hydrostatic, number of harmonics used to force the open boundary, choice of friction model and turbulence closure schemes, numerical solver methodologies used, and the accuracy of the algorithms

used to estimate parameters. Some form of quantification of the sensitivity of the parameters to factors that can be controlled will help inform best practices for parameter estimation.

2.5 Summary of Recent, Related and Relevant Research

Table 2-4 summarises the results of an up-to-date literature review that was conducted following reporting of the specification work in Deliverable D2.1. It was conducted to help ensure that any successful online (hence re-configurable) measurement campaigns could be tailored based on the current state-of-the-art. Due to the unavailability of the D10 TEC it was not used for this purpose, but is included here for reference.

Table 2-4: Summary of related and relevant research since previous report

Title	Authors	Year	Area	Key Findings
Assessment of tidal current resources in Clarence Strait, Australia including turbine extraction effects	Marsh et al. [54]	2021	2D numerical modelling (COMPAS)	Model of Clarence Strait (Northern Australia), ADCP validation; arrays of 10m & 20m TECs; minimal farm influence on flow field.
Turbulent flow mapping in a high-flow tidal channel using mobile acoustic Doppler current profilers	Guerra et al. [55]	2021	Resource char. (ADCPs, fixed & floating)	Resource char. and TEC wake effects measured (Bay of Fundy, Canada); platform mounted TECs; vertically confined wake detected from operational turbines.
Tidal energy site characterisation in a large tidal channel in Banks Strait, Tasmania, Australia	Cossu et al. [56]	2021	Resource char. (ADCPs); wave-current	Full year campaign at Banks Strait (Tasmania); significant wave-current interaction; turbine design, installation and operation insights.
Wave-turbulence separation at a tidal energy site with empirical orthogonal function analysis	Togneri, Masters & Fairley [47]	2021	Numerical wave-turbulence decomposition (ADCP)	Empirical orthogonal analysis for detecting waves from ADPC data; good correlation with linear theory and buoy data for large waves.
Turbulence measurements: An assessment of Acoustic Doppler Current Profiler accuracy in rough environment	Mercier et al. [57]	2021	Virtual ADCP accuracy modelling (LES/LBM)	Accuracy assessments of ADCP configurations relating to Reynolds stress observation; ADCPs simulated to underestimate Reynolds stresses, especially within rough boundary layers
Modelling an energetic tidal strait: investigating implications of common numerical configuration choices	Mackie et al. [15]	2021	3D numerical modelling (Thetis)	Detailed bathymetric calibration of numerical model; impact of Manning coefficient greatest at spring flood; implications on model configuration discussed for developers.
Evaluation of wave-turbulence decomposition methods applied to experimental wave and grid-generated turbulence data	Perez et al. [46]	2020	Numerical wave-turb. decomposition (tank tests)	Linear wave and Synchrosqueezing Wave Transform (SWT) assessed for decomposing waves and turbulence; SWT demonstrated as suitable for common conditions at tidal sites.
Assessing the turbulent kinetic energy budget in an energetic tidal flow from measurements of coupled ADCPs: TKE budget in an energetic tidal flow	Thiébaut et al. [58]	2020	TKE production vs dissipation	Reynolds stress evaluations from ADCP field measurements (Alderney Race, France); local TKE dissipation exceed production during ebb and flow; non-local TKE of importance.
One year of measurements in Alderney Race: Preliminary results from database analysis: In situ measurements in Alderney Race	Furgerot et al. [45]	2020	Significant field campaign	Oceanographic and meteorological records, Alderney Race 2017-2018 (almost 1 year); up to 7m/s currents, 8m waves; impact on wave height and turbulence caused by wind and wave direction; storm observations.

Title	Authors	Year	Area	Key Findings
Underway velocity measurements in the Alderney Race: Towards a three-dimensional representation of tidal motions: Underway velocity measurements	Sentchev et al. [59]	2020	Tidal jet char-acterisation, use of towed ADCPs	Local dynamics of tidal jets studied (Alderney Race), including power law characterisation, with correlation to tidal conditions.
Characterization of the vertical evolution of the three-dimensional turbulence for fatigue design of tidal turbines: 3D turbulence for fatigue design of TEC	Thiébaut et al. [60]	2020	Impact of turbulence on fatigue in TECs	Streamwise TI, shear and normal stress, and vertical integral lengthscale impact on fatigue and power output; high streamwise TI at measurement site (Alderney Race).
Flow field impact assessment of a tidal farm in the Putuo-Hulu Channel	Zhang et al. [61]	2020	Large TEC farm simulation; ADCP validation	Flow field impact due to a large TEC farm using Delft3D and BEMT model; localised increases and reductions in tidal flow, potential for sedimentation where seabed shear stress reduces significantly
On the use of a single beam acoustic current profiler for multi-point velocity measurement in a wave and current basin	Jourdain de Thieulloy et al. [24]	2020	Tank tests of horizontal ADCP application	Single Beam ADP tested in horizontal application, with comparison against ADV, 0.6-1.2m/s range, improved correlation above 1m/s demonstrated; 2% bias recorded
Investigation of the error of mean representative current velocity based on the method of bins for tidal turbines using ADP data	Rathnayake et al. [62]	2020	TEC power uncertainty from ADCP measurements	Uncertainty of standard IEC method for Mean Representative Velocity (MVR), relating to TI, tilt, noise and beam misalignment; temporal-spatial method (TSM) proposed as alternative
Wake field study of tidal turbines under realistic flow conditions	Thiébot et al. [63]	2020	Numerical modelling: Telemac-3D, AD	Numerical modelling of TEC arrays (Telemac-3D plus Actuator Disk); 16% higher output when staggered, min 5D spacing, lateral spacing can be reduced for inline, however, turbulence propagates more rapidly
A comprehensive assessment of turbulence at a tidal-stream energy site influenced by wind-generated ocean waves	Thiébaut et al. [44]	2020	Turbulence characterisation	Spectral vs structural function method for estimating ε and integral lengthscale l; spectral method produced lower std. dev.; removal of wave and Doppler noise essential
On the variation of turbulence in a high-velocity tidal channel	Greenwood, Vogler & Venugopal [64]	2019	Resource characterisation	Turbulence characterisation; localised flow effects around headlands; ADCP make/model variation reported
Engineering analysis of turbulent flow measurements near Kuchinoshima Island	Imamura, Takagi & Nagaya [65]	2019	Resource characterisation	Spectral analysis of ADCP measurements for turbulence characterisation (Japan)
Merging velocity measurements and modeling to improve understanding of tidal stream resource in Alderney Race	Thiébaut, Sentchev, du Bois & Bailly [66]	2019	Resource characterisation	Optimal interpolation algorithm used evaluate velocity field evolution, calibrated against ADCP records and 2D model (MARS); largest discrepancy at ebb; method provides enhanced spatial detail

3 IMPLEMENTATION: IN-SITU CAMPAIGNS

No single sensor or modelling solution exists that can capture in a techno-economically viable manner the full extent of the varying underlying conditions. Instead, a pragmatic approach must be taken that focuses on the immediate and upcoming requirements of the tidal sector: those uncertainties that are presenting barriers to the roll out of or reliable operation of the technology. RealTide builds on components of previous R&D and academic projects and took a holistic approach to resource characterisation. The measurement campaign designs and their execution, and the modelling methodologies and subsequent analyses were conducted specifically to align with the development of engineering tools that could improve reliability of tidal energy. Existing guidance from IEC TS 62600-201 [49] was used to inform the measurement campaign. For further information on the specification of the campaigns see RealTide D2.1 [1]. In-situ campaigns were carried out in parallel to new hydrodynamic site modelling that was designed, built and executed from "the ground up" as described in detail in Section 5.

Implementation involved three category of activity:

- **TEC-Mounted Systems** (see Section 3.1)
- **Seabed-installed sensor systems** (see Section 3.2)
- **Advanced turbulence sensing** (see Section 3.3)

Figure 3-1 shows the final campaign design that was initially targeted. It features sensor systems retrofitted to the Sabella D10 turbine based on design work. No sensing could be designed to the front of the machine due to the lack of slip-rings in this machine. A rear-facing Nortek Signature 500 device was placed in the rear flooded bub of the D10 along with a surface-facing RDI Workhorse 600. The D10 was also used as a shore-wired instrument connection point to the seabed-mounted systems. **Error! Reference source not found.** summarises the completion status of the RealTide in-situ campaigns.

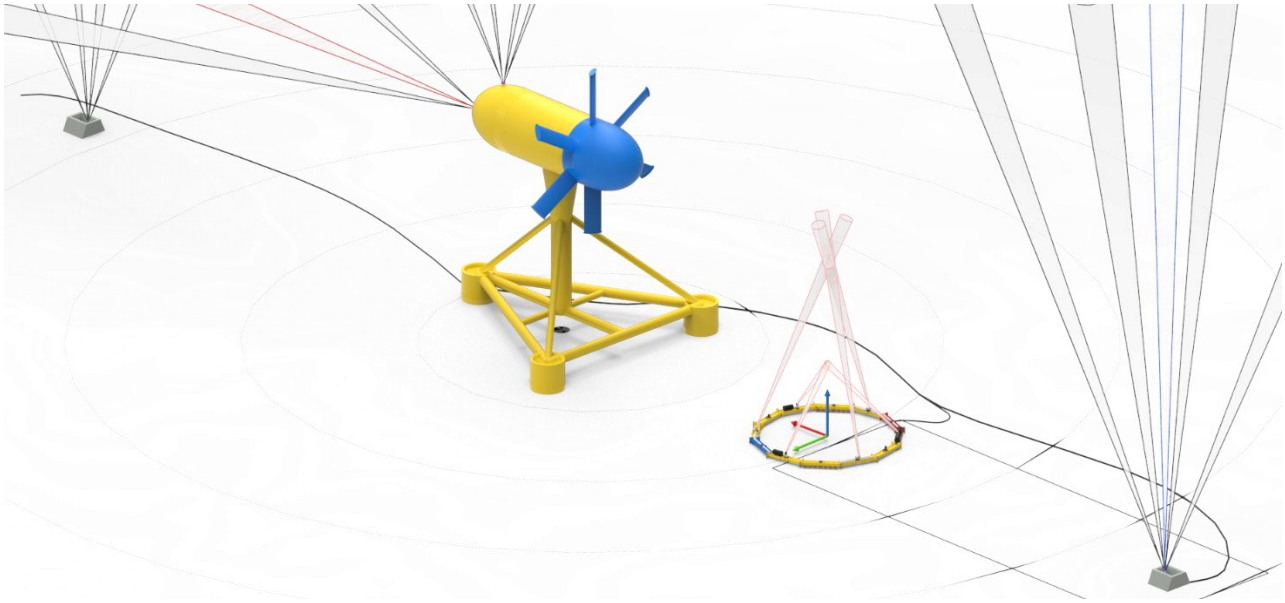

Figure 3-1: 3D Sketch of the *planned* RealTide Fromveur Strait deployment campaign specification showing (top-left) 5-Beam 600kHz ADCP, (centre) Sabella D10 with rear-mounted horizontally aligned 5-Beam 600kHz

ADCP and top-mounted vertically aligned 4-Beam 600kHz 4-Beam ADCP, (centre-right) the UEDIN advanced turbulence sensor package, and (right) 5-Beam 600kHz ADCP.

3.1 TEC-Mounted Systems

3.1.1 Design Work

Multiple sensor systems were designed and installed on the Sabella D10 TEC as a retro-fitting exercise. This required mechanical, electrical, communications and IT design work to be carried out in partnership with the turbine developer. Examples of the work conducted are shown in Figure 3-2 and Figure 3-3. Most systems and sub-systems were designed using Computer Aided Design (CAD). Electrical interfaces between the D10 TEC and the instrument systems were modified multiple times based on changing requirements or as technical issues encountered. This required high levels of coordination between project partners - which was much more efficient when face-to-face meetings were possible and site visits could be conducted with ease. Control apparatus was heavily modified to increase resilience and reduce risk as part of the second TEC deployment following operation learning and the ability for the turbine developer to make internal changes to their systems.

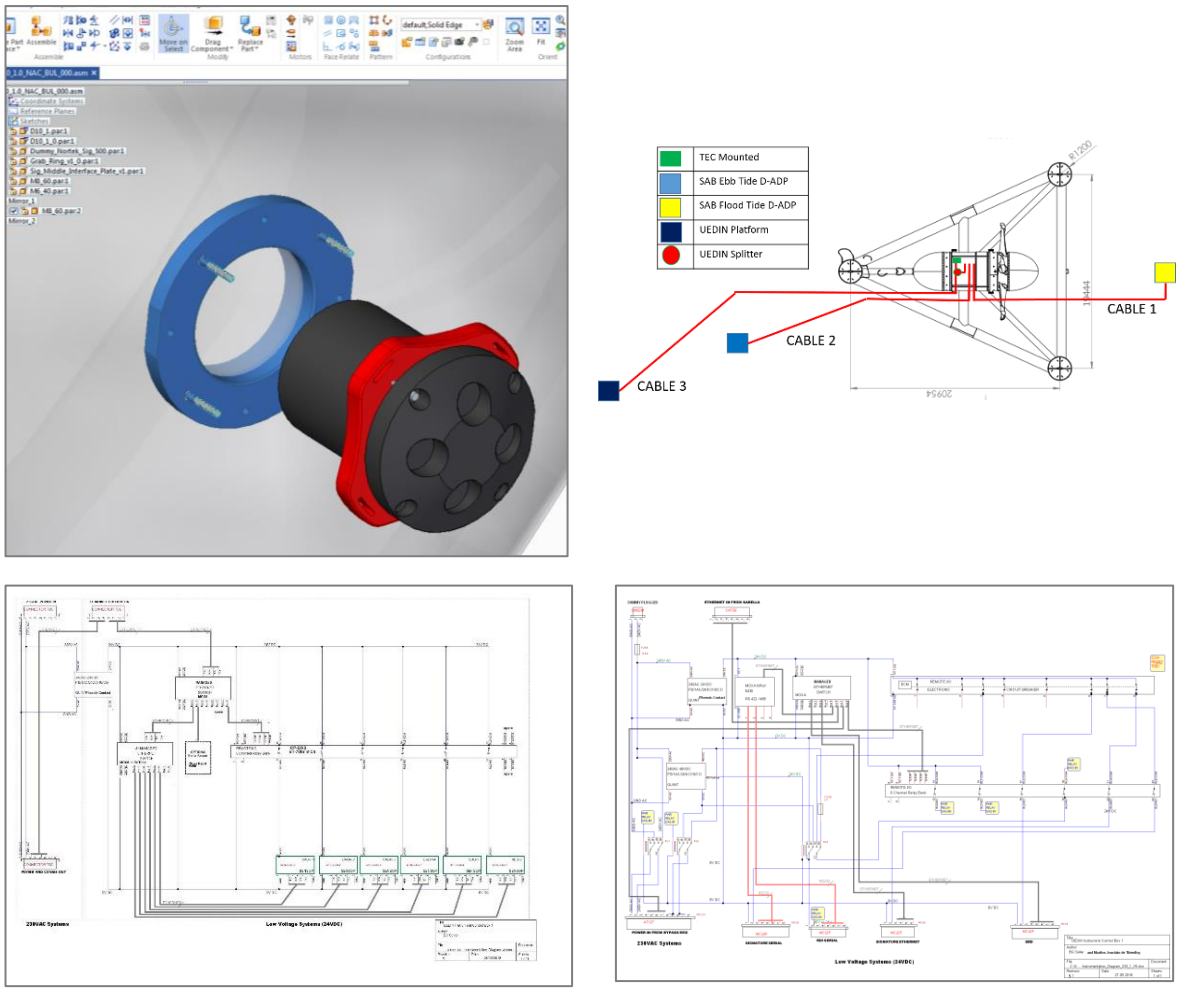

Figure 3-2: (top left) 3D CAD model of UEDIN rear-mounted hub-height ADP and Sabella D10 rear bulb assembly. (top right) one of many turbine-sensor concept layouts (bottom left) and (bottom right) examples of multiple electrical and communications interfaces developed to integrate sensor systems and the D10 turbine.

Figure 3-3: Iterative development of instrument control boxes (ICBs) from left to right featuring altered internal components (smaller with more redundancy) to affect increased resilience.

3.1.2 TEC-to-surface and wave measurement

An RDI Workhorse Sentinel 600kHz 4-Beam ADCP was interfaced with the D10 TEC to allow remote operation over the internet. It was installed atop the rear flooded bulb on a custom bracket and orientated so as to be facing vertically when deployed at sea, taking into account measured angular offsets of the machine on its tripod. Successful installation can be seen in Figure 3-4.

Figure 3-4: Sabella D10 turbine rear bulb showing RDI Workhorse Sentinel 600 installed in vertical orientation to capture above-turbine current flows and wave action.

3.1.3 Advanced Flow Sensing: Horizontally mounted ADP

A Nortek Signature 5-Beam ADCP was also interfaced with the D10 TEC to allow remote operation over the internet. It was installed as close as possible to the centreline of the turbine on the rear flooded bulb on a custom bracket and orientated so as to be facing horizontally when deployed at sea, taking into account measured angular offsets of the machine on its tripod. Successful installation can be seen in Figure 3-5

3.2 Seabed-Installed Systems

Seabed-installed systems comprised multiple ADCPs that were available to the project team integrated with new or modified gravity moorings. The turbine developer designed and implemented custom gimbal-less moorings, whereas UEDIN supplied existing 3000kg concrete-based large open-bay

mooring frames for use with modified gimbals to accommodate the 5-Beam Nortek Signature 1000 ADCP. This instrument was loaned to the project team by the MONITOR project as part of a data sharing agreement that enabled the device to be deployed and for UEDIN's Signature 500 to be made available for installation on the D10 machine. Figure 3-6 shows CAD sketches of the final implemented designs of the frame and gimbal system. The mooring featured modular and readily changeable stainless steel channel framing and acetal clamps for fitting multiple subsea cannisters containing batteries and smart (ethernet controlled) relays, fuses, power management and diagnostic sub-systems). Battery packs were connected in parallel via custom cable assemblies and a power and comms hub was implemented that would allow remote reallocation of control from stand-alone battery operation to online (via internet and a virtual machine) control via power and communications form the D10 turbine

Figure 3-5: Sabella D10 turbine rear bulb showing Nortek Signature 500 installed in horizontal orientation to capture behind-turbine (on ebb tide) and ambient-to-turbine inflows (on flood tide) at turbine hub-height.

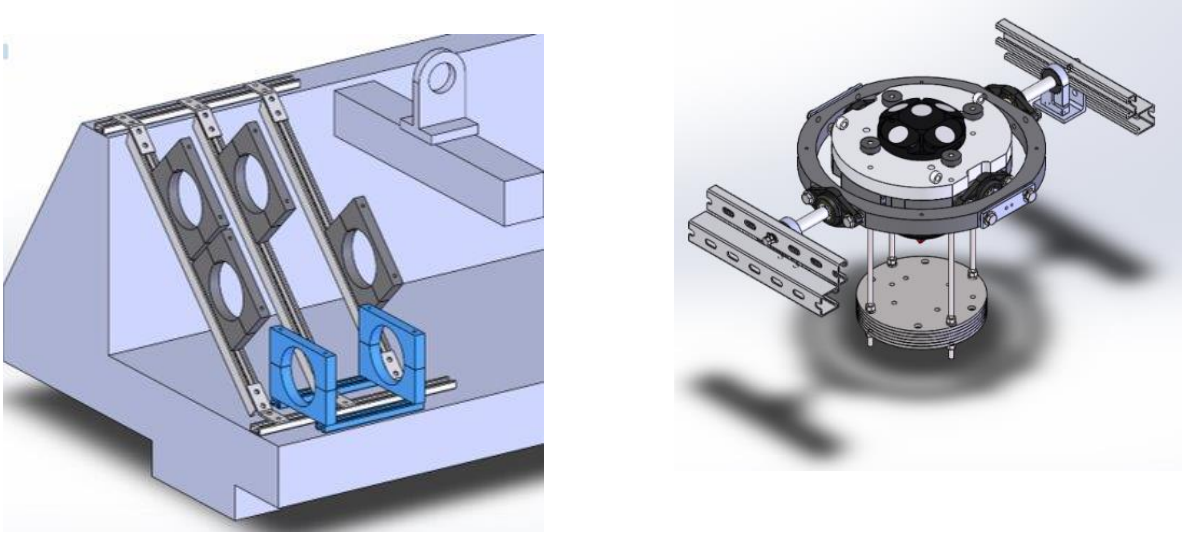

Figure 3-6. Seabed moorings and instrument attachment mechanisms. Design work: 3D CAD sketches (left) 3T concrete frame and flexible/modular component holder, (right) damped gimbal and rails system.

Figure 3-7 shows a collection of images related to the implementation of the RealTide Fromveur Strait measurement campaign. The top left image shows the completed frame (following assembly and testing at the quayside in Brest) aboard a heavy-lift vessel during deployment of the D10 TEC. It shows a coiled "extension-lead" ready for diver connection to a pre-installed 80 m main cable linking the D10 tripod to the target location of the ADCP. The instrument fixing was designed to be diver-removable: a feature that was successfully trialed upon instrument recovery. Top right and middle photographs

show the frame being during its deployment. The deployment exploited the considerable capacity and capability of the D10-deployment vessel. Visual confirmation of deployment location and stability was confirmed via ROV-operated cameras. The photograph at bottom left shows footage from the ROV as it detaches the main lowering hook from the gravity frame. The photograph at bottom right was taken by a diver team during preparations to connect the RealTide subsea instrument packages to the D10 turbine.

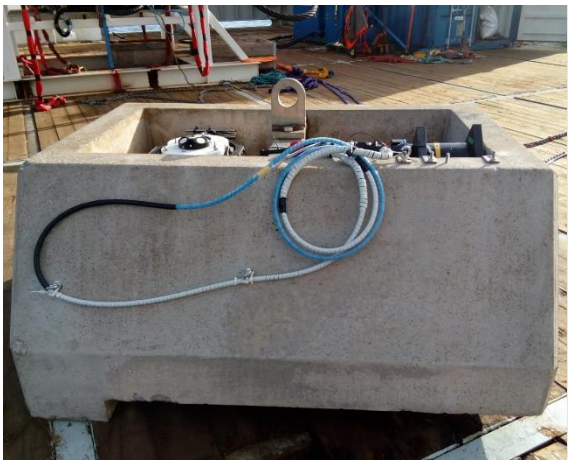

UEDIN concrete gravity mooring with diver connectable "extension-lead" to allow connection to Sabella D10 TEC

RealTide ADCP being deployed in Fromveur Strait September 2019 as part of D10 deployment.

RealTide ADCP being lowered to ~58m depth in Fromveur Strait September 2019.

RealTide seabed sensor being monitored by ROV and crane operators.

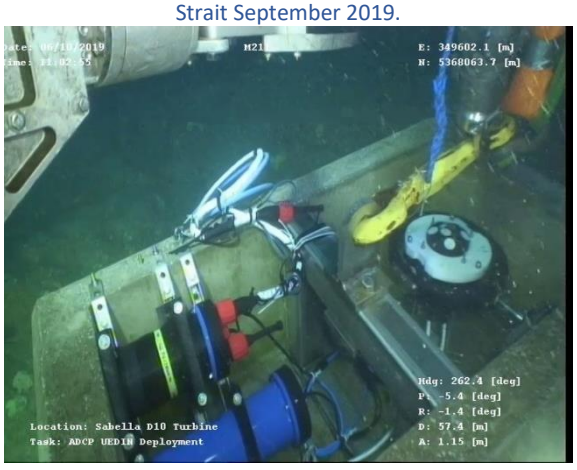

RealTide seabed sensor being left on seabed. The ROV is in the process of detatching the crane hook.

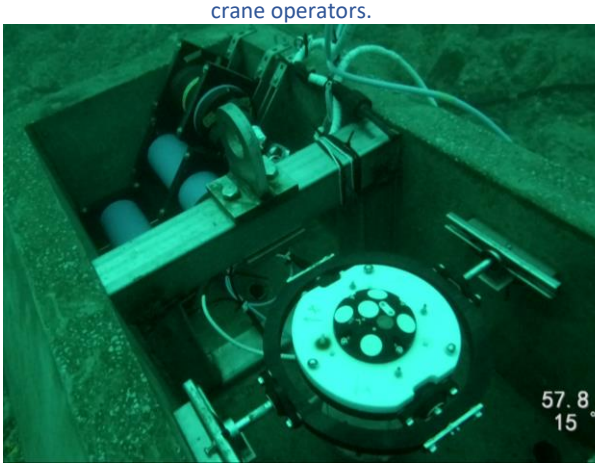

RealTide seabed sensor being inspected by divers during laying of the turbine-sensor connection cables.

Figure 3-7: Deployment of the Seabed-installed RealTide sensor packages.

3.3 Advanced Sensing – Convergent Acoustic Doppler Profilers (C-ADP)

The use of ADCPs is widespread for the characterisation of bulk flow velocities in rivers, the open ocean and tidal currents. These instruments are based on the measurement of water velocity in the direction of multiple acoustic beams (beam-wise) which are transmitted in multiple diverging directions from a single instrument. The processing of the velocity data from the beam directions to a three dimensional velocity estimate utilises the assumption that the flow velocity is identical between all of the beams at a given elevation in the water column. This is an effective assumption for the measurement of mean current velocities, however the processing has the effect of spatially averaging velocity fluctuations with length scales below the order of the beam separation.

By inverting the standard divergent-beam ADCP (or D-ADP) and arranging the acoustic beams to meet at "a point" i.e., a small volume, the corruption of measurements sampling non-homogeneous flow regimes at distant locations is greatly reduced. A convergent-beam (C-ADP) arrangement reduces uncertainty in instantaneous flow measurements and enables the measurement of velocity fluctuations with significantly smaller length scales. Such improvements are relevant to understanding flow regimes featuring high spatial variability, such as high-speed tidal channels and in areas of fluid-structure interaction [67, 23, 68].

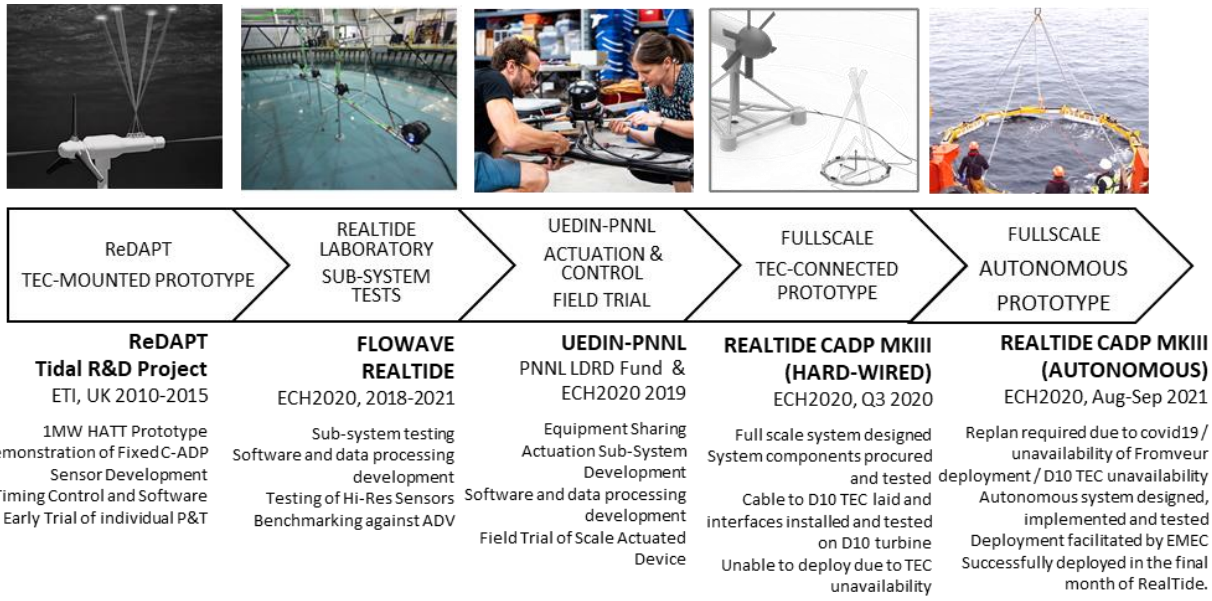

Figure 3-8: The timeline, phases and sub-system development of C-ADP systems for tidal energy applications from the first field-scale C-ADP demonstrated atop the DeepGEN IV tidal turbine to the deployment of a full-scale seabed-mounted and autonomous system featuring actuated re-orientable measurement location.

The goal of C-ADP development in the context of RealTide is to capture 3D flows in high-resolution at regions important to tidal energy e.g., rotor regions. These datasets would be of high value for the verification of standard off the shelf (OTS) systems, to help provide uncertainty bounds on OTS systems as they reach the limits of their performance capabilities in highly turbulent flows and to build 3D "maps" of inflow conditions which has value to the development of engineering tools to help improve reliability and lower cost to the sector. The route to these improvements would be through the development of better analyses using more reliable input conditions. RealTide followed an iterative and phased approach to the development of the C-ADP, testing sub-systems in the laboratory and developing and testing software algorithms for the design and operation of the systems.

The RealTide variant - C-ADP MkIII - has multiple key and ambitious enhanced capabilities over the first prototype deployed during ETI ReDAPT in 2014, namely:

1. Scale-optimized (large) to capture data from seabed to TEC hub-heights (e.g., 10m to 20m).
2. Using modular, single-beam (SBD) instruments with x 2 the spatial resolution and x 4 the temporal resolution to previously available (and heavily used units).
3. Capable of moving the sensor geometry through electro-mechanical actuation to target specific locations of interest in 3D space.

The opportunity to field-test the actuation sub-system arose in 2019 due to a collaboration between the University of Edinburgh and Pacific Northwest National Laboratory, (PNNL), USA.

3.3.1 Advanced Turbulence Sensor: Laboratory Testing

This work tested the performance of the modular single-beam SB-ADP sensors in a controlled laboratory environment under a range of available flow speeds. The sensor used offered 2 x spatial resolution and 4 x temporal resolution over the legacy units available at project commencement. The units are Nortek 1MHz 16Hz SB-ADPs based on the architecture of the Nortek Signature 1000 devices.

Single Beam (1D) Configuration: Measurements from a single-beam ADP under various flow conditions were evaluated against measurement from a traditional laboratory flow point instrument, a Nortek ADV. Results provides the uncertainty of the measurement associated with one unit, provided the conditions required to test the converging array of profilers and allowed the standard and custom API control software to be trialed / verified. This work as also highlighted the use of profiling instruments for tank testing applications [69, 24]. Results show good agreement with a high-precision laboratory benchmark instrument, an ADV, as shown in Figure 3-10 (right). Instrument-to-instrument comparison was studied along a 10 m profile. Results indicate a bias in velocity that varies between approximately 0% to 2% when comparing ADV results to those of the single-beam ADPs – which are of course designed for use in at sea and capable of readily capturing flows of 5 m/s.

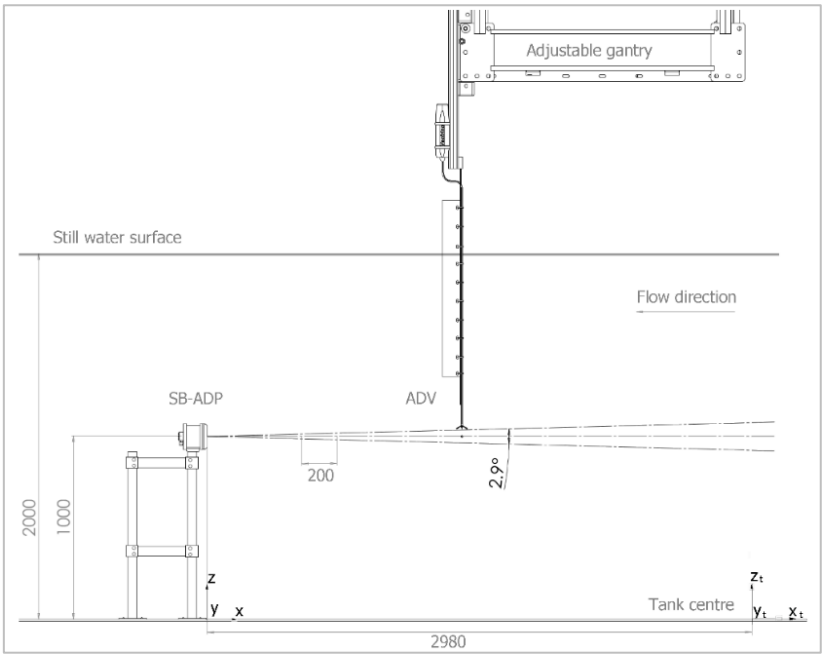

Figure 3-9: Component testing as part of phased C-ADP development. Technical drawing of laboratory setup during benchmarking of new high-resolution single-beam ADP against lab. standard instrument (ADV) [24].

Multi-Beam (3D) Configuration: Following on from individual instrument tests a multi-instrument statically orientated C-ADP was designed and operating in FloWave. Figure 3-11 and Figure 3-12 show one such setup which enabled an assessment of geometry on measurement error against a laboratory point measurement benchmark instrument (ADV). A converging array of 7 single-beam ADPs, whose acoustic beams were geometrically converging at a focal point was laboratory tested. This set-up allows for the derivation the 3D velocities from the measurements, and assess the impact of changing the system geometry on the measurement of the 3D velocities and associated turbulent parameters. Outside the focal point the impact of acoustic beam separation on the derivation of 3D velocities is studied, providing an estimation of the incertitude associated with traditional measurements. This work is currently being submitted as part of a PhD thesis and will be of value to the design of any future variant C-ADP systems and the processing of acquired measurements.

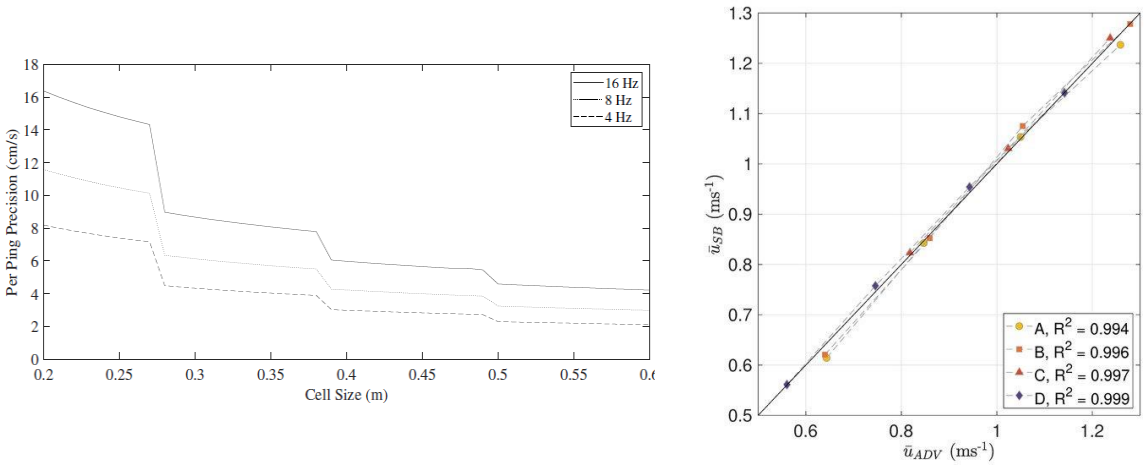

Figure 3-10: (left) Results of systematically probing instrument software settings and their affects: here showing effect of changing cell sizes in software on the resulting per-ping precision estimates. (right) Results from detailed tank-testing: direct inter-comparison of mean velocities measured by SB-ADP and reference instrument (ADV) at the target locations A, B, C, and D. The straight line depicts a 1:1 relationship between the SB-ADP and ADV velocity measurement values [24]

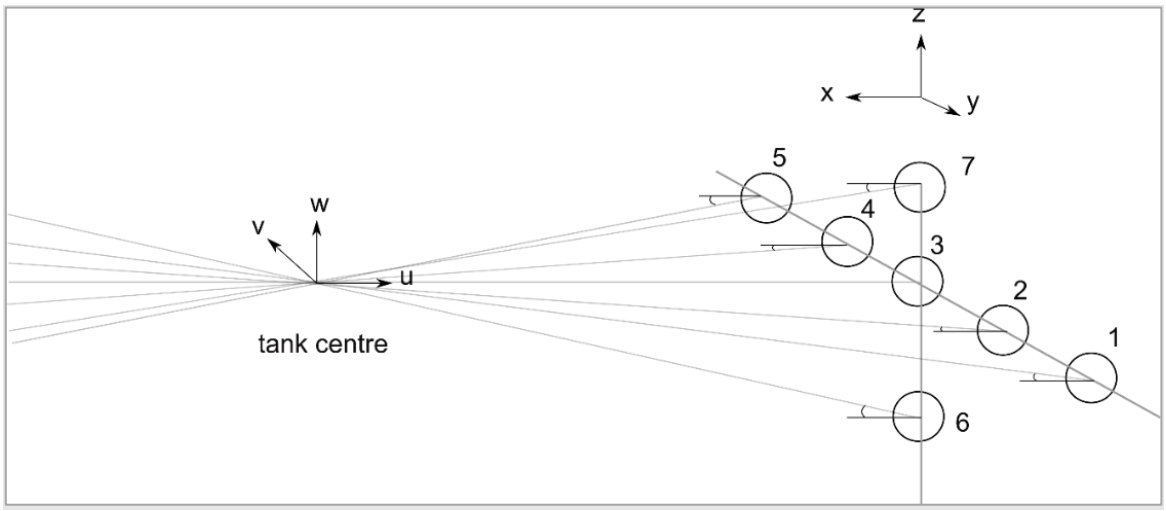

Figure 3-11: Sub-system testing in a controlled environment as part of phased C-ADP development: schematic of C-ADP coordinate system and geometry as deployed and tested in FloWave, University of Edinburgh.

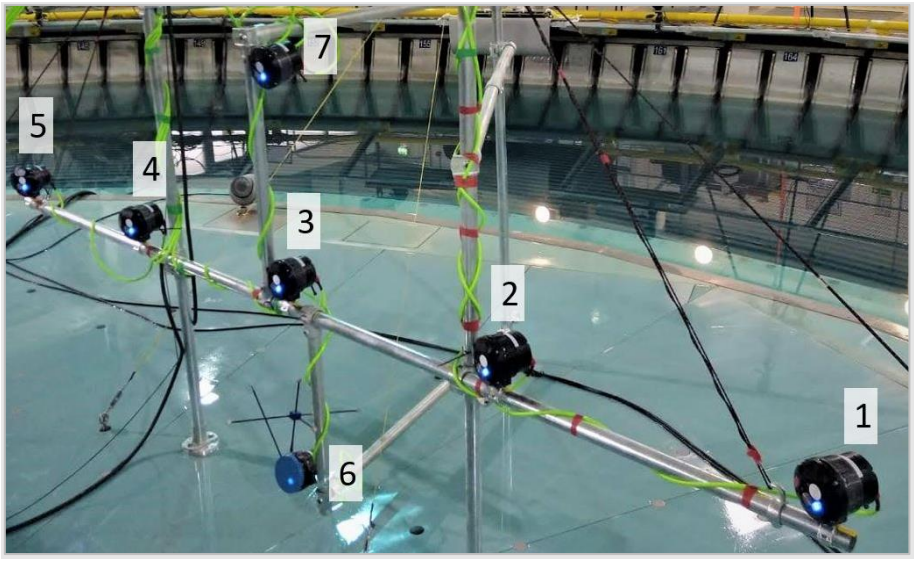

Figure 3-12: Sub-system testing in a controlled environment as part of phased C-ADP development: Photograph of the implemented prototype C-ADP in FloWave, University of Edinburgh [25].

3.3.2 Field Trial of the First Actuated C-ADP

A collaboration between the Pacific National Northwest Laboratory, PNNL, USA and the University of Edinburgh enabled the development and testing of a scaled version of the envisaged RealTide full-scale device, labelled the C-ADP MkII. The ready-to-deploy C-ADP is shown in Figure 3-13 having been assembled in the workshops of PNNL. Four SBDs can be seen in the corners of the 4.9m wide frame with a fifth SBD positioned centrally. A subsea control box that supplies power and communications to the instruments is also installed. Cables are run down to the system from the pier which has mains electricity and Wi-Fi connections.

Figure 3-14 shows the coordinate system for the actuated C-ADP MkII and the installation concept at the pier of the Marine and Coastal Research Laboratory, Sequim, WA, USA [22]. Summary details of the test setup are shown in Table 3-1 which is taken from [23], where further information on the successful demonstration of an actuated C-ADP velocimeter can be found.

Table 3-1: Summary configuration information on the Actuated C-ADP MkII [23]

	Beam 1	Beam 2	Beam 3	Beam 4
Actuator mounting points (x,y) (m)	(2.24, 0.89)	(2.24, -0.89)	(-2.24, -0.89)	(-2.24, 0.89)
Focal Point Locations (m)	$-1.5 \leq x \leq 1.5$; $-0.75 \leq y \leq 1.5$; $z = 3.21$			
Yaw angle (°)	$90 \leq \phi_1 \leq 270$	$90 \leq \phi_2 \leq 180$	$0 \leq \phi_3 \leq 90$	$-90 \leq \phi_4 \leq 90$
Pitch angle (°)	$30 \leq \theta \leq 90$			
Transmit Offset (Δt) (ms)	0	24	48	72

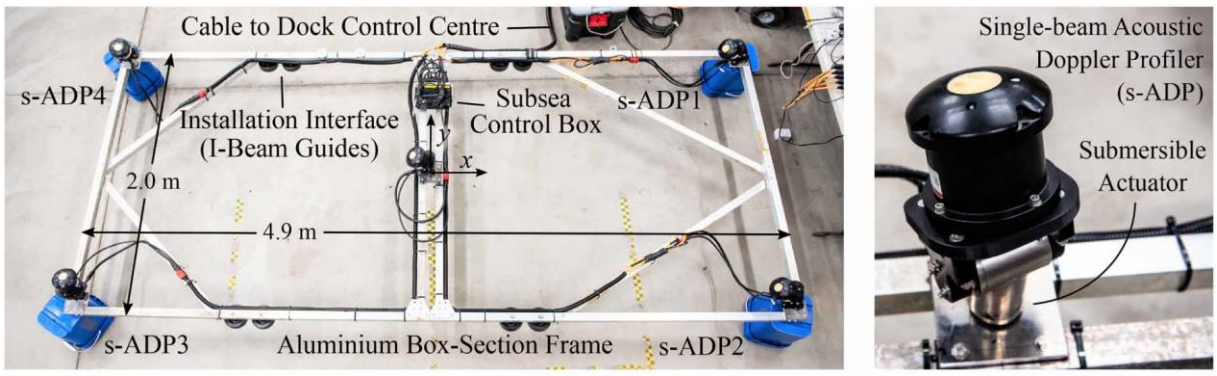

Figure 3-13. Photographs of the C-ADP MkII following assembly and testing at PNNL, USA.

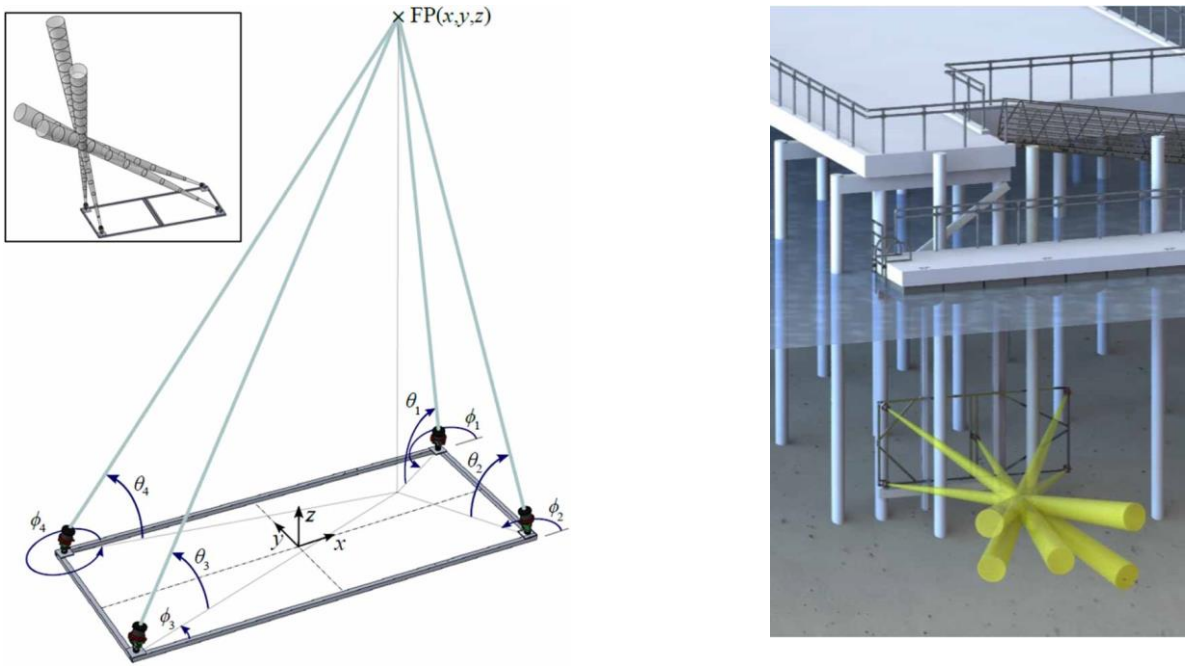

Figure 3-14: The actuated C-ADP MkII showing (left) the geometry and coordinate system essential to the control software and data-processing algorithms and (right) the final installation concept on the pier of the Sequim, WA test site [22].

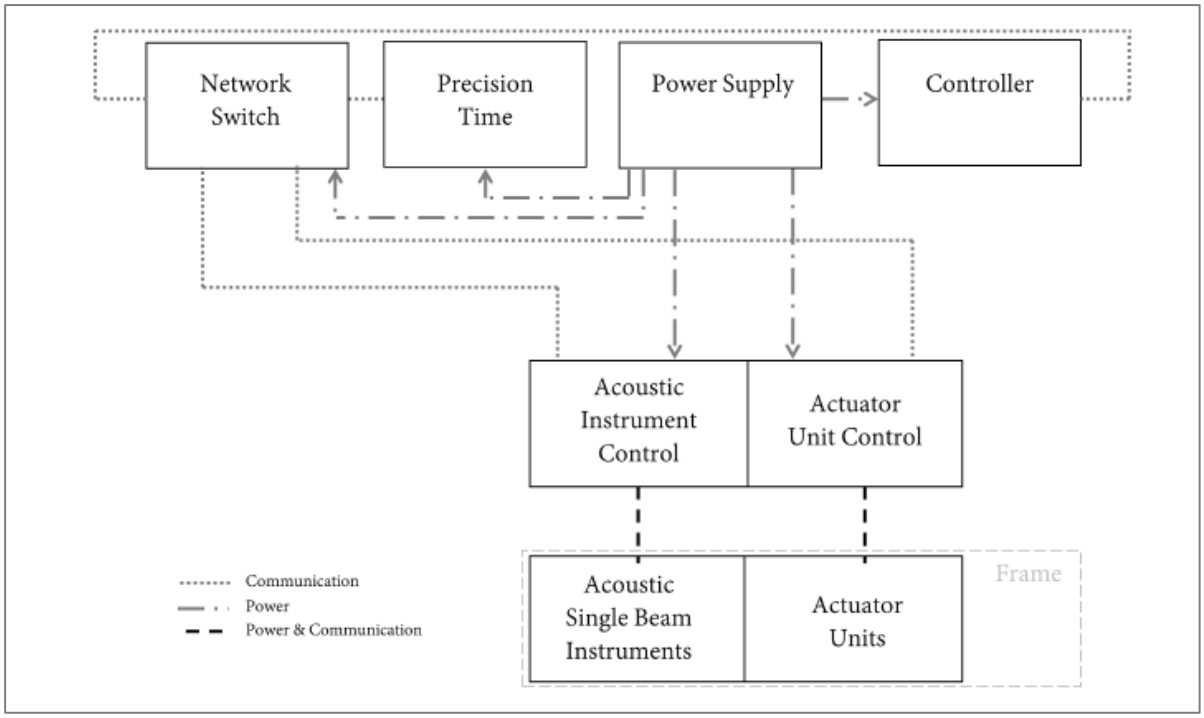

Figure 3-15: Schematic of C-ADP II subsystems and their integration to obtain remote and high resolution velocity measurement at multiple locations within a flow volume at field scale.

Figure 3-15 shows the final system diagram for the successfully demonstrated C-ADP MkII. Software was implemented with MATLAB and python code. The left-hand figure of Figure 3-16 shows a system verification checks being undertaken. Here, torches installed to the subsea sensors are being used to verify 3D coordinate transforms and the control software: the lights allow directionality and locations to be targeted (Note: in the image additional overlayed lines have been shown to help visualise the verification process).

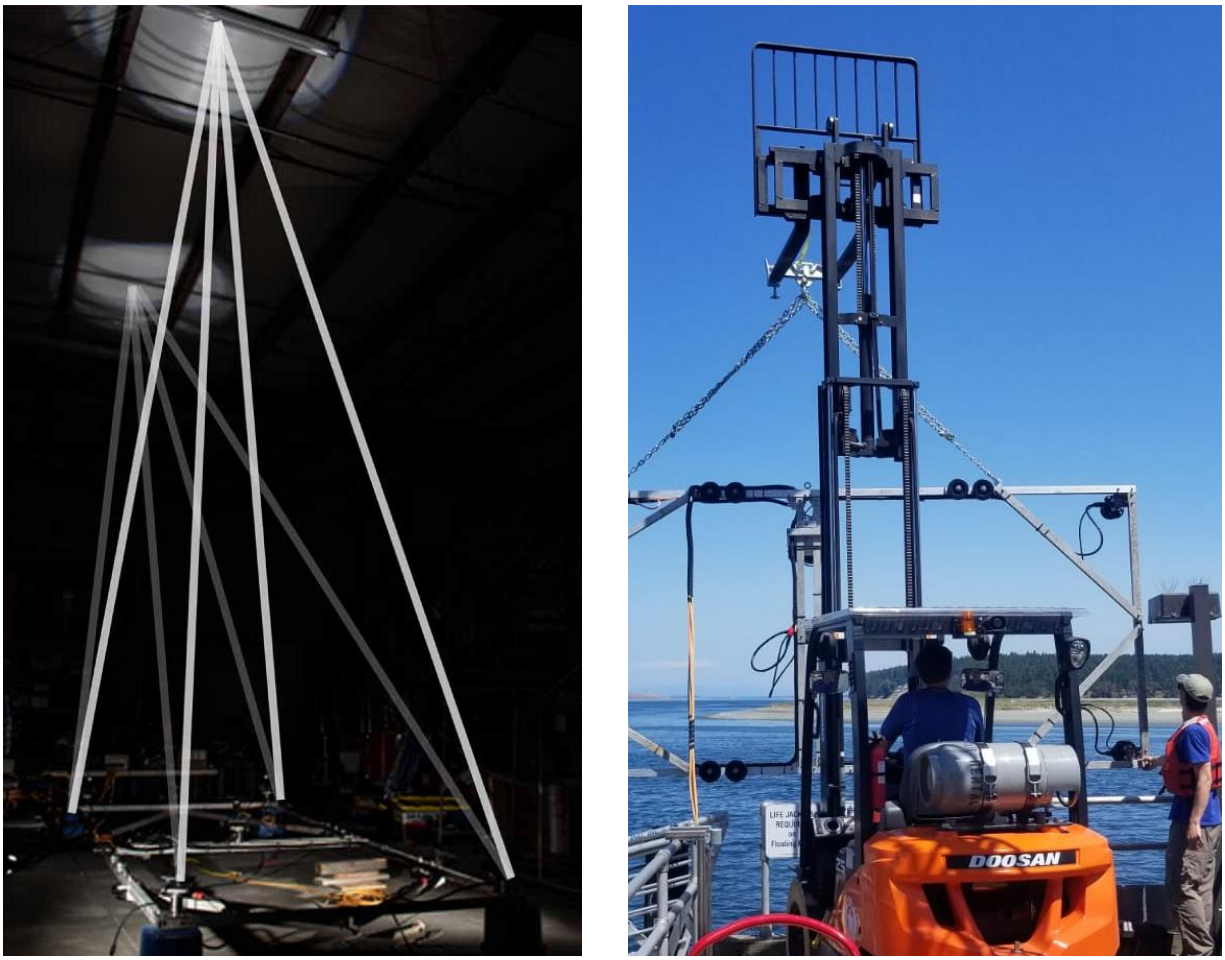

Figure 3-16: Implementation: laboratory testing at PNNL, USA showing system verification tests underway. Torches have been affixed aligned to the S-BD profilers and the system is undergoing actuation tests to verify coordinate transforms (Note: the white lines are overlayed for clarity) (left) and (right) field installation via forklift off the pier at the Marine and Coastal Research Laboratory, PNNL, Sequim, WA, USA.

Results of the field trial are reported in [23]. Key outputs are shown in Figure 3-17, where the top left inset image shows agreement between a proximal marine-variant ADV and the C-ADP system. The main plot shows time-series plots of the CADP output at the “focal point” (FP) for nine separate measurement locations – which have been achieved through the system re-orientating to these target positions.

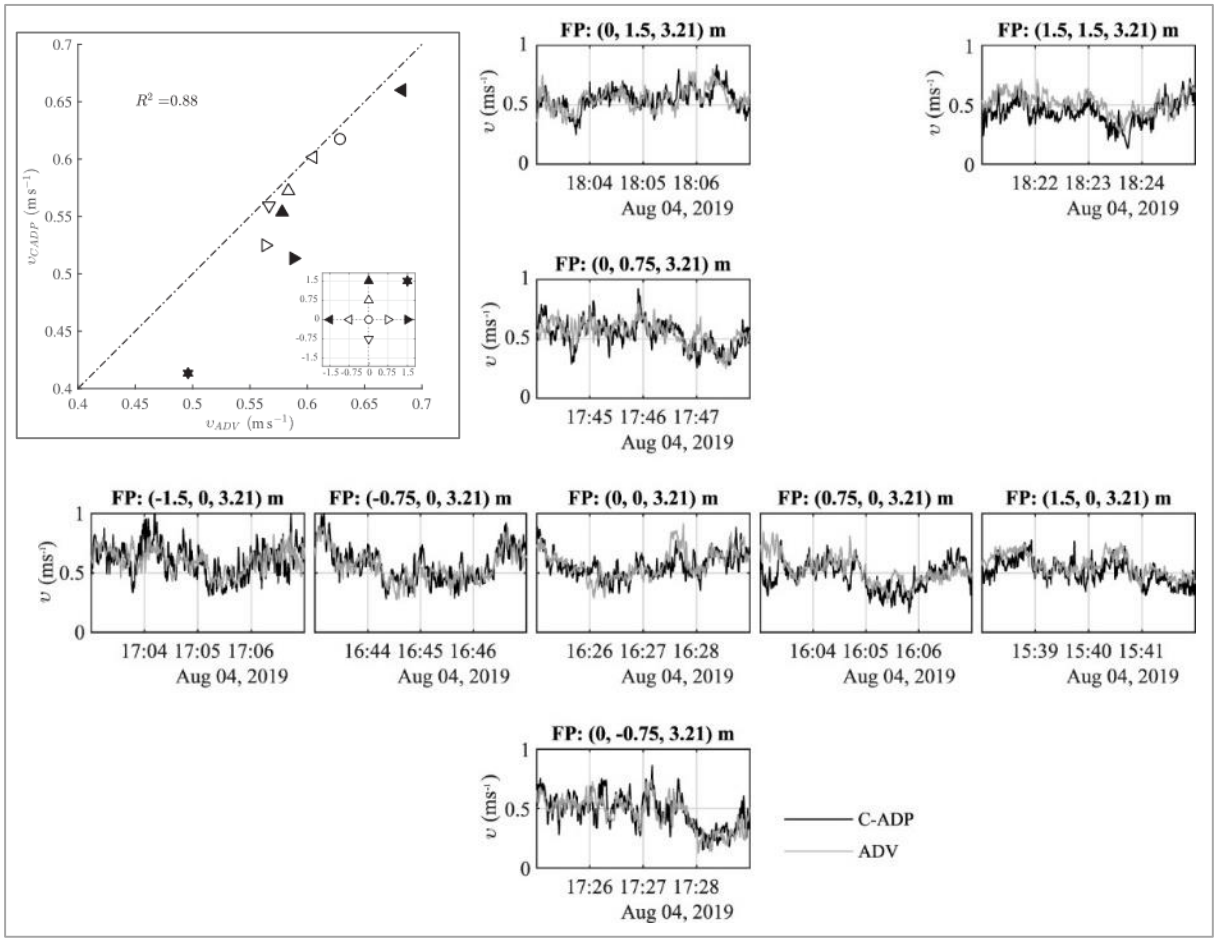

Figure 3-17: Off-axis actuated C-ADP results from field testing at Sequim, WA, USA 2019 [23]. Subplots are arranged to geometrically match the sensor targets from the perspective of the sensor frame looking into the page. The plots summarise data from the C-ADP and a proximal ADV. (top-left inset) Comparison of ADV and C-ADP mean velocity magnitude. Inset: Location of each of the nine focal points [23].

3.3.3 Summary of Phased Development of C-ADP Systems and Sub-Systems

Extensive design work incorporating mechanical engineering and low-power direct-current (DC) electrical systems was carried out in the development of C-ADP sub-systems. Work on communication systems and timing protocols was also required. Subsequent implementation and testing of the collated sub-systems was conducted during RealTide to develop a full-scale system that could be deployed in front of an operating tidal turbine. Whilst the envisaged setup was ultimately not realised – due to turbine unavailability – the sub-systems and assembled C-ADP variants proved successful. Some key points on progress are summarised below:

- Tests conducted at FloWave assessed the performance of the RealTide single-beam ADPs, and allowed extensive testing of the devices' software and company-supplied API. This was required in order to develop software to interface with the devices and to understand the effects of commands on measurement performance and system stability/instability.
- Test conducted at FloWave reveal that there may be scope for improved tank-testing through lab-focused variants which is the subject of ongoing work.
- The FloWave laboratory tests together with field work at Sequim, WA, USA provided valuable input to the design of the full scale actuated and autonomous C-ADP MKIII.
- Software was successfully produced to allow configuration of an C-ADP of arbitrary geometry – essential for the RealTide actuated (move-able) concept, and subsequent data processing.

3.4 Advanced Turbulence Sensor: Full-scale Prototype - C-ADP MKIII

The C-ADP MkIII was conceived to enable the collection of 3D measurements of velocity from regions of interest to tidal energy developers e.g., across the rotor plane in in near-field of the turbine, where flow is extremely heterogeneous and where the use of standard instrumentation is either infeasible or would lead to large uncertainty in derived descriptions of the flow. It was developed in a phased manner as outlined in previous sections. It is an objective of the sensor package (which is a multi-sensor system featuring both standard and novel C-ADP devices) to generate data that can allow the uncertainty quantification of existing techniques as tidal conditions vary so as to be able to use existing technology in better ways or with better knowledge of any limitations.

3.4.1 System Design and Key Features

Multiple variants of geometries, layouts and fabrication methods were assessed. The final RealTide design was formed from opportunities and constraints that included:

- Envisaged vessel availability
- The availability of divers
- The availability of a hard-wired power cable and to-shore / to-cloud data connection
- Close proximity to an operating TEC of hub-height 12 metres
- Operating depths of up to 80 metres

3.4.2 External Impacts

Covid19: Throughout 2020 and 2021 the covid19 pandemic had a severely negative impact on access to equipment, materials, consumables, staff, suppliers and facilities including offices, construction yards and laboratories. Wherever possible delays and issues were mitigated.

Brexit: The uncertainty due to Brexit, the late nature of information of the terms of exit and the timing of Brexit during complex UK-France marine operations increased project delivery risk, which had to be mitigated. Examples of problems caused included the need to re-consolidate scientific instruments and tools that had been previously openly shared between project partners and re-planning required around delays to shipping of equipment, consumables and sensors.

3.4.3 Design Change: From a Hard-Wired to Autonomous System

As it became evident that due to technical and logistical issues it would likely not be possible to deploy the RealTide MkIII prototype in a connected-to-TEC configuration, mitigative work commenced on developing an autonomous control system that would enable operation on the seabed without any access to originally planned human interventions. This required a considerable amount of unforeseen engineering and system development, particularly around power supply, data backups, subsea timing protocols and decision-making software.

3.4.4 Final Design Concept

Multiple system topologies were reviewed based on lessons-learned from previous developments, arising opportunities and in discussion with the turbine developer, vessel operators and the local dive-team.

The final design concept captured the following features/requirements:

- A 12-sided dodecagon form to enable multiple sub-C-ADP systems arranged in 120 degree increments i.e.,
    - a set of fixed SBDs in triple arrangement
    - set of moveable SBDs in triple arrangement.
- A frame size that could be deployed by a relatively small vessel, not relying on the availability of any turbine-deploying heavy-lift vessel.
- A frame size that would allow good measurement using convergent beams at rotor heights
- Sufficient "floor-plan" for large number of battery cannisters, OTS benchmarking instruments including an 5-Beam ADCP and multiple instrument control boxes.
- Cable routing path to allow the majority of cables to be semi-protected from the flow-field
- A four point lifting system.
- A frame that could be readily adapted on site should any changes be required.
- A frame that could maintain station, preferably in a surface-facing pose once deployed, hence the inclusion of flexible.

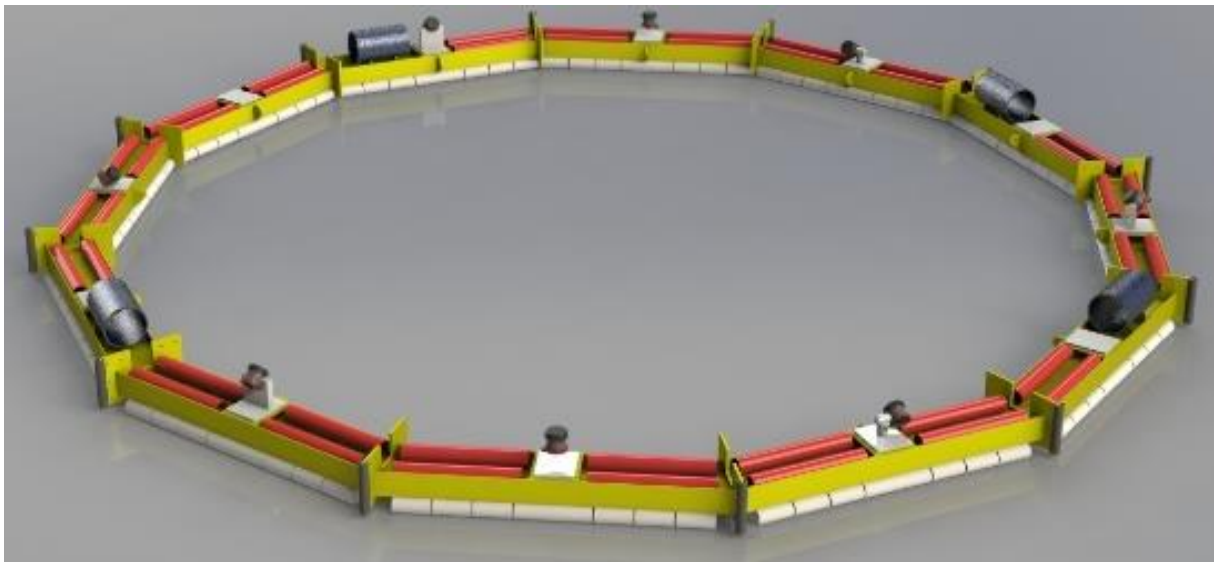

Figure 3-18. Final Design Concept based off of the selected steel frame section and prior to detailed engineering design for all components.

Figure 3-18 shows a 3D CAD render of the CADP MkIII design at the stage of having selected the dodecagon arrangement/variant using steel frame elements and prior to detailed engineering design across all components and sub-systems. An original frame size of 15 m was reduced to 9 m to align with available vessels at the intended deployment site. The frame is a bolted assembly for ease of shipping to/from deployment sites. Figure 3-19 shows the near-"as-built" configuration with labelled elements described in Table 3-2. Figure 3-20 shows various stages of the structural design and fabrication of the CADP MkIII steel frame sections.

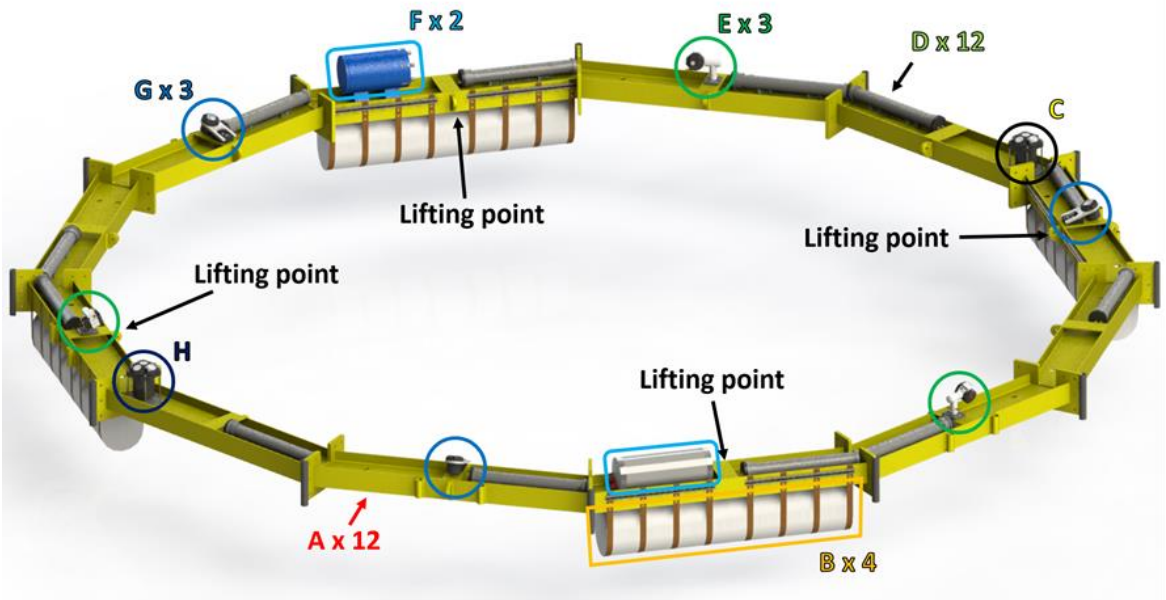

Figure 3-19: Schematic showing close to "as-built" C-ADPMKIII system. See Table 3-2 for further information.

Table 3-2: Expanded description of the C-ADPMKIII system (refer to labels in Figure 3-19)

Label	Description
A	**Steel section** – The C-ADP3 sensor's dodecagon frame is formed by 12 similar steel sections of mass 160 kg. Instruments, integrated frame ballast bags, batteries and controller enclosures are mounted onto the various frame sections. Each frame section has a lifting pad eye rated to 6.5 T on the internal face of the frame section. 3 of the frame sections have lifting pad eyes rated to 6.5 T on their outer faces.
B	**Integrated frame ballast bag** – 4 integrated frame ballast bags are located around the C-ADP3 sensor. These provide additional mass to the sensor and due to their compliant nature will shape to the seabed providing additional stability. They will be filled by locally acquired aggregate to aid logistics.
C	**500 kHz ADCP** Nortek Signature operating off of pre-programmed schedule.
D	**UEDIN Battery tube** – 12 battery tubes are located around the C-ADP3 sensor to supply power to its systems. 9 of the battery tubes have integrated IMUs to record deployed sensor status.
E	**Actuated Single Beam ADCP** – 3 actuated Single Beam ADCPs are located around the C-ADP3 sensor. These instruments will move to facilitate adjustment of a volume of measurement focal point.
F	**Instrument Control Box** – 2 instrument control boxes are located on the C-ADP3 sensor to control its operation.
G	**Fixed Single Beam ADCP** – 3 fixed Single Beam ADCPs are located around the C-ADP3 sensor. These instruments are set-up to focus at a volume of measurement focal point, 10 - 12 m above the centre of the frame.
H	Acoustic modem for confirmation of frame landed status and other diagnostic signals

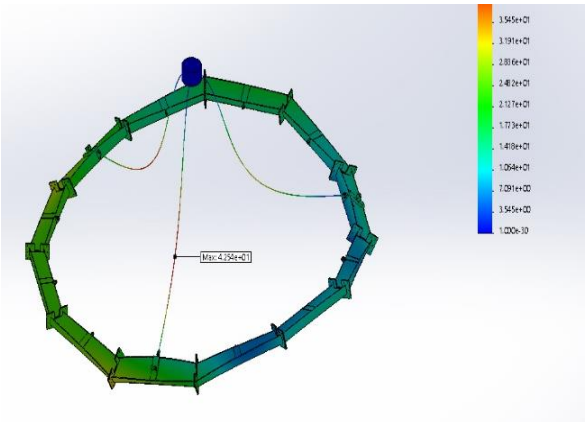

Sketch showing the results of finite element analysis simulations used as part of the structural design work.

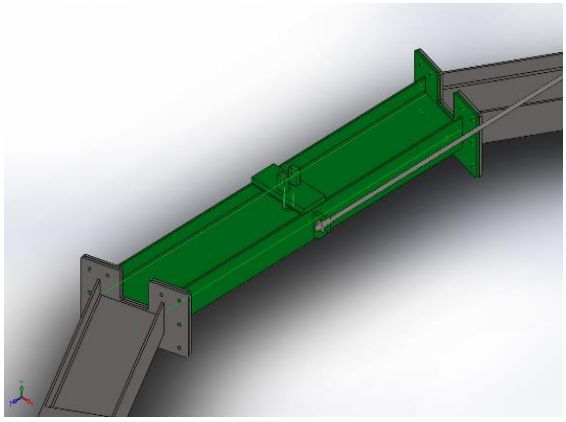

3D image showing the designed steel sections in a 3D CAD assembly as part of the structural design work

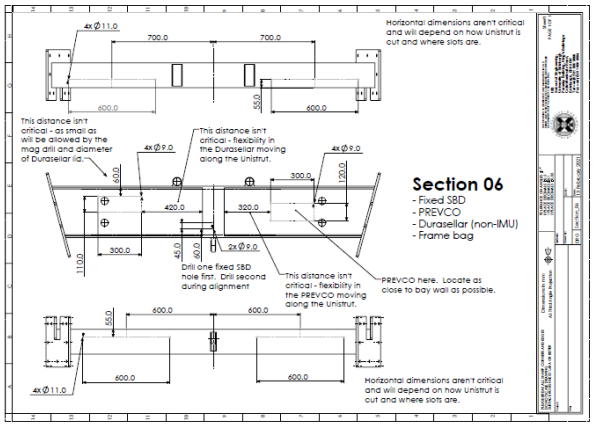

Detailed technical drawings produced from the full system model for drilling of attachment points

Frame sections post-fabrication awaiting cleaning and coating

Frame sections awaiting final top-coat of marine paint

Frame sections being fabricated: end flange plates being cut-out of sheet steel.

Figure 3-20. Structural design works including finite element analysis, CAD model creation and frame section fabrication and painting.

3.4.5 Battery Packs: modular, smart and reduced-cost

Pressure vessels are a critical and often an expensive part of the field deployment of sensors. Whilst the project team had access to existing supplies of various sizes the loss of access to the D10 TEC and related seabed-installed power cables increased dramatically the requirement for stand-alone battery power provision. Therefore, a new design of battery cannister was developed (see Figure 3-21) as a mitigation. The battery cannisters were coupled to a hybrid cable assembly that provided multi-channel redundancy with some cannisters connected in parallel. These hybrid cables (multiple connectors "T-ed" off of one main connector helped to reduce costs and reduced the number of required penetrators in pressure vessel end-caps. **Smart end caps:** A system requirement for the autonomous C-ADP is knowledge of frame pose. Therefore a network of low-cost 6 degree of freedom (6DOF) Inertial Measurement Units (IMUs) was designed into the end-cap of the pressure vessels. These end caps were manufactured by the workshop of the School of Engineering and FloWave staff, University of Edinburgh. An RS485 bus was integrated to the multi-channel power cables. Power was run at 48V DC nominal. Battery packs were custom made and of modular design of Alkaline chemistry.

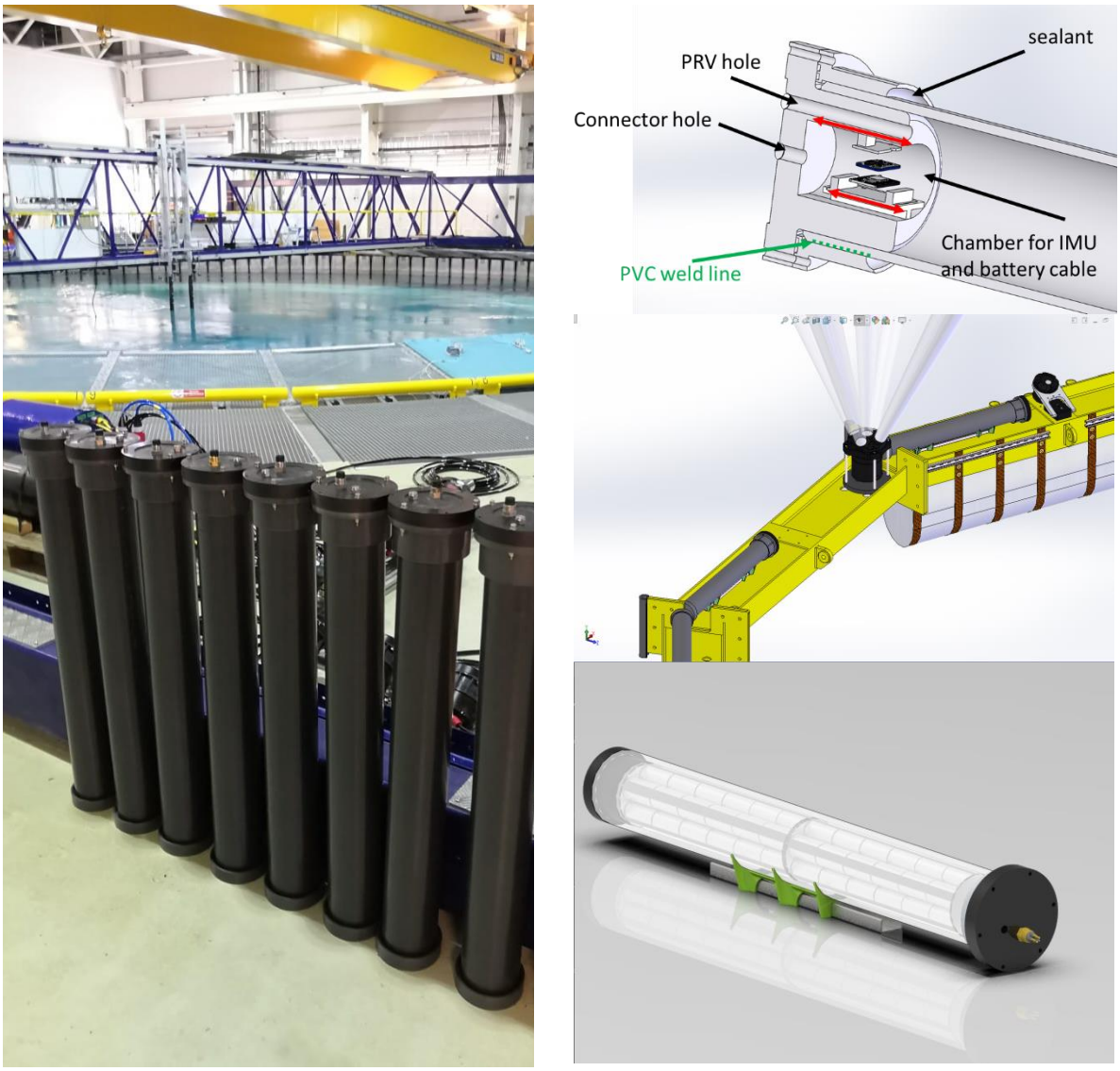

Figure 3-21: RealTide PVCu/acetal battery cannisters. (left) eight battery cannisters in final assembly phase at FloWave, (top) 3D CAD sketch of smart-cap with IMU, microcontroller and communications bus, (middle) The as-deployed configuration of battery packs and (bottom) a 3D render of the final design assembly.

3.4.6 Frame Assembly: Fit Test and Alignment Verification and Lift Testing

The C-ADP MkIII frame required assembly test-fitting to check alignment and to develop an assembly user manual to mitigate the possibility that UEDIN staff would not be permitted to travel to the final assembly and deployment location due to covid19 restrictions which were subject to change.

Frame assembly checks showed that the frame was straightforward to assemble using hand tools and a single pallet truck and "closed-up" reliably upon tightening into the desired shape. Assembly and disassembly of the main frame took up to 2 hours per trial run. A later test-fit of all instruments, cables and instrument control boxes and additional ballast bags was conducted prior to shipping to the deployment site. This was to ensure that as much time as possible was available for commissioning and system checks as opposed to equipment assembly.

Figure 3-22.Frame assembly tests at FloWave (left). Test fitting additional compliant ballast bags (right).

Figure 3-23. Lift testing of the C-ADP frame via the designed four-point lifting method, prior to dismantling and shipping to EMEC for re-assembly and instrument fit-out.

3.4.7 Bench Testing of Components and Sub-Systems

Bench testing was conducted at component and sub-system level. Tested systems included:

1. Battery cannisters and caps for correct microcontroller, communications and IMU operation.
2. Pan and Tilt electro-mechanical actuators via a dedicated test rig.
3. Single-beam acoustic Doppler Profilers (SB-ADPs) on the bench and deployed in FloWave.
4. Onboard low-power computers.
5. Onboard PTP Timing Protocol implementation.
6. Power bus and power management system.
7. Computer controlled relay units.
8. Smart fuse system.
9. Actuated C-ADP positioning control software via dedicated test rig featuring SB-ADP pose tracking
10. Data management checks to confirm correct backing-up of acquired data between redundant systems located in separate subsea enclosures.

3.4.8 Pre-Deployment Assembly, Commissioning and Testing

Deployment of the C-ADP MkIII was arranged by the European Marine Energy Centre (EMEC) who also provided a secure quayside working area and facilitated the necessary logistics and administrative tasks. The frame was shipped to Hatston Quay, Kirkwall, Orkney in August where it was assembled by UEDIN and EMEC staff before UEDIN staff conducted commissioning works and final system tests. The fully commissioned system and final systems checks being conducted can be seen in
Key stages of work included:

1. Mechanical Assembly.
2. Additional mooring bag attachment and filling with local aggregate.
3. Instrument attachment.
4. Battery packs attachment.
5. Extensive cable runs and connections and securing.
6. System power up.
7. Instrument configuration.
8. Software pre-deployment checks.
9. Test run in accelerated and in real-time deployment mode and confirm proper operation.
10. Deploy the system and confirm operation via LED indicator lights on selected instruments.

Figure 3-24. RealTide C-ADP MkIII fully assembled (left) and undergoing final system checks (right) at Hatston Quay, Kirkwall, Orkney prior to deployment.

3.4.9 Field Deployment

The C-ADP system was lifted off of the quayside by the C-Odyssey vessel operated by Leask Marine. A custom frame was fabricated to allow the frame to be accommodated onboard and to be stowed for transit. Figure 3-25 shows the frame aboard the C-Odyssey in transit from Hatston Quay to the Fall of Warness, in footage via drone arranged and made available by the European Marine Energy Centre.

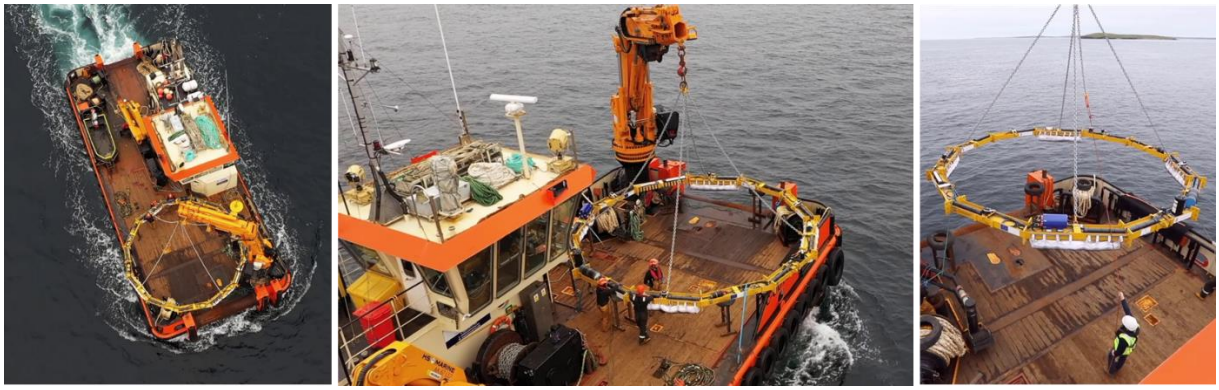

Figure 3-25. Photographs taken and provided by EMEC of the C-ADP MkIII being deployed at the north west end of the Fall of Warness, tidal energy site.

Figure 3-26. Photographs of the deployment of the C-ADP MkIII. (left) being lowered to the seabed, (right) footage from a subsea camera showing the landed frame and operational SB-ADP (active LED indicator).

3.4.10 Recovery of the C-ADP in September 2021

The C-ADP MkIII could not be recovered during the originally planned neap tide due to vessel availability and weather, hence a delay of two weeks was incurred. This resulted in a longer-duration deployment (which improves data-collection duration) but which left little time for detailed analysis of the recovered sensor systems. The frame was recovered on 18th September and the system was accessible – remotely via EMEC staff in Orkney the following week. Only very preliminary investigation on the system has been possible in the time available prior to reporting. Early indications are that the diagnostic systems have functioned including the network of inertial measurement units and the autonomous scheduler and PTP timing functionality appears to have been operational throughout the deployment until battery depletion around the 30-day mark. However, early indications show corrupt/damaged and/or missing files on the SB-ADP sub-systems. This cannot be fully investigated

until the system is shipped back to UEDIN for thorough investigation. While this is underway, analysis, QC and publishing of the valuable Nortek Signature 500 5-beam ADCP has been prioritized and is discussed in Section 3.5. In summary, this data set is confirmed as acquired and high quality. Preliminary analysis highlights significant levels of wave action from an area of the Fall of Warness that is shallower than previously studied areas. It is envisaged that the dataset will be valuable to the sector as the location of deployment is proximal to ongoing tidal energy converter deployments.

3.5 Results of Implementation

Post-processing of successfully executed measurement campaigns reveals that sensor package mooring systems performed well, resulting in deployments with sensors orientated correctly and with levels of vibration and oscillation ranging from exceptionally low (see Section 3.5.1) to low (See Section 3.5.2) . Figures

Table 3-3. Stability of instrument packages in highly energetic tidal flows

Deployment	Pitch (mean) (degs)	Pitch (std) (degs)	Heading (mean) (degs)	Heading (std) (degs)	Roll (mean) (degs)	Roll (std) (degs)
Fromveur Signature 500 ADCP	1.7	0.3	214.8	0.7	-1.2	0.1
Fromveur Signature 1000 ADCP	1.6	0.4	100.2	0.2	0.0	0.4
C-ADP-EMEC Signature 500 ADCP	2.2	0.1	40.0	0.4	0.9	0.2

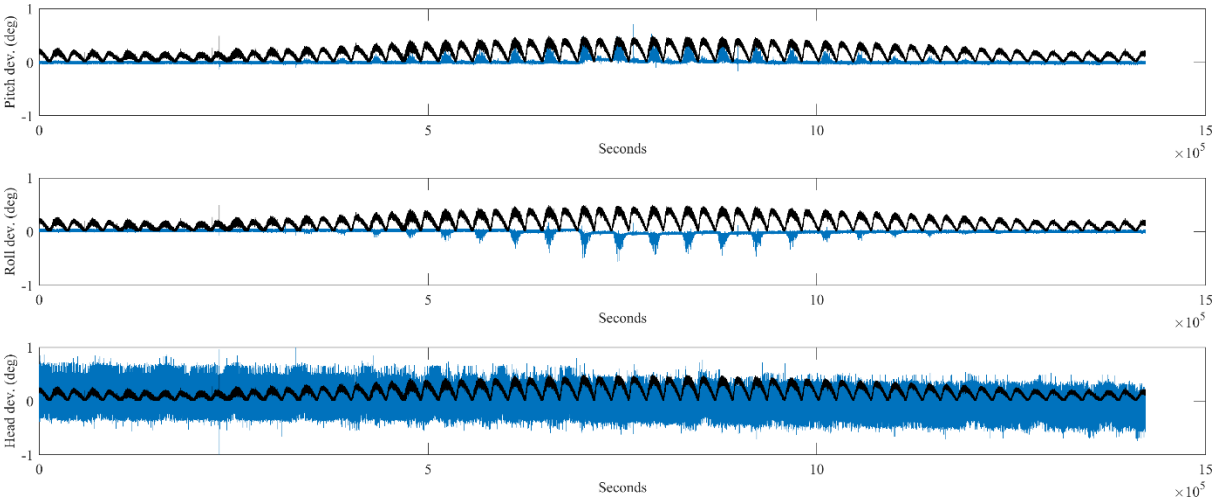

Figure 3-27: Stability of RealTide 5-Beam ADCP deployment at ~IEC 5D . Raw data at 1Hz. Pitch mean = 1.8degrees, Roll mean= -1.2, heading mean 214.5 degrees. Scaled tidal current magnitude (in black) shows relationship between tidal speed and direction on deviation of the sensor orientation.

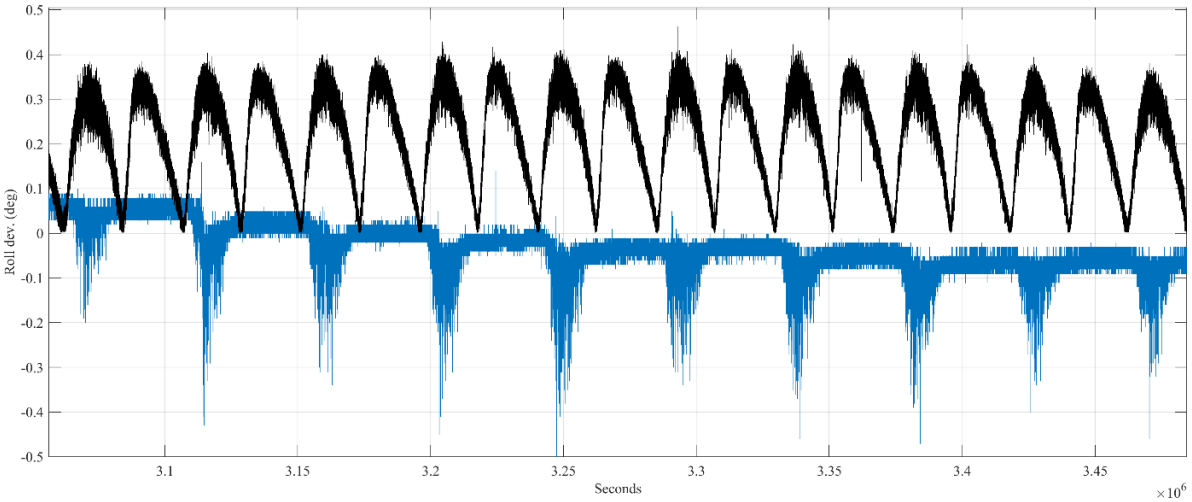

Figure 3-28. Time-series of multiple tidal cycles showing deviation from mean value of Pitch, Heading and Roll for ADCP Signature 500.

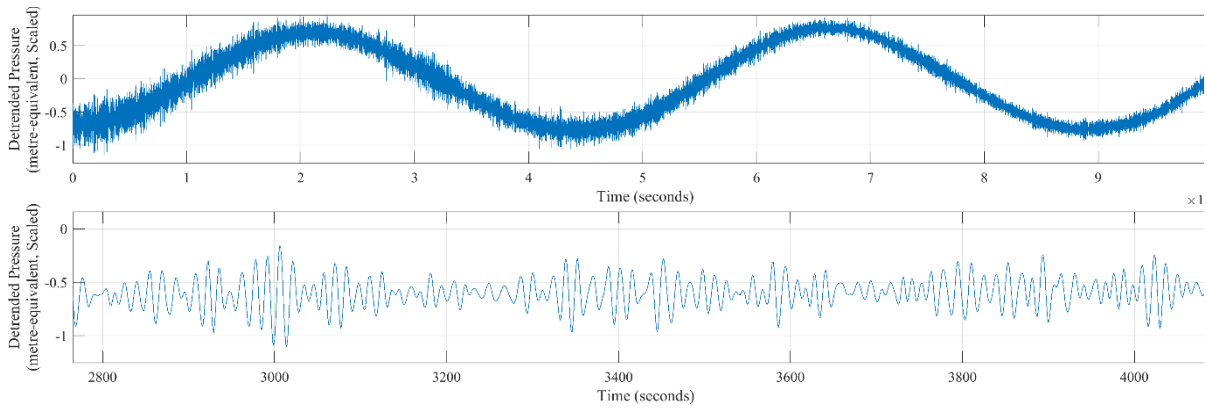

Figure 3-29. Time-series of two segments of Fromveur Strait 500kHz ADCP dataset showing quality of the pressure measurements. (Top) rescaled data showing tidal cycle, (bottom) rescaled data showing surface wave groups as measured by the on-board ADCP pressure gauge.

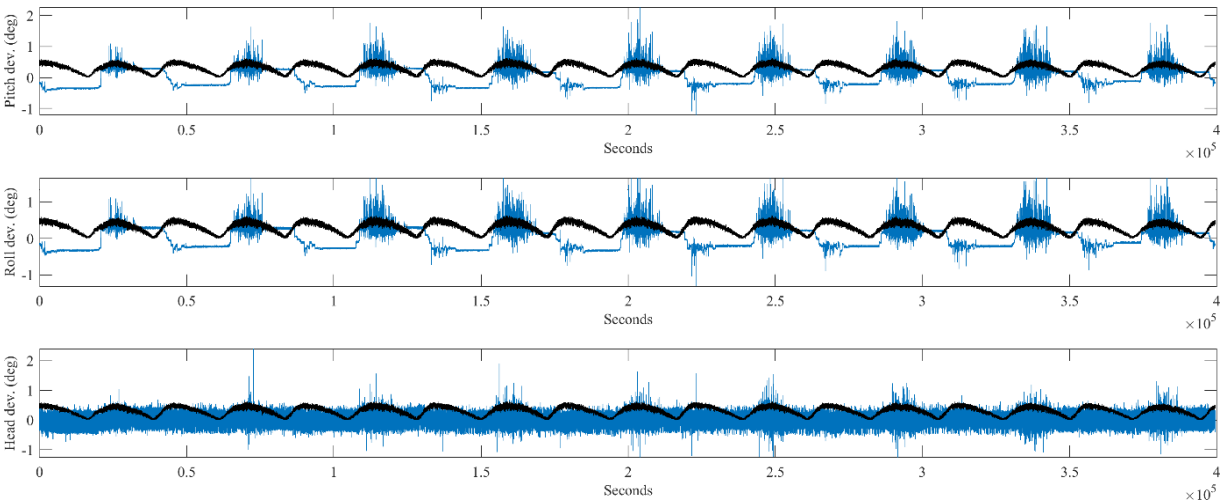

Figure 3-30. Time-series of multiple tidal cycles showing deviation from mean value of Pitch, Heading and Roll for ADCP Signature 1000.

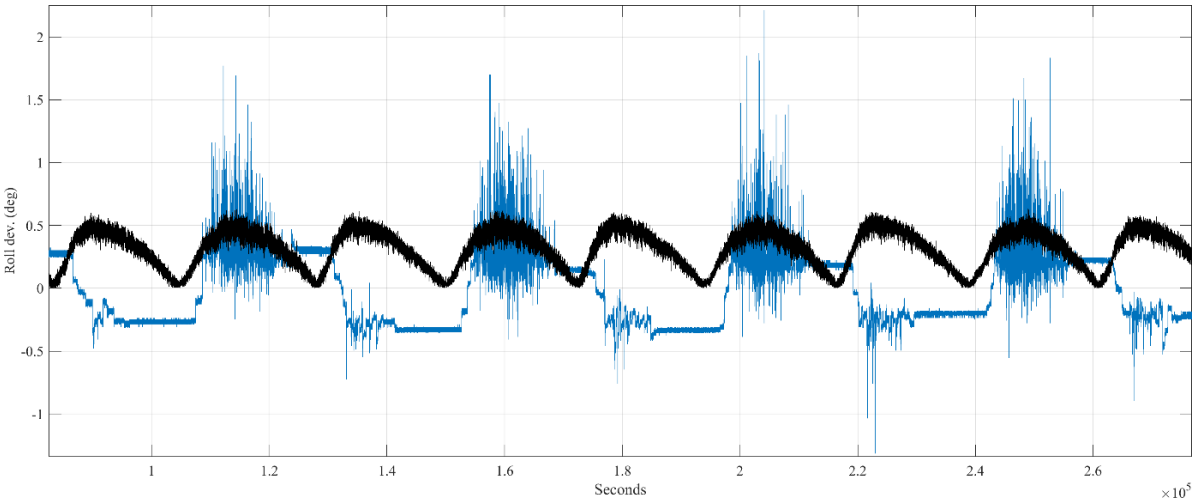

Figure 3-31. Time-series of multiple tidal cycles showing deviation from mean value of Roll for ADCP Signature 1000: zoomed-in to show dynamic behaviour with changing tides.

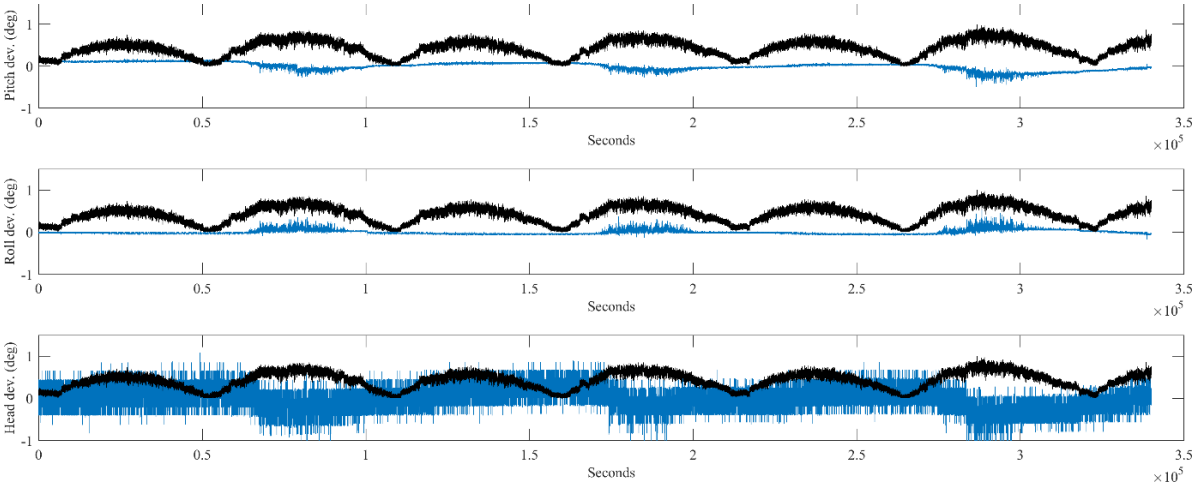

Figure 3-32: Time-series of multiple tidal cycles showing deviation from mean value of Roll for ADCP Signature 500 deployed as part of the C-ADP Aug/Sep 2021 deployment at Fall of Warness, EMEC.

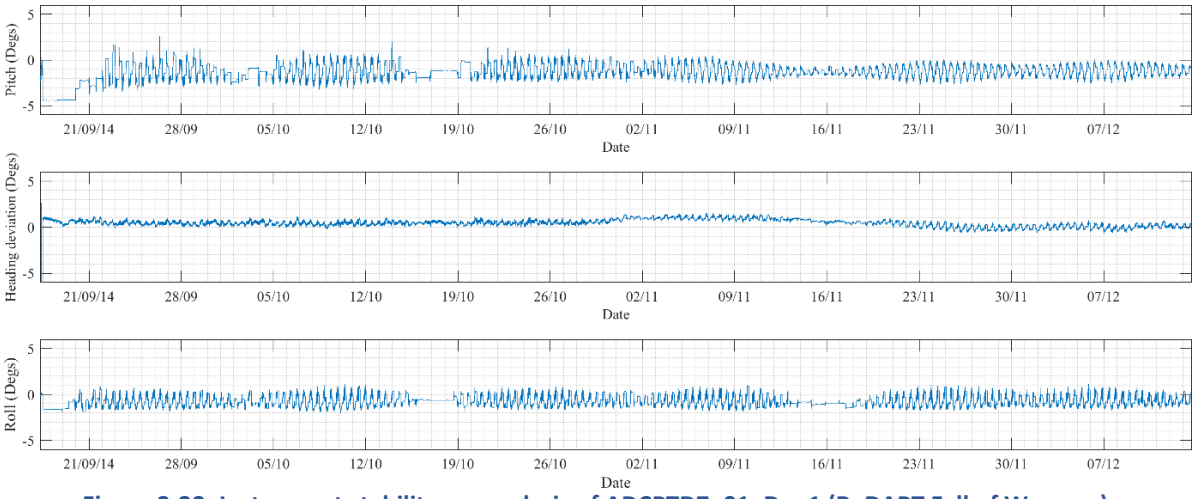

Figure 3-33: Instrument stability: re-analysis of ADCPTD7_01_Dep1 (ReDAPT Fall of Warness).

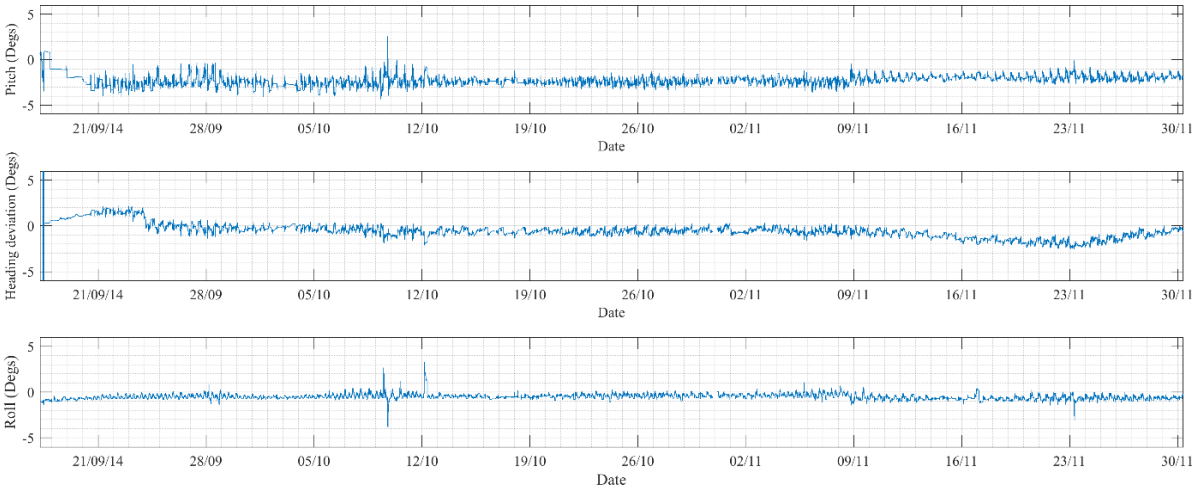

Figure 3-34. Instrument stability: re-analysis of ADCPTD7_02_Dep1 (ReDAPT Fall of Warness).

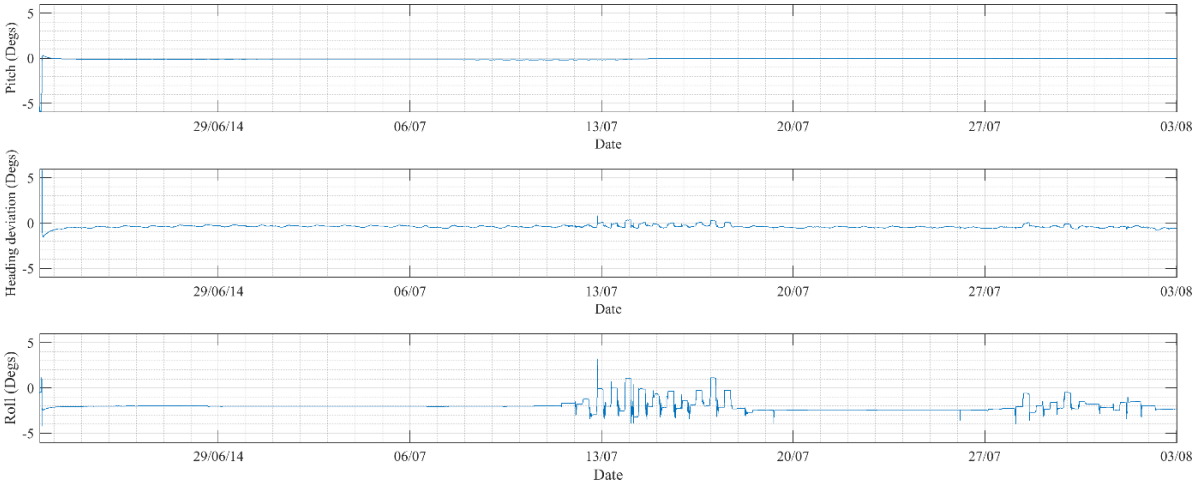

Figure 3-35. Instrument stability: re-analysis of ADCP01_NW_Dep5 (ReDAPT Fall of Warness).

3.5.1 ADCP02_NW_Dep5

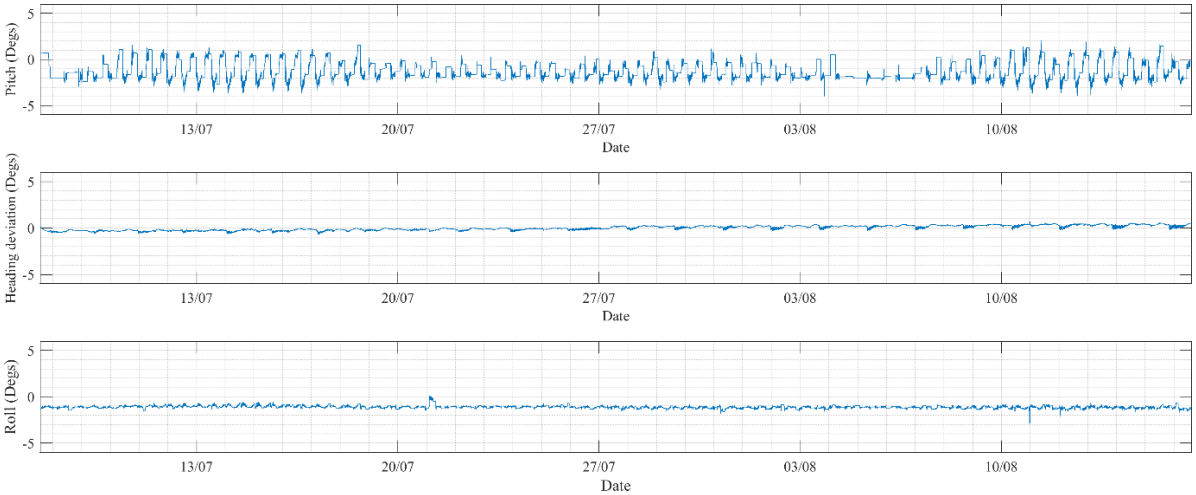

Figure 3-36. Instrument stability: re-analysis of ADCP02_NW_Dep5 (ReDAPT Fall of Warness).

3.6 Summary of Implementation

Table 3-4 collates and summarises RealTide WP2 tasks and sub-tasks categorised by four main strands of work, namely TEC-installed activities around the first and second trial deployments, seabed-installed sensor packages and the multiple phases of development of the C-ADP advanced turbulence sensor. Completion status is listed from design, through implantation and testing to data retrieval.

Table 3-4: Summary of RealTide in-situ sensor campaign types and completion status across system/component design, implementation, testing, deployment and data acquisition.

System & Features	Completion Status				
	Designed	**Implemented**	**Tested**	**Deployed**	**DATA**
TEC Deployment 1 Implemented the specification developed in RealTide D2.1 - **Engineering / Marine Systems Design:** extensive work in partnership with turbine developer Sabella. - **Logistics**: Procurement of off-the-shelf (OTS) components, shipping of equipment between UK-France including 3000kg gravity moorings. HSE management. Marine operations, liaison with divers, vessel operators and wide supply-chain. - **Mechanical:** Diver removable elements, marinized bracketry and turbine fixings, 3rd party simulations of TEC D10 bulb to assess impact of sensor penetrations. Alignment tasks. Mechanical fabrication & machining via UEDIN and ext. workshops - **Electrical** design of smart relays, fuses and multi-voltage, multi-path, multi-redundant power supplies housed in multiple pressure vessels. - **Control & Comms:** Extensive design and testing of small embedded computing, back-up architecture, communications networks based on RS232, RS485 and ethernet controlled by various developed software including MATALB and Python on Arduino, Linux and Windows OS. - **Sensors:** Integrated a horizontally orientated ADCP to D10 rear. Integrated a vertically orientated ADCP to D10 top. (Designed system for Single-Beam Doppler integration but did not install due to prioritizing testing of highest priority systems.)	yes	yes	Yes - partial - some D10 sub-systems not available quayside	yes	None - before unplanned TEC recovery
TEC Deployment 2 **Redesign for improved resilience:** a full review of the design was carried out to exploit re-designed D10 auxiliary electrical system to mitigate previous failures / potential-failure points and to improve system resilience. - New "bypass" cabling system to de-couple UEDIN seabed systems with the UEDIN D10-installed systems - Improved fusing, redundancy, inrush-current protection and miniaturization which gave more flexibility on the choice of installed pressure vessels (to allow for the possibility of extended D10 deployment). - Battery-operated back-up on D10 Sig500 implemented to "guarantee" data collection should the D10-TEC experience a problem. **Testing:** UEDIN-Sabella designed and implemented extensive system checks at quayside with the turbine electrical and IT systems setup in "as-deployed" setup, involving up to six staff checking operation of external sensor systems – all passed including seabed systems connected via 100m seabed cable assemblies.	yes	yes	Yes - extensive	yes	Yes - before unplanned TEC recovery

System & Features	Completion Status				
Seabed-installed sensor systems - **Hybrid power:** Power defaulted to extended stand-alone battery packs but could be switched remotely to human control via connection of a successful pre-installed cable to the D10 via diver operations planned for near-turbine works. Safe-switchovers to D10 control implemented via smart relays - **Sensor Stability / Data Quality:** UEDIN's proven damped gimbal setup manufactured for RealTide campaigns. Gravity mooring re-configured to accommodate extended battery cannisters and computer-control / smart-switch-over. Oversized central lifting point for ROV proved successful with French vessel operators. - **Campaign Flexibility:** Diver removable sensors and battery packs designed, implemented and successfully used to provide flexibility in the marine operations depending on required deployment lengths / changing requirements. - **Sensors:** Integrated a Signature 1000 5-Beam high-resolution ADCP to 2D upstream of D10. Integrated a Signature 500 5-Beam high-resolution ADCP to 5D upstream of the D10.	yes	yes	Yes (extensive)	yes	Yes (extensive)
Actuated Convergent acoustic Doppler Profilers:					
- Design of system and control software to enable instrument configuration based off of required/programmed "focal" point (point of intersection of acoustic beams).	Yes	Yes	Yes	Yes	Yes
- High-resolution sensor unit performance tests to check performance levels / behavior under controlled laboratory conditions at FloWave.	Yes	Yes	Yes	Yes	Yes
- C-ADP testing in controlled environment: as above but multi-sensor in concert. Geometrical configuration and timing offsets being varied to assess interference levels	Yes	Yes	Yes	Yes	Yes
- C-ADP with novel actuation capability. In collaboration with PNNL, USA a scaled field C-ADP was designed and tested in USA demonstrating control software and post-processing algorithms.	Yes	Yes	Yes	Yes	Yes
- Full-Scale Tests: C-ADP deployed on turbine-provided power allowing remote operation and user-intervention/configuration remotely via the D10-provided internet connection.	Yes	Yes	No	No	No
- Full-Scale Tests: With risk increasing that deployment at Fromveur Strait would not be possible extensive mitigations applied: Autonomous system designed, tested, fabricated, tested and commissioned. Successfully deployed and retrieved to/from the Fall of Warness, EMEC, UK.	Yes	Yes	Yes	Yes	TBC

4 DATASETS

In-situ measurements processed and used within RealTide are shown in Table Table 4-1. Where the data is publicly releasable it can be accessed via the work of the database and data access activities of RealTide Task 2.3 - see RealTide D2.3 [2] and www.tidalenergydata.org. As per the objectives of RealTide WP2 data comprised both re-analysis of existing data including UEDIN-held and Sabella-held previously acquired datasets, and data sets specifically targeted from the design and execution of new measurement campaigns.

Table 4-1. Summary of in-situ datasets showing temporal coverage and location.

Instrument	Primary Measurement	Temporal Coverage of Data			Location UTM 30N
		From	To	Duration	
ROWE WEST	u, v, w, p	10-Oct-2016	29-Nov-2016	50 days	Fromveur D10+4D
ROWE EAST	u, v, w, p	10-Oct-2016	24-Nov-2016	45 days	Fromveur D10+3D
SIG1000	u, v, w, p	05-Nov-2019	10-Jan-2020	66 days	Fromveur D10+2D
SIG500	u, v, w, p	06-Oct-2019	16-May-2020	222 days	Fromveur D10+5D
C-ADP MkII [23]	u, v, w, p	Aug-2019	Aug-2019	6 days	429157mE 623009mN
C-ADP MkIII	u, v, w, p	06-Aug-2021	16-Sep-2021	42 days	509968mE 6556364mN
C-ADP MkIII-SIG500	u, v, w, p	06-Aug-2021	16-Sep-2021	42 days	509968mE 6556364mN
ADCPTD7_01_Dep1	u, v, w, p	17-Sep-2014	13-Dec-2014	88 days	511144mE 6555329mN
ADCPTD7_02_Dep1	u, v, w, p	17-Sep-2014	30-Nov-2014	75 days	511078mE 6555286mN
ADCP01_NW_Dep5	u, v, w, p	05-Jun-2013	18-Jul-2013	44 days	511054.2mE 6555328.9mN
ADCP02_NW_Dep5	u, v, w, p	05-Jun-2013	18-Jul-2013	44 days	511151.1mE 6555241.1mN

Fromveur Strait, North West France

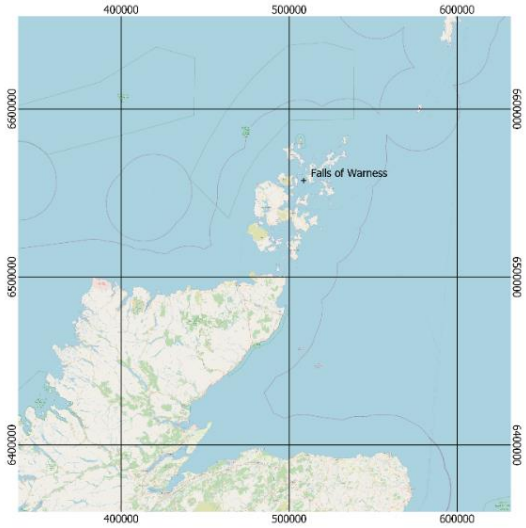

Falls of Warness, Orkney, UK

Figure 4-1. Maps of the regions considered in RealTide: (left) The Fromveur Strait, France and (right) Falls of Warness, Orkney, UK

4.1.1 ADCPTD7 datasets

Dataset ADCPTD7_01_Dep1 and ADCPTD7_01_Dep1 were used extensively to test the ability of the RealTide developed modelling techniques to capture multi-scale flow features. Demonstrating the combined model-in-situ data approach at the European Marine Energy Centre enables the results to be publicly shared since the EMEC tidal energy test site does not have confidentiality restrictions on the data. This work is described in detail in Section 5 of the report. These datasets were also used to trial the implementation of a post-processing tool to convert pressure gauge data to 1D wave spectral information, as shown in Figure 4-2.

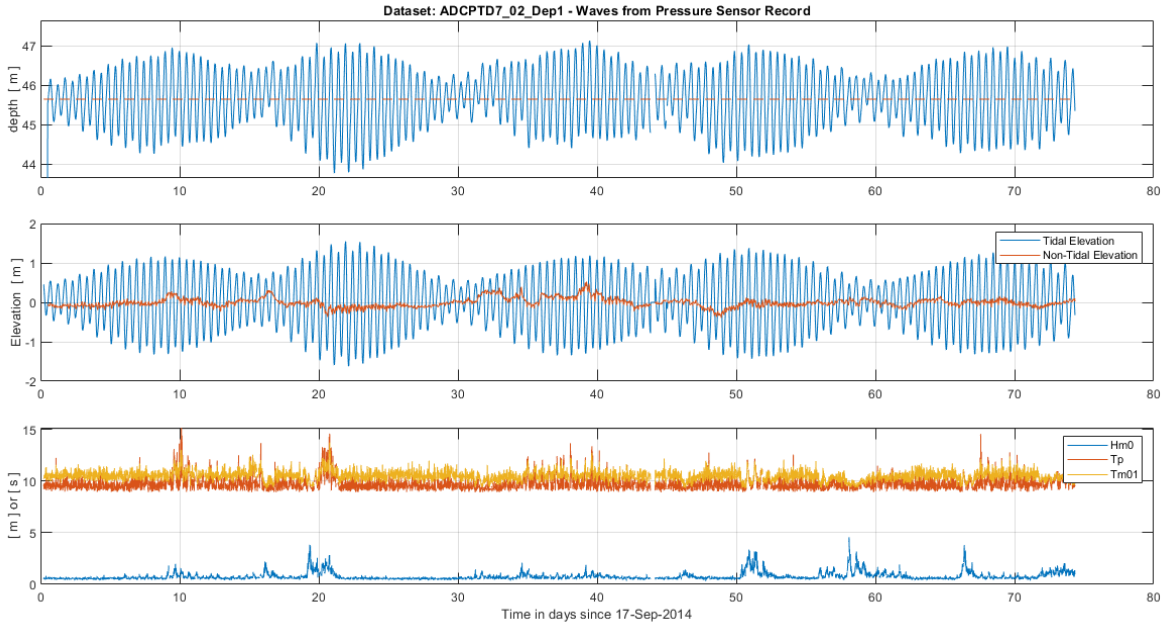

Figure 4-2. Pressure gauge to 1D wave spectra conversion: timeseries plots of the process trialled on the ADCPTD7 datasets.

4.1.2 ROWE legacy datasets

Two ADCP datasets, ROWE East and ROWE West, collected prior to the RealTide project commencement were provided by Sabella to UEDIN and processed using new processing scripts developed in the Python programming language. Velocity and surface-elevation (converted from pressure readings) timeseries were used in the calibration and validation of multiple RealTide developed 3D hydrodynamic models. The data is commercially sensitive. Snapshots of the datasets are shown below in Figure 4-3 which show unscaled flood and ebb tidal cycles and include information on the stability of the sensor via instrument pitch and roll readings.

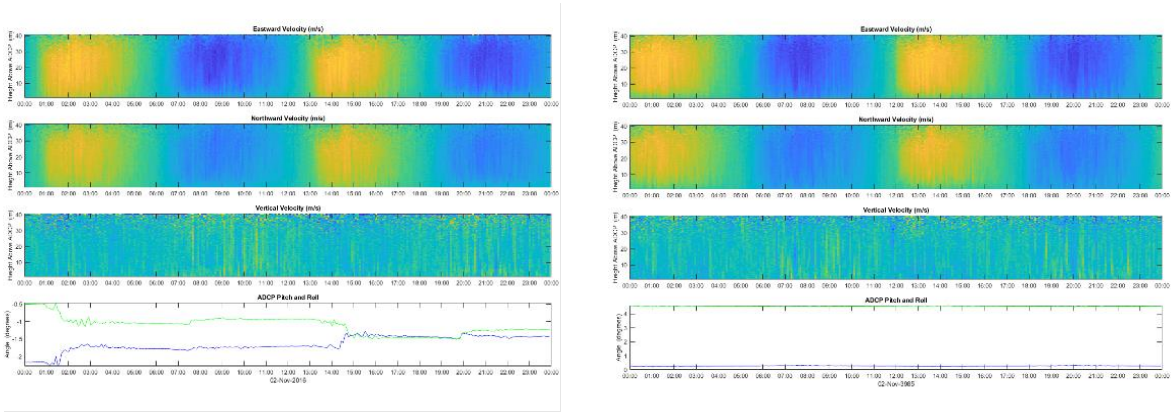

Figure 4-3 – Fromveur Strait Datasets: ROWE East and ROWE West re-processed for use in model development work.

Table 4-2: Implemented processes, use cases and data availability for data retrieved through re-analysis of pre-existing datasets

Instrument Label	Processed	QC	Archived	Data Availability	Primary Use Case
ROWE EAST	Yes	Yes	N/A	Confidential	Fromveur Strait model calibration and validation and to inform Sabella next-generation turbine systems
ROWE WEST	Yes	Yes	N/A	Confidential	Fromveur Strait model calibration and validation and to inform Sabella next-generation turbine systems
ADCPTD7_01_Dep1	Yes	Yes	Yes	Public (New)	Spatial variation and large-scale eddy studies
ADCPTD7_02_Dep1	Yes	Yes	Yes	Public (New)	Spatial variation and large-scale eddy studies
ADCP01_NW_Dep5	Yes	Yes	Yes	Public (Improved)	Spatial variation and power performance assessment as part of related projects. Results being prepared.
ADCP02_NW_Dep5	Yes	Yes	Yes	Public (Improved)	Spatial variation and power performance assessment as part of related projects. Results being prepared.
TEC Mounted SBD	Yes	Yes	Pending	Public (New)	Studies on the performance and possible limitations of D-ADPs in energetic environments.

4.1.3 Auxiliary Meta-data for the Interpretation of Fall of Warness ADCP Datasets

Since the ADCP datasets reanalysed under RealTide were originally captured in close proximity to an operating commercial prototype 1MW TEC, the DeepGEN IV, knowledge of the system state of the TEC is required when interpreting the data. This is due to the fact that the presence and operating point of the machine strongly affects local flow structures. Therefore key machine properties have been included in the re-analyses and included in the RealTide dedicated databasing and data access activities. These include temporally averaged (e.g., 5-min) records of turbine presence, turbine heading, turbine power and a common timestamp.

4.2 Fromveur Strait Measurement Campaign

Between 2018 and 2020 retrofitting of multiple ADP-based instruments and associated cabling and power and communications equipment was carried out. Further information on the specification of this field campaign can be found in RealTide technical report D2.1 Deployment and Instrument Specification for Advanced Flow Characterisation [1] and in the previous section (Section 3) of this report. Derived datasets are summarised in Table 4-3.

Table 4-3: Implemented processes, use cases and data availability for data retrieved through multiple measurement campaigns in the Fromveur Strait

Instrument label	Processed	QC	Archived	Data Availability	Primary Use Case
ADCP_FROM_SIG1000	Yes	Yes	Confidential	Confidential	Developer - Multiple
ADCP_FROM_SIG500	Yes	Yes	Confidential	Confidential	Developer - Multiple
ADCP_FROM_SIG500_TEC*	No	No	Confidential	Confidential	Instrument Benchmarks
ADCP_EMEC_SIG500_C-ADP	Yes	Yes	Yes	Public-New	Developers - Multiple

*Recently a small section of data, initially believed not to be captured, has been recovered from the D10-installed horizontally-installed 5-beam ADCP. The data covers several tidal cycles during neap tides (slower tidal currents). It has not been possible to analyse this data at the time of reporting but it will be carried out as a priority as part of ongoing internal research. Any research findings – anticipated to concern differences in derived flow metrics between direct (middle-beam) and averaged (divergent-beam) processes - will be added to and executed under the post-project publication plan.

4.2.1 Fromveur Strait Signature 500 Dataset

Whilst data collected in the Fromveur Strait has publishing constraints imposed due to commercial sensitivity, general observations can be reported. As an example, Figure 4-4 indicates using non-dimensional values as a proxy for wave action, specifically the ratio of vertical velocity to horizontal velocity magnitude. Strong bands of colour highlight periods where vertical velocities make up a large proportion of the total flow magnitude and are associated with wave activity, and it can be seen that the depth penetration of these "events" varies in time. Within the 220 days of data acquired there were multiple periods where wave action could be described as highly significant for all classes of turbine considered within RealTide, i.e., floating, mid-depth and small bottom-mounted. During these periods the loading of the turbine and the magnitude and quality of the power produced would be dominated by the wave field. Figure 4-5 shows the same velocity ratio for three selected range bins (distances from seabed) corresponding to hub-heights of a floating TEC, mid-depth TEC and low height TEC where in this small section of data the largest (relative) vertical component of velocities occur during slack tides (where of course the horizontal velocities are lowest).

More generally, across the dataset the occurrence of high wave action at different phases of the tide from slack-water to periods of fastest flow suggest that further clustering and classification of combined wave-current conditions are required, as the different regimes will have different consequences to e.g., operations and maintenance access windows – where interventions would be planned around slack-water periods, to maximum loading and design load cases, where extreme wave conditions coinciding with maximum tides could cause concern.

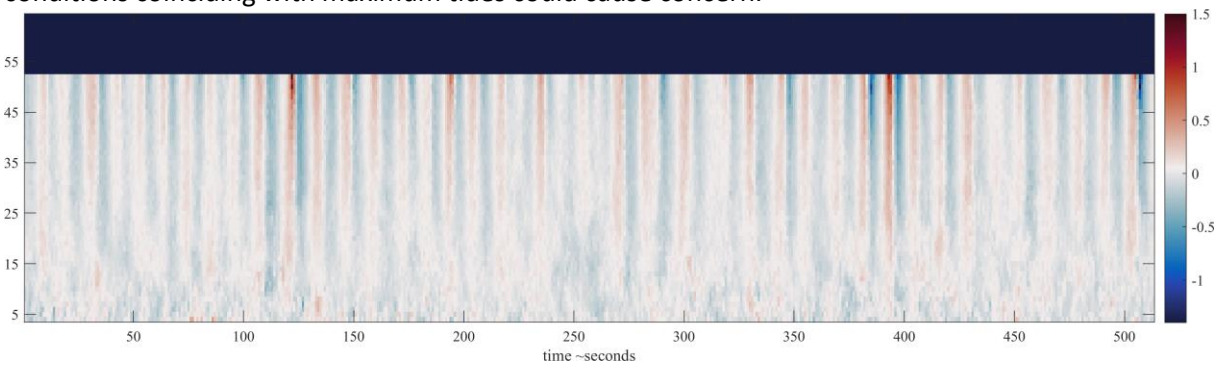

Figure 4-4: Pseudo-wave action: Spatial-Time map of the ratio of vertical velocity to horizontal velocity magnitude during a period of high wave activity and average flow speeds of approximately 2m/s. Data acquired by 5-Beam 500kHz ADCP.

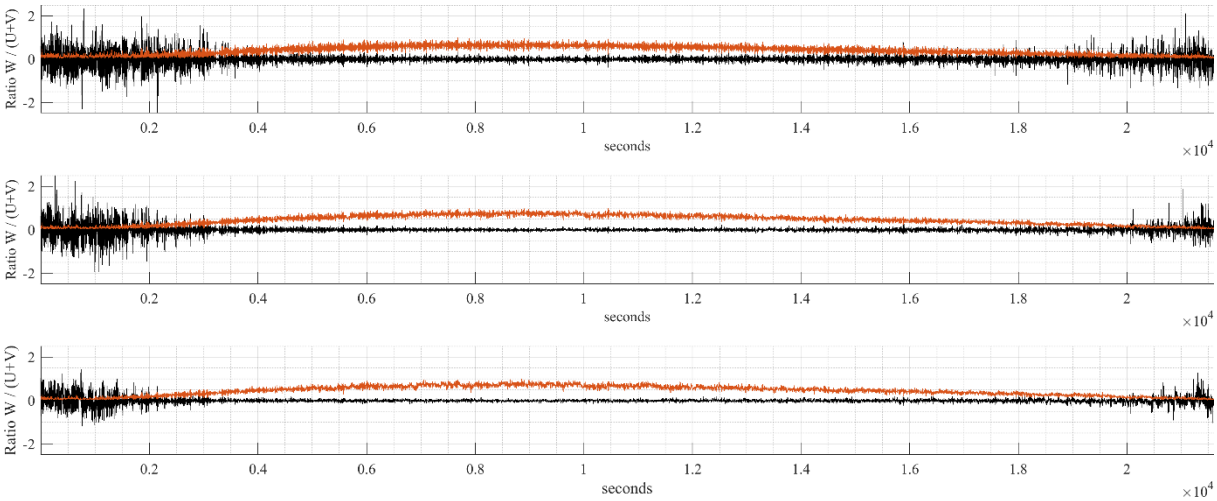

Figure 4-5: Pseudo-wave action timeseries from three selected depths of the water column corresponding to the approximate location of the three RealTide TEC classes: floating (top), mid-depth (middle) and close-to-bed small turbine (bottom).

4.2.2 Fromveur Strait Signature 1000 Dataset

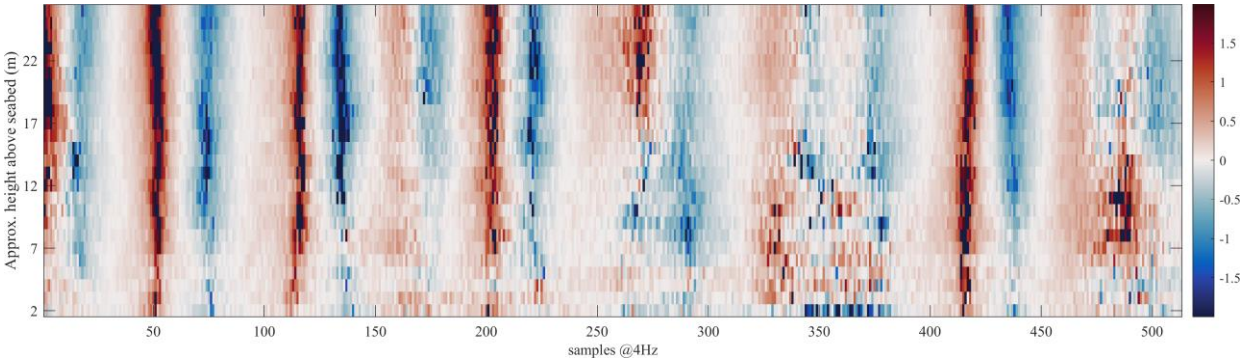

Figure 4-6: Pseudo-wave action: Spatial-Time map of the ratio of vertical velocity to horizontal velocity magnitude during a period of high wave activity and average flow speeds of approximately 2m/s. Data acquired by 5-Beam 1MHz ADCP.

Figure 4-6 is of similar form to Figure 4-4 above, with the range of measurement curtailed to approximately 25m due to the higher acoustic emission frequency (1MHz compared to 500kHz). The higher temporal sampling rate, however, of 4Hz (compared to 1Hz of the 500kHz device) provides greater temporal resolution and for studies of complex near-bed turbulent structures could be of value. More generally, across this data set, detailed structures can be seen from seabed to ~25 m particularly prevalent when capturing flow that is in the wake of the installed turbine tripod.

4.2.3 Fall of Warness 5-Beam ADCP Dataset captured via C-ADP MkIII Deployment

At the time of reporting (October 2021) the following data has been recovered from the RealTide C-ADP MkIII deployment conducted at the north west region of the Fall of Warness, Orkney, UK. As shown in Figure 4-7 the instrument was configured with a non-continuous duty-cycle, specifically 12 minutes on, 8 minutes off for 43 days between 3rd August 2021 and 15th September 2021. Preliminary data analysis shows very stable instrument siting and confirms that the design of the C-ADP multi-instrument frame to be low to the seabed and to take advantage of novel semi-compliant gravity bags has been successful.

Table 4-4: Dataset recovery status as of October 2021 from the RealTide C-ADP MkIII

Data Source	Data Recovered	Note
C-ADP SBDs	No	Ongoing Analysis
Nortek Signature 500	Yes	Data QC'd and Made Public
C-ADP Diagnostics and auxiliary sensors	Partially	Ongoing Analysis

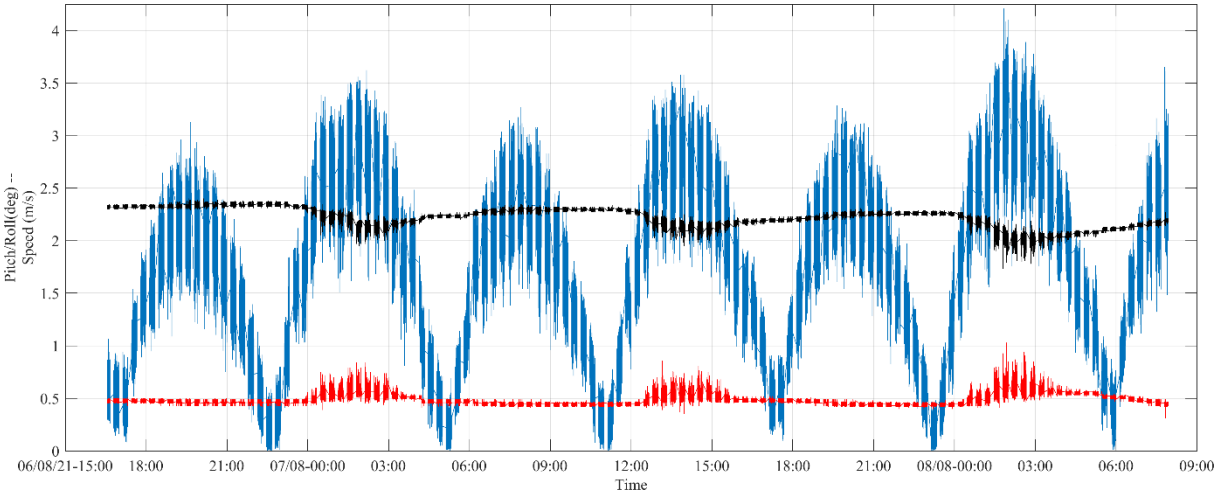

Figure 4-7. Timeseries of (blue) Current speed magnitude (m/s), (red) sensor roll and (black) sensor pitch (degrees) showing highly stable platform offered by the RealTide C-ADP deployment at EMEC, Aug.-Sep. 2021.

Figure 4-8 shows the results of implemented QC processes on the recently acquired Signature 500 dataset from the C-ADP deployment. Interestingly the approach using Qartod recommendations as the starting point of a tailored QC procedure for very high energy sites (tidal channels) are picking up the periods of instrument-to-instrument interference that was expected on this multi-sensor frame. These can be seen as periods of outlier velocity readings and strong bands of QC flags (red squares) during these periods. This is due to overlap between emitting instruments on the pre-programmed scheduler but is an encouraging result.

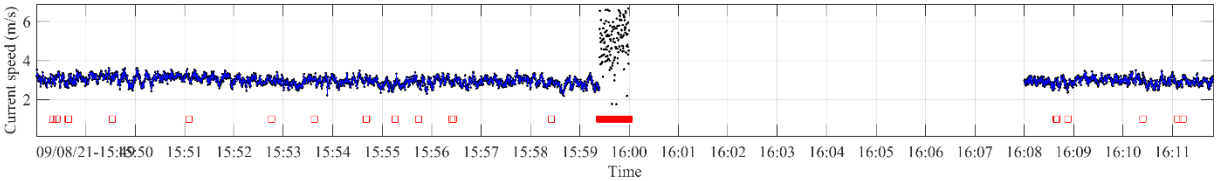

Figure 4-8. Timeseries indicating functioning QC processes where a period of instrument-instrument int3errference of n the C-ADP frame has been detected using the implemented QC. (red squares are QC-Fail flags).

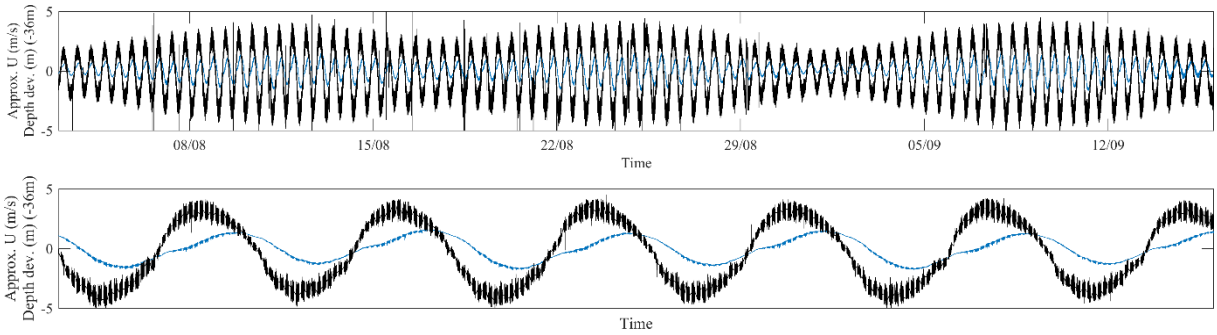

Figure 4-9: Preliminary analysis of ADCP_C-ADP_SIG500_Dep1 (pre-QC) showing approximate streamwise velocity, in black and detrended pressure in blue. Instrument to Instrument interference can be seen in the top plot.

Figure 4-9 highlights the requirement for QC procedures where large spikes can be seen (top) figure. Without correction these would strongly corrupt estimates of turbulence parameters. In this case they are likely the result of instrument-to-instrument interference occurring at small periods at the end of each data capture window due to a specific setup of the multi-instrument deployment. Figure 4-9 (bottom) shows very high flow speeds (for a few days of the deployment) and interesting elevation signal. The full dataset will be published on the RealTide website by December 2021 when QC and initial analyses are complete.

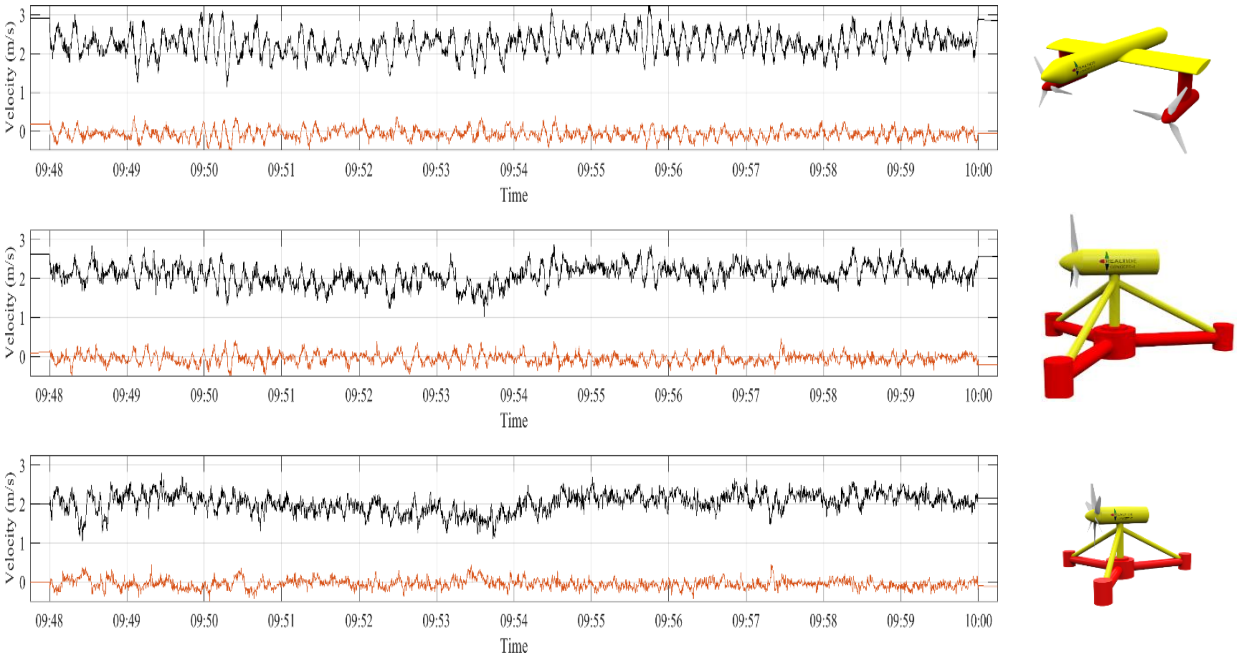

Figure 4-10: Timeseries plot showing approximate streamwise velocity (black) and vertical velocity (red) at approximately 25m, 18m and 12m above seabed (from top to bottom).

Figure 4-10 shows the results of initial post processing where the dataset has been re-orientated into a new coordinate system via an initial estimate of the mean streamwise flow direction for a given tide. The level of wave action is clearly visible for this period selected (selected visually from the dataset as being the period of high wave activity). The horizontal velocity variation is very strong in the top and middle plots – corresponding to the hub-height velocity that would be experienced by a TEC of RealTide class "floating" and "mid-depth" respectively. These classes are shown to the right of the figure. Figure 4-11 emphasises the level of wave action at this location where deviation of the instantaneous velocity profile from a temporal and spatial average current field is shown. Positive deviation is shown in red, with stronger colours corresponding to larger deviation. Negative deviation

is similarly highlighted in blue shades. The velocity field shown here for this recently acquired dataset is varying from mean values of (approximately and under preliminary analysis) 2.5 m/s up to 4.0 m/s and down to 1.5 m/s. This flow field would have strong impact on any operating tidal turbine both in terms of power produced and cyclic loading. It should also be noted that in this plot data has been curtailed before the full sampling range of the instrument as further post-processing is required on approach to the sea surface at ~35 m – where velocity fluctuations are even higher but where instrument performance is most uncertain.

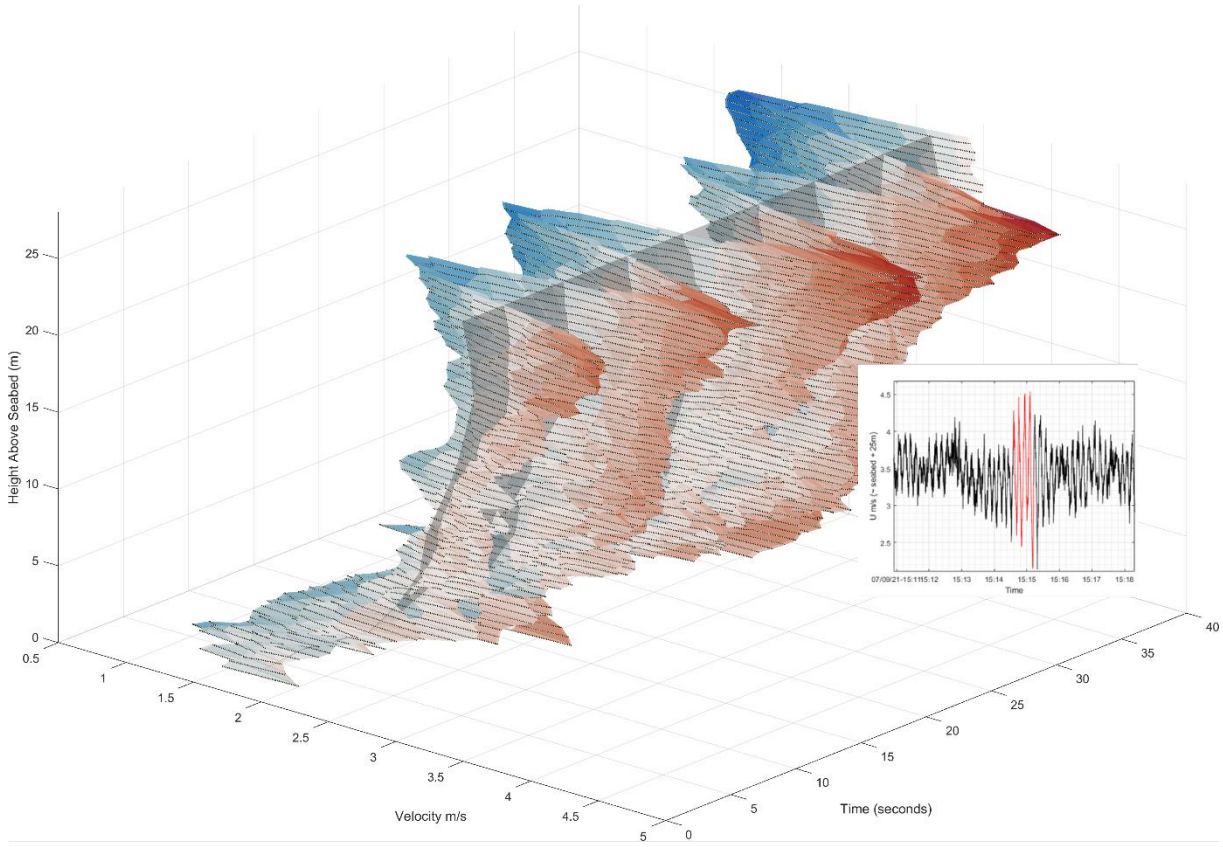

Figure 4-11. Data visualisation for the 5-Beam ADCP dataset acquired as part of the recovered (Sep. 2021) C-ADP MIII multi-sensor deployment at the north west region of EMEC's tidal energy test site. Deviation from a temporally and spatially averaged mean current depth profile (grey plane) is indicated by strength of colour with red being positive deviation and blue being negative. The influence of waves on the velocity field can clearly be seen. (inset) the corresponding time-series data of horizontal velocity (black) for a single sample depth bin with the matching time period (red).

4.3 Meta-Data, Quality Control and Data Processing Tools

A core objective of WP2 was to create high quality data outputs for use across the project activities and moreover to publish datasets externally. Sharing data puts higher requirements on data management e.g., transparency, provenance and reliability.

4.3.1 Improved Meta-Data

Data analysis and acquisition was conducted in parallel to the development of a prototype tidal energy database. Refer to RealTide Technical Report D2.3 for more information [2]. This has led to improved meta-data capture on new data and improved meta-data re-capture / gap-filling on previously acquired data. It is hoped that the improved datasets will make it easier for stakeholders to exploit the RealTide data outputs. Some of the steps taken are listed below:

- Re-analyses includes time offsets referenced to UTC
- Re-analyses have had missing descriptive fields added
- Re-analyses have had missing units fields added
- New data processing scripts were produced to extract and convert as much information from the raw proprietary instrument files as possible
- Parallel processing and the now routine availability of solid-state disks has been exploited to speed up conversion and internally beta-testing of large quantities of raw binary data into useable data format

4.3.2 Quality Control

Data quality control (QC) is essential for ensuring confidence in results derived from the measured data. Recommendations for QC of acoustic velocity instruments data recorded in the open ocean water environment have been made available in reports (QARTOD [27]), toolboxes (IMOS [28, 29]), articles [70, 71, 72], and by the instrument manufacturers (Nortek [73, 74], RDI operation manuals [75, 76, 77, 78, 79]). However, these guidelines are typically for open ocean measurement and may not apply to data measured in highly energetic and turbulent flow such as tidal sites. Typical QC strategies involve studying the physical status of the instrument e.g., pressure, pitch, roll, heading, temperature and accelerations, and studying aspects of the returned signal from which measurements are derived e.g., signal strength, signal to noise ratio, signal strength decrease along profile, pulse correlation, and the along beam velocities (e.g., spikes and rates of change etc.).

To arrive at reasonable/baseline QC parameters an analysis was conducted on a subset of an ADCP dataset acquired at the EMEC tidal test site in Orkney, UK . Of the 20 recommended in Qartod, twelve were selected. For each test, QC thresholds were varied and their impact on the data was studied against depth cell and ambient flow velocity. This has enabled to investigate the stable QC tests for high energetic flows as well as giving initial insight on the input thresholds for these tests. This has also shown that without relaxation of filtering thresholds, some of the recommendations result in very large occurrences of “fail flags” throughout the water column– mainly due to how dynamic the velocity fields are in these tidal sites.

In summary, the Qartod-described tests in Table 4-5 have been implemented at the time of reporting using the listed thresholds and limits. It is important to note that these are not universally applicable thresholds and further work is required - and is ongoing - on establishing thresholds with wider applicability. A summary of the implemented QC steps and example figures showing typical effects on an RDI Workhorse Sentinel 600kHz deployed at EMEC can be seen in Figure 4-12, Figure 4-13 and Figure 4-14. The RealTide database has been designed to be readily updatable as QC flagging is iteratively improved.

On completion of the QC processes on the ADCP datasets a simple new data structure is created which contains time-series arrays for each QC process. Where data has passed a particular QC stage data will be flagged with a 1, where data has failed to be checked – usually due to the technique employed – data will be flagged with a 2, where data is suspect – usually falling within a relaxed threshold – it will be flagged with a 3, and where data has failed it will be marked with a value of 4. The end-user of the data then has the flexibility to select any or none of these flags in their downstream processing.

Table 4-5: Quality Control implemented within RealTide for ADCP datasets

#	Test Name	Thresholds Used	
		RDI Narrowband [broadband]	**Nortek Signature 500 / 1000**
Q6	*Signal Strength*	90 [45] counts	30 dB
Q8	*Correlation Magnitude*	85 %	85 %
Q9	*Percent Good*	90	N/A
Q10	*Current Speed*	6 m/s – 8 m/s	6 m/s – 8 m/s
Q14	*Error Velocity*	0.1 m/s – 0.2 m/s	0.1 m/s – 0.2 m/s
Q15	*Rate of Change of Tilt Sensors*	2.5 deg/s – 5 deg/s	2.5 deg/s – 5 deg/s
Q17	*Flat Line*	Not implemented	Not implemented
Q18	*Echo Intensity*	8 [4] counts	6 dB
Q20	*Current Gradient*	0.8 m/s	0.8 m/s
C1	*Deployment Depth*	80% of expected depth	80% of expected depth

TEST6- Signal strength

Signal strength reduces with distance from the instrument. This test ensures that the strength of the returned signal is sufficient to produce good data. This test is applied to each beam of the sensor. A data point is flagged as PASS if all the individual beams pass the test, SUSPECT is one beam fails, and FAIL if more than one beam fails the test. Sensitivity analysis on EMEC data show the test is stable with a null to very low variation with flow speed. Tests could not be conducted across alternate instrument configurations. Thresholds vary depending on manufacturer, which use differing units.

TEST8 -Correlation magnitude

This test ensures that the correlation magnitude between pulses is above an acceptable threshold. This test is applied to each beam of the sensor.

A data point is flagged as PASS if all the individual beams pass the test, SUSPECT is one beam fails, and FAIL if more than one beam fails the test. Results have shown that this test is relatively stable with a low variation with flow speed. Note that the recommended threshold might depend on the individual instrument performance + units varies depending on manufacturer in counts (RDI) and % (Nortek)

TEST9 - Percent good

This test ensures a percentage of high data quality measurements to produce good velocities (or good ping per sample). Signal quality tests are applied to each beam of the sensor. A data point is flagged as PASS if all the individual beams pass the test, SUSPECT is one beam fails, and FAIL if more than one beam fails the test. Not all brands of ADCP return a percent good value; Nortek does not.

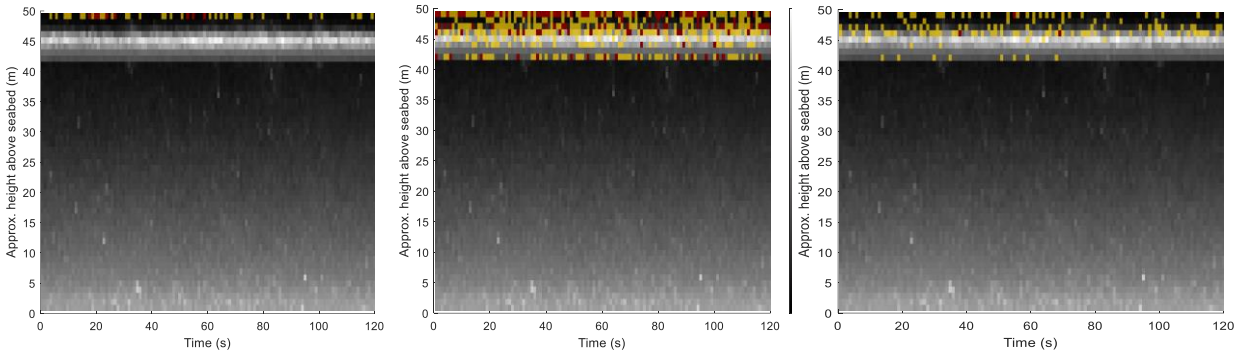

Figure 4-12: QC processes 6, 8 and 9. Flag=2, Not Evaluated - Blue , Flag=3, Suspect - Yellow , Flag=4, Failed - Red

TEST10 - Velocity magnitude

This test checks for unrealistically high current speed. It contains two thresholds: (1) a maximum threshold over which the velocity is flagged as FAIL, and (2) a minimum threshold. Velocity data between the min and max thresholds are flagged as SUSPECT. Data under the minimum thresholds are flagged as PASS.

TEST14 - Error Velocity

This test checks the difference in vertical velocity measured between beam pairs 1,2 and 3,4.
The error velocity is defined by

$$Ev_z = \frac{(b_1 + b_2) - (b_3 + b_4)}{2\cos\theta} = V_{12z} - V_{34z}$$

The error velocity is also a proxy measure of the flow inhomogeneity and the uncertainty in the measurements induced by beam separation.

TEST15 - Rate of Change of Pitch, Heading, Roll

This test ensures that the pitch/roll/heading rate of change in deg/s is

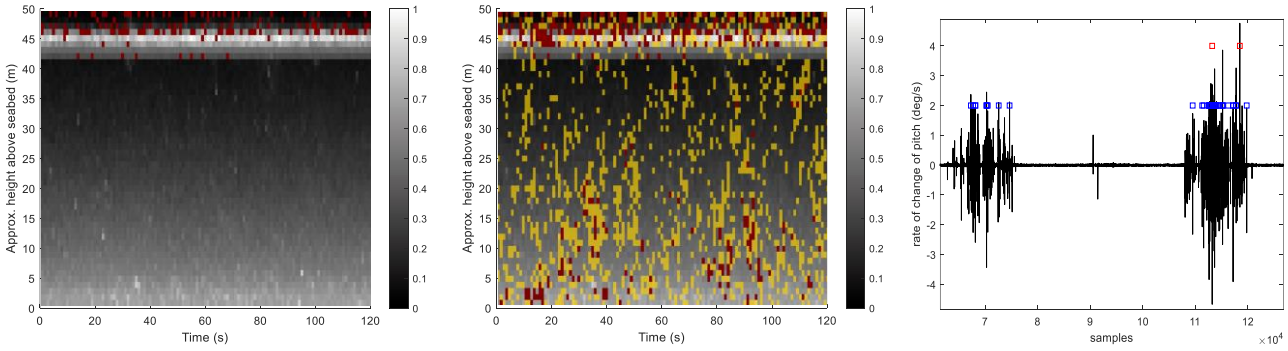

Figure 4-13: QC processes 10, 14 and 15. (left and middle) Flag=2, Not Evaluated - Blue Flag=3, Suspect - Yellow Flag=4, Failed – Red. (right) Yellow squares: Suspect Red squares: Fail.

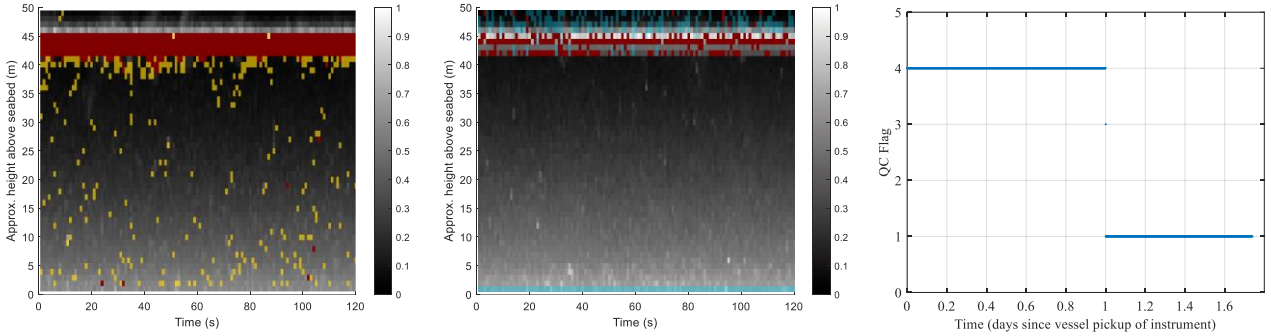

Figure 4-14: QC processes 18, 20 and C1. (left and middle) Flag=2, Not Evaluated - Blue Flag=3, Suspect - Yellow Flag=4, Failed – Red. (right) blue-line showing data failing (=4) or passing (=1).

TEST18 - Echo Intensity Spikes
This test checks for echo intensity increase from previous bin that may indicate interactions with the surface, bottom, or in-water structures. This test is applied to each beam of the sensor. A data is flagged as PASS if all the individual beams pass the test, SUSPECT is one beam fails, and FAIL if more than one beam fails the test.

TEST20 - Current Gradient in Vertical Direction
This test checks for excessive current speed changes in the vertical profile. The velocity magnitude between adjacent bins n and n-1 is compared. If the difference exceeds a given threshold the data is flagged as FAILED.

TESTC1 - Deployment Depth
This checks that the instrument depth as reported by any installed pressure sensor is close in value to the expected water depth at the location of deployment. Useful for QC'ing data where there are extensive pre-deployment/post-recovery records (e.g, during vessel transit).

4.3.3 Data Processing Tools

Multiple post-processing tools have been developed. Identified subsets have been prepared and packaged for public release. The following scripts will be available on the RealTide website www.tidalenergydata.org

1. Data extraction tool for datasets in a legacy file format for one manufacturer
2. Time-series extraction from a prescribed hub-height from a 4D vector field -> 2D vector field
3. Pre-processing for key parameters e.g., tidal direction and peak-flows etc.
4. Tidal reduction using surface elevation or velocities
5. Spectral analysis of non-tidal component of modelled and measured signals
6. Pressure to 1D wave spectra
7. Beam-wise acoustic Doppler Profiler turbulence processing toolset
8. Model output visualization tools including the visualization of flow rotation.

Other data processing tools are currently being collated will be added in due course as aligned projects continue and as the tools are quality checked.

5 REGIONAL MODEL

An appropriately designed regional model provides information that is complimentary to that derived from *in-situ* measurements. In particular a model provides information on the spatial variability of the flow, parameters such as vorticity, surface gradients, and circulation that cannot be derived from single point measurements. Regional scale numerical simulations require the discretization of both the spatial and temporal dimensions of the physical states being modelled, therefore regional model also has limitations on what can be simulated. When designing regional models there is always a pay-off between resolution, accuracy and computational cost. For developers it is typically the cost that is the dominant controlling factor. With this in mind a range of regional models have been built to allow the impact of model construct on the prediction of key flow classification parameters to be assessed.

A number of different variants of the models were constructed and run during the development of the final set of model constructs. It was clear during the iterative development of the Iroise Sea model that far-field processes associated with persistent large-scale eddies may modify the flow through the Strait. This observation raised questions about the interpretation of IEC guidance on model development provided to developers. The guidelines acknowledged that large-scale flow structures need to be considered, but do not provide any further detail. There are recommended mesh resolutions within the region of interest depending on the end-use of the model data, but no discussion of the extent this region should cover. It was decided that this was a fundamental question that needed to be addressed before advancing to the full wave modelling. Time and resource constraints meant that proposed wave modelling work could not be addressed in the project time frame.

Many of the intermediate constructs were used to select an optimal set of numerical parameters that will produce stable models, to develop post-processing software tools, and to better understand the workings of the OpenTELEMAC software. It should also be noted that over the timeframe of the RealTide project, the quality and availability of bathymetric and substrate data significantly improved. The final versions of the model constructs all use the most up to date data. For these reasons, only the final clean set of model constructs used for the final analysis presented in this document are discussed and the associated results archived for integration with the database developed in RealTide D2.3 [2].

5.1 Numerical Solver

A review of available tools was carried out to determine which tools to use for the development of the regional models, and candidate short list was defined. Then a set of selection criteria were defined and used to select the appropriate software tool. The short list of numerical solvers have been tabulated against the selection criteria in Table 5-1. Where a criteria is met the table cell has been ticked. The model or models to be considered for use must meet the majority of our selection criteria. It was decided early on that we should limit ourselves to OpenSource tools, this not only reduces costs but makes the model constructs accessible to a broader group of potential end-users. The OpenSource tools that meet the majority of criteria are OpenTELEMAC, OpenFOAM, and FVCOM. After consultation with consortia partners it was decided that the OpenTELEMAC numerical solver would be used for the regional modelling work.

Table 5-1: Modelling tool selection criteria

Criteria	OpenTelemac	Delft-3D	MIKE 3	OpenFOAM	ADCIRC	FVCOM	FLUIDITY	SUNTANS	SELFE	ROMS	POM	MARS	COAWST	COAMPS
OpenSource	✓	✓		✓		✓	✓	✓		✓	✓		✓	✓
Source code	✓	✓		✓		✓	✓	✓	✓	✓			✓	✓
Quality assured	✓			✓		✓								
Regular updates	✓	✓	✓	✓										
Docker package				✓			✓							
Finite Difference				✓						✓	✓		✓	✓
Finite Element	✓	✓	✓	✓	✓	✓	✓	✓	✓			✓		
2-D solution	✓	✓		✓	✓		✓	✓		✓	✓	✓	✓	
3-D solution	✓	✓	✓	✓	✓	✓	✓	✓	✓	✓	✓	✓	✓	✓
Adaptive Mesh				✓			✓	✓						
Parallel code	✓	✓	✓	✓		✓	✓	✓	✓	✓	✓	✓	✓	✓
Orthogonal Grid	✓			✓				✓		✓		✓	✓	✓
Curvilinear Grid	✓			✓						✓	✓	✓	✓	✓
Unstructured Grid	✓	✓	✓	✓	✓	✓	✓	✓	✓					
Sigma Levels	✓	✓				✓		✓	✓	✓		✓	✓	✓
Nested Grids						✓				✓			✓	✓
Meshing tool	✓	✓	✓	✓	✓	✓				✓		✓	✓	
Free Surface	✓	✓	✓	✓	✓	✓	✓	✓	✓	✓	✓	✓	✓	✓
Wetting/Drying	✓	✓	✓	✓	✓	✓	✓	✓	✓	✓			✓	
Diffusion	✓	✓	✓	✓		✓	✓	✓		✓	✓		✓	✓
Turbulence: GLS	✓	✓	✓	✓	✓	✓	✓	✓	✓	✓	✓	✓	✓	✓
Turbulence: RAS	✓	✓		✓		✓	✓							
Turbulence: LES				✓			✓				✓			
Turbulence: DES				✓										
Non-hydrostatic	✓	✓	✓			✓	✓	✓	✓	✓			✓	✓
Tidal forcing	✓	✓	✓	✓	✓	✓	✓	✓	✓	✓	✓	✓	✓	✓
Surface forcing	✓	✓	✓	✓	✓	✓	✓	✓	✓	✓			✓	✓
Sediment transport	✓	✓	✓	✓	✓	✓		✓	✓	✓			✓	
Wind wave generation	✓	✓	✓	✓	✓	✓	✓	✓	✓	✓	✓		✓	✓
Waves coupling – 1 way	✓	✓	✓	✓		✓				✓			✓	✓
Waves coupling – 2 way	✓												✓	✓
Energy extraction	✓		✓	✓		✓	✓		✓					
Data assimilation (EnKF)	✓	✓				✓			✓					
Adjoint (4DVAR)	✓									✓			✓	✓
Users group	✓	✓	✓	✓		✓	✓	✓			✓			
Workshops/courses	✓	✓	✓	✓		✓	✓							
Support package	✓	✓	✓	✓	✓									

OpenTELEMAC has robust software verification, the hydrodynamic code is based on high-quality code developed by EDF for the modelling of nuclear reactors. There is a large user community who readily share solutions to issues as they arise. The hydrodynamic code supports a good range of numerical methods, turbulence closure models, and bottom friction models. The code can be readily modified to add user-defined functionality and to import data with a format other than those currently supported. The user has full control over the choice of numerical schemes used and the level of tolerance required for solution convergence. There is an associated wave model, TOMAWAC, integrated with OpenTELEMAC for full 2-way wave-current model coupling. The BlueKenue hydraulic modelers tools are designed to support mesh generation for OpenTELEMAC and can be used to visualize model output.

5.2 Computing Facility

There were a range of options available from running the regional model constructs. All had pros and cons, but the main constraints were cost and accessibility. The University high-performance computing facilities were considered too costly, and their user operating windows were too restrictive for model development, testing and long-period runs. The compromise solution was to purchase a dedicated 48-core server blade with access restricted to the IES group working on RealTide and IS support. The server was setup as a managed system so that IS had control of the maintenance and systems upgrades. The users could request standard packages and libraries be installed and could install specific packages locally for their own use. IS initially install an early version of OpenTELEMAC, this was subsequently upgraded to latest versions by the RealTide users.

5.3 Model Construction

Models have been constructed for two separate sites: (1) The Iroise Sea covering Ushant Island, Fromveur Strait and the Molène Archipelago, (2) The Orkneys including the Pentland Firth, Pentland Inner Sound and the Falls of Warness. The Iroise Sea model was developed to compliment the field data collection campaigns in the Fromveur Strait, where Sabella have deployed their D10 tidal turbine used to supply power the Ushant integrated energy supply, and the Orkneys model was developed to compliment the ReDAPT data collected at the EMEC Tidal Energy test site in the Falls of Warness. There is a large volume of open-access data for this site that can be used to develop flow classification methodologies. Multiple versions of the models for these two sites have been constructed where the mesh resolution and bottom friction definitions have been altered to test parameter sensitivity to (un)resolved physical processes.

(a) Ushant and Molène Archipelago, France

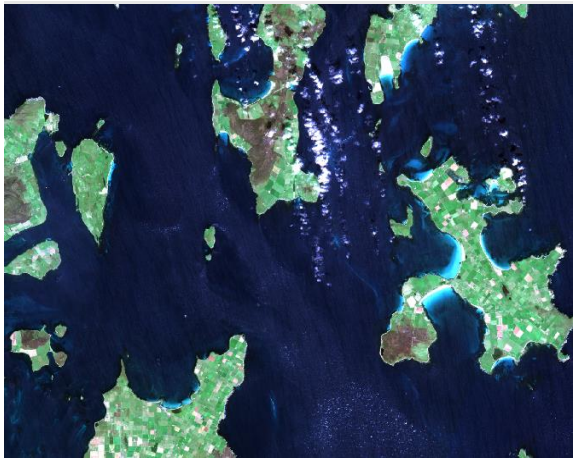

(b) Falls of Warness, Orkney

Figure 5-1: Sentinel 2A false colour images of the regional modelling sites.

The two sites have different topographical structures, so provide information on a range of physical response that may be encountered at tidal energy extraction sites. Fromveur Strait is essentially a channel through a headland. The Molène Archipelago and Ushant Island act as a barrier to the propagation of the shelf-sea tidal wave producing a dynamic head that drives flow through the gaps between the Molène Islands, Fromveur Strait, and the by-passes flow around Ushant. Fromveur Strait is open to Atlantic Ocean swell and exposed to local storms. In contrast the Falls of Warness lie within a channel formed between a pair of Islands. The in-flow is complicated by flow in and around the Orkneys Archipelago, and the presence of Muckle Green Holm Island within this channel. Atlantic swell is filtered by the shape of the channel and the distance of the EMEC site from the open ocean entrance to the channel. The Islands modify local winds, but this site is still fairly exposed to local storms.

The purpose of the multiple model constructs is to determine how well key physical processes are represented in a given model construct, and what the corresponding impact is on the prediction of parameters relevant to the tidal energy sector. From satellite imagery (see Figure 5-1a), it is known that large persistent eddy structures are formed as a result of the tidal flow through Fromveur Strait. The presence or absence of the large rotational fluid structures in the model will alter the dynamical balance of the fluid flow to the forcing around Ushant Island and through Fromveur Strait. Changes in this dynamical balance can affect the magnitude, direction and phase of the tidal flow through Fromveur Strait. The model constructs for this site are focused on vary the resolution over the regions where the tidally driven eddies persist. The Orkney models are focused on the Falls of Warness (see Figure 5-1b), where the mesh resolution is highest. The ReDAPT data show that the vertical profile of the flow is strongly modified on the north side of the channel. Flow structures along this channel edge will vary between flood and ebb tides. During flood tides trapped eddies formed in and around Seal Skerry Bay as the flow passes the outlying Seal Skerry rocks. On the ebb tide eddies are shed from the War Ness headland on the southwest corner of Eday. The form of these eddies and the impact on the channel flow are scale-dependent.

5.3.1 Domain Definition and Mesh Design

Experience has shown that effort put into building the best possible domain mesh leads to more stable and accurate models, limiting the amount of computing time lost to model run failures. The choice of domain extent depends on the purpose of the model and how accurately the open-boundary forcing can be defined. The mesh resolution should allow key bathymetric structures and islands to be resolved while maintaining mesh quality. All models are built using an unstructured mesh. For both regional modelling sites the coastline was hand-digitized in Quantum GIS (QGIS) using a mixture of Open Street Maps base layers and Sentinel 2 satellite imagery. A number of available coastline products were reviewed, but in general the resolution was too varied and most had missing small-scale islands. Hand digitization allows better control on hard-boundary resolution where it is most relevant to the intended purpose of the model output. The model domain meshes were generated using the BlueKenue hydraulic modelers software tool. Increased resolution across the regions of interest (RoI's) is achieved by generating and embedding sub-meshes within the model domain. The BlueKenue tools allow the user to set the triangle growth rate from the domain open and hard land boundaries, and to control how the triangles are distributed along the open boundaries.

OpenTELEMAC supports a full range of coordinate reference systems (CRS) on which the model geometry can be defined. For the development of the regional models for the two sites, it was decided that a Universal Transverse Mercator (UTM) projection would be used for the CRS. The specific UTM used is the WGS84 UTM Zone 30N (or EPSG:32630). The UTM allows all spatial measurements to be made in metres and simplifies the generation of a coastline to the required spatial scales. The vertical position is set relative to mean sea level (MSL). The limitations of a UTM coordinate systems is that the lengths are distorted with latitude, the closer to the poles the greater the distortion. For the location and areas being modelled this distortion is considered negligible. All time stamping is referenced to UTC, this is the same time reference standard used for *in-situ* data collection.

Iroise Sea Model	
CRS: WGS84 UTM Zone 30 Area: ~ 165km x 195km Bathymetry: SHOM HOMONIM 100m Bottom Friction: EMODnet Substrate Tidal Forcing: OSU TPXO AO2011 Solver: OpenTELEMAC v8p2r0	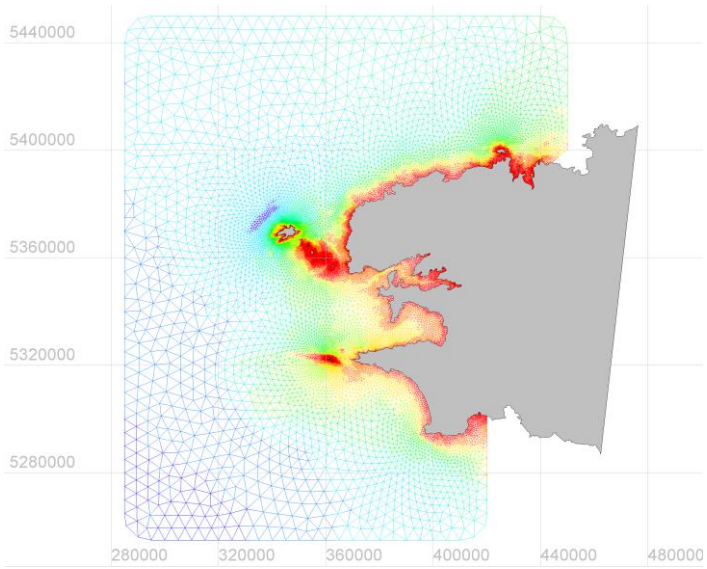

Figure 5-2: Iroise Sea model domain description

The extent of the Iroise Sea model was chosen to get the majority of the open boundary into areas where there are reliable tidal forcing records, and to encompass the key coastal and areas of persistent large-scale flow structures relevant to Fromveur Strait dynamics. A set of four model meshes were constructed that vary the mesh resolution through Fromveur Strait and the extent beyond the Strait that the high-resolution mesh component covers. For each model the outer domain was kept the same and only the interior mesh was modified. The reason for this approach was to keep the open-boundary forcing the same for all construct so the impact of the internal mesh can be determined. Figure 5-2 shows the full model domain with a brief description of the construct.

Iroise Sea - MODEL A	
Mesh Statistics Number of Nodes: 48040 Number of Elements: 91039 Number of Layers: 11 Min. Edge Length: 4m Max. Edge Length: 8330m Fromveur Edge Length: ~30m Mainland Edge Length: ~250m Open Boundary Edge Length: ~5000m Mid-Channel Edge Length: ~200m	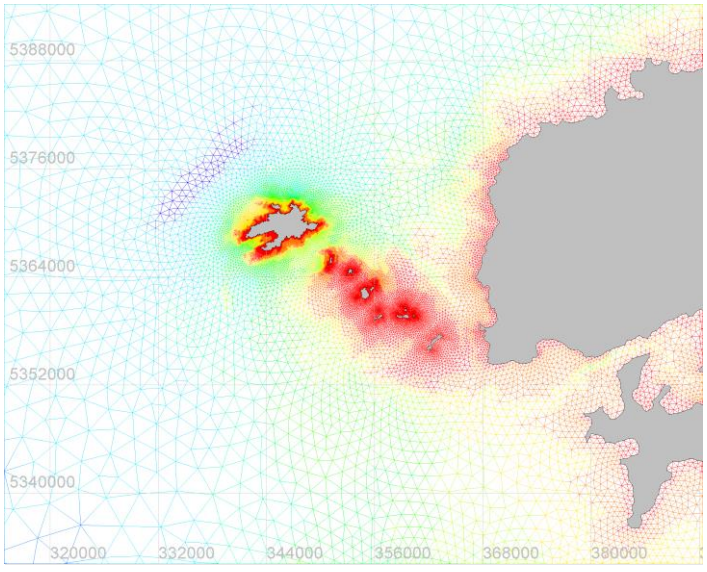

Figure 5-3: Iroise Sea MODEL A mesh description

MODEL A is the most basic form of mesh where the only constraints of the mesh resolution are the coastline and open boundary resolution and the chosen element growth rate. This gives limited control

on the mid-channel mesh resolution in the Fromveur Strait. This model has the lowest overall resolution so is the cheapest and fastest to run. Figure 5-3 shows the mesh over the Fromveur Strait and surrounding Islands with a list of the relevant mesh statistics.

Iroise Sea - MODEL B	
Mesh Statistics Number of Nodes: 54440 Number of Elements: 98944 Number of Layers: 11 Min. Edge Length: 4m Max. Edge Length: 7370m Fromveur Edge Length: ~30m Mainland Edge Length: ~250m Open Boundary Edge Length: ~5000m Inner Mesh Edge Length: 50m Outer Mesh Edge Length: 500m	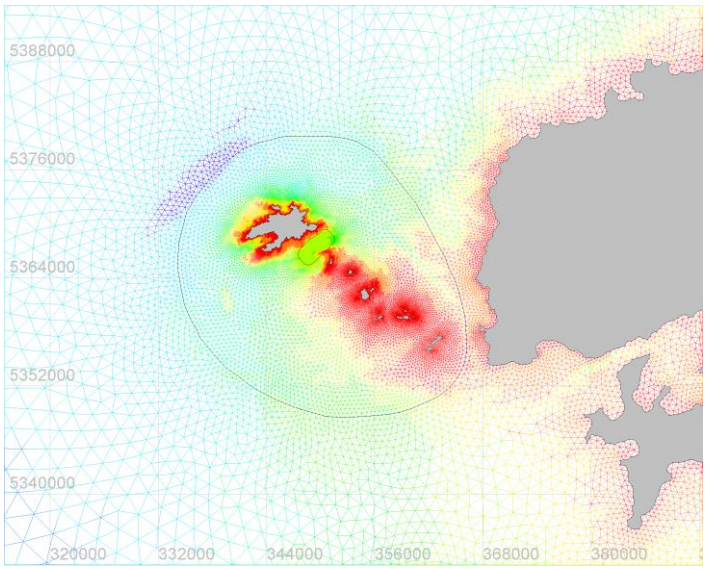

Figure 5-4: Iroise Sea MODEL B mesh description

In MODEL B the centre of Fromveur Strait has be forced to 50m resolution elements by the inner sub-mesh. This is then extended out to the outer sub-mesh which has a fixed edge length of 500m to limit the growth. This sub-mesh is then extended out to the open boundary which has a fixed edge length of 5000m. This represents the IEC recommendation for site characterisation. Figure 5-4 shows the boundaries of the inner and outer sub-mesh domains and the associated change in resolution and lists the key mesh statistics. The number of elements in this mesh about 12% more than the simple mesh of MODEL A, so there is a small increase in computational cost.

Iroise Sea - MODEL C	
Mesh Statistics Number of Nodes: 191455 Number of Elements: 377926 Number of Layers: 11 Min. Edge Length: 4m Max. Edge Length: 7495m Fromveur Edge Length: ~30m Mainland Edge Length: ~250m Open Boundary Edge Length: ~5000m Inner Mesh Edge Length: 50m Outer Mesh Edge Length: 500m	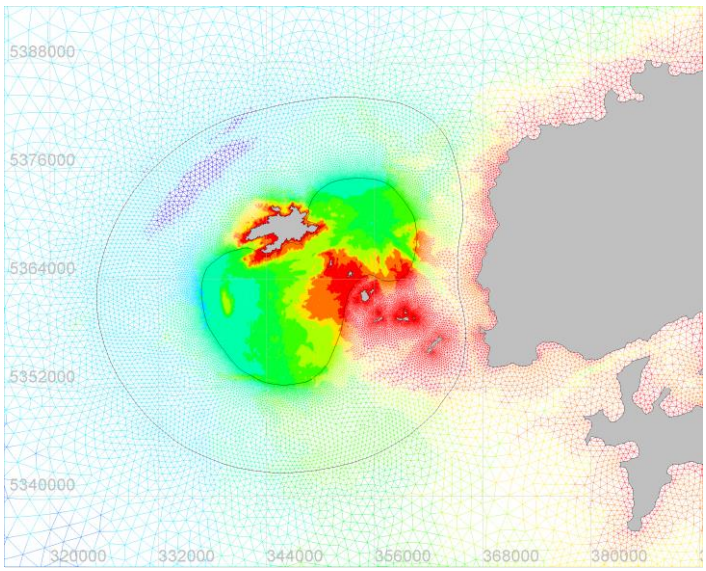

Figure 5-5: Iroise Sea MODEL C mesh description

MODEL C takes this a step further by extending the 50m resolution inner sub-mesh to cover the areas where the large-scale tidal eddies persist. The outer sub-domain has been extended to better encompass the inner sub-mesh. Figure 5-5 shows the impact of the extended inner and outer sub-meshes on resolution and lists the key mesh statistics. The number of elements in this mesh is 3.5 times that of the MODEL B mesh, therefore it imposes a significantly high computational cost.

Iroise Sea - MODEL D	
Mesh Statistics Number of Nodes: 490722 Number of Elements: 971580 Number of Layers: 11 Min. Edge Length: 4m Max. Edge Length: 7680m Fromveur Edge Length: ~30m Mainland Edge Length: ~250m Open Boundary Edge Length: ~5000m Inner Mesh Edge Length: 50m Outer Mesh Edge Length: 500m	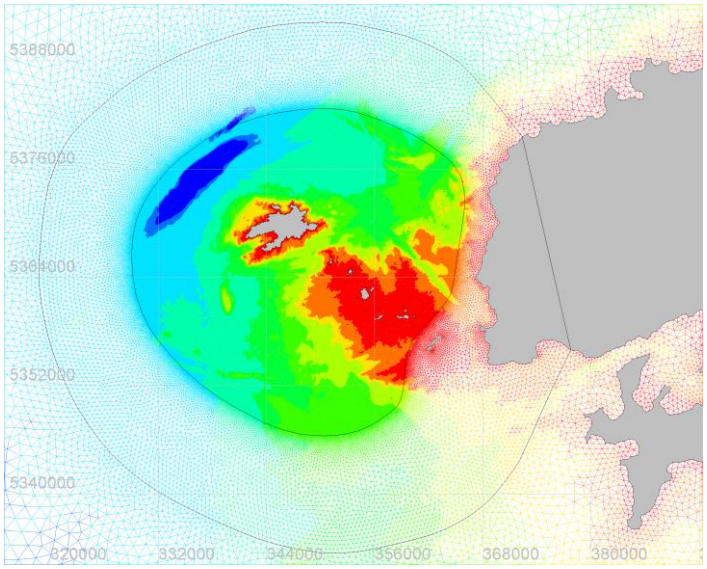

Figure 5-6: Iroise Sea MODEL D mesh description

Finally, MODEL D is the most extensive of the mesh constructs. It aims to capture the full dynamical response change by including the by-pass around Ushant. This mesh has 2.5 times the number of elements in MESH C and 9 times the number of mesh elements in MODEL B. This is a very computationally expensive mesh to run. Figure 5-6 shows the extent of the inner and outer sub-meshes and lists the key mesh statistics.

The extent of the Orkney Islands model was chosen to cover the areas in Northern Scotland where marine renewable energy development is active. The open boundary was extended to a distance sufficiently to avoid the blockage of large-scale fluid processes and to get the best possible open-boundary forcing. The domain was set with a view to future extension to include wave forcing, the domain in this case requires a sufficient distance to reproduce the fetch for local wind-generated waves. The full domain is shown in Figure 5-7.

Orkneys Model	
CRS: WGS84 UTM Zone 30 Area: ~ 145km x 155km Bathymetry: EMODnet 100m Bottom Friction: EMODnet Substrate Tidal Forcing: OSU TPXO ES2008 Solver: OpenTELEMAC v8p2r0	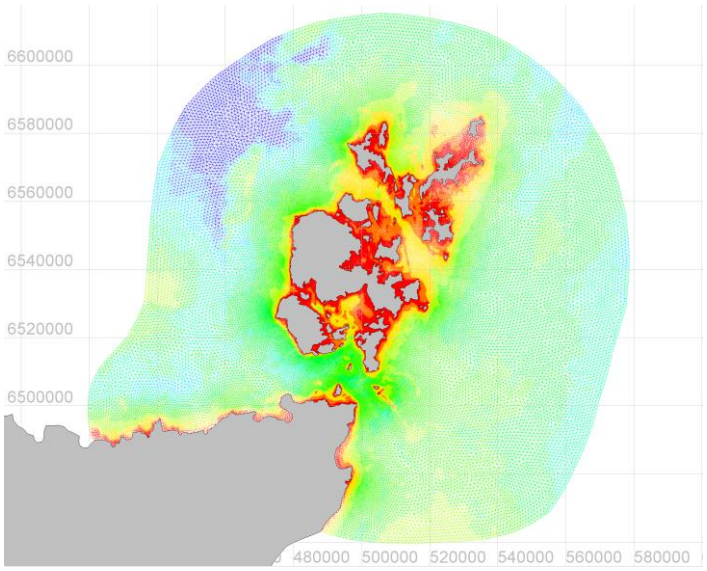

Figure 5-7: Orkney base model domain description

Two separate meshes where constructed for intercomparison, these are shown in Figure 5-8 and Figure 5-9. In the construction of the first mesh, BlueKenue was set to build the mesh using a 10% growth rate from the boundaries. Resolution across the Falls of Warness was controlled by the resolution of the Island coastline. The second mesh included a 10m resolution region covering the Falls of Warness. The purpose of this model was to support the analysis of the ReDAPT data sets.

Orkneys Model – ORK_BASE	
Mesh Statistics Number of Nodes: 157699 Number of Elements: 296828 Number of Layers: 15 Min. Edge Length: 6m Max. Edge Length: 1530m Falls of Warness Edge Length: ~30m Mainland Edge Length: ~200m Open Boundary Edge Length: ~1000m Mid-Channel Edge Length: ~80m	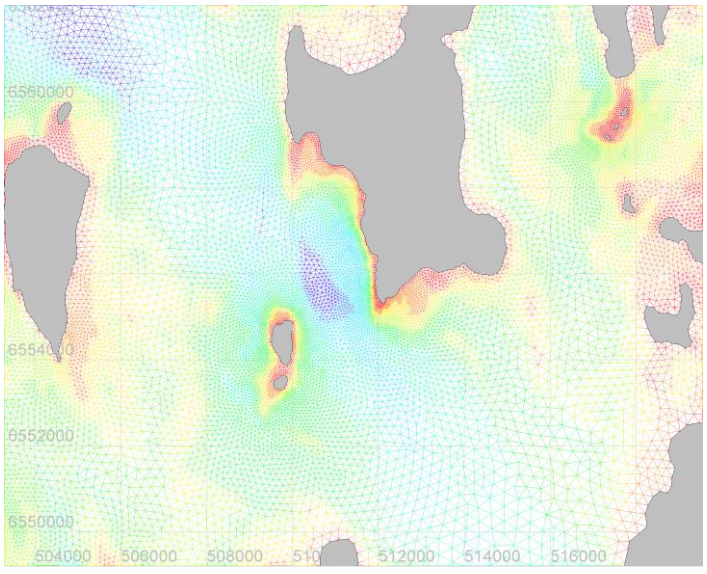

Figure 5-8: Orkneys base model mesh description

Orkney Model – FOW_HiRes	
Mesh Statistics Number of Nodes: 319227 Number of Elements: 629450 Number of Layers: 15 Min. Edge Length: 6m Max. Edge Length: 2355m Falls of Warness Edge Length.: ~30m Mainland Edges Length: ~200m Open Boundary Edge Length: ~1000m Inner Mesh Edge Length: 10m	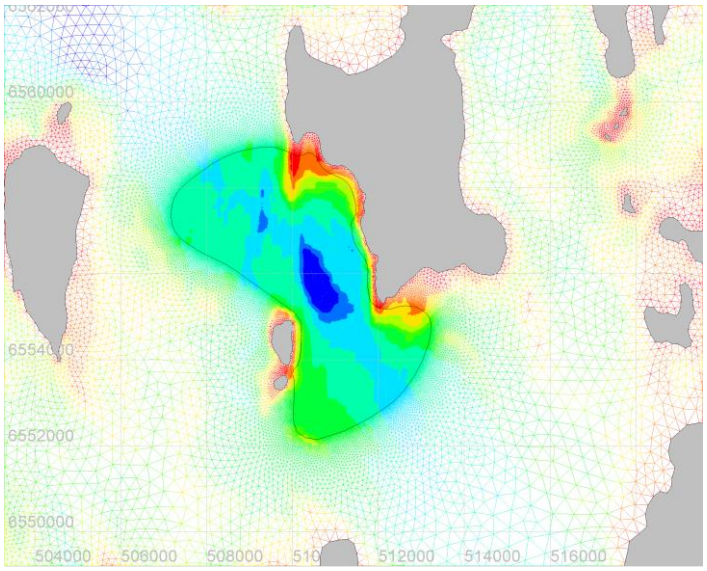

Figure 5-9: Orkneys Falls of Warness high-resolution mesh description

5.3.2 Bathymetry and Bottom Friction

The bottom topography of the model domains was derived from standard data archives. The bathymetry for the Iroise Sea models was taken from the Homonim Atlantic bathymetry data set (MNT_ATL100m_HOMONIM_WGS84_NM_ZNEG) provided by the French Naval Hydrographic and Oceanographic Service, SHOM. These data are nominally at 100m spatial resolution provide on a regular Lat/Lon grid using the WGS84 spherical CRS. In this dataset the bathymetry is defined as a vertical elevation relative to mean sea level (i.*e.* the depths are negative values). A subset of these data covering the model domain were extracted and converted, using QGIS, to WGS84 UTM CRS for mapping onto the model mesh.

The bathymetry for the Orkneys model was extracted from the EMODnet bathymetric archive. This data archive has been standardised from data collected from a wide range of European source and has been strictly quality control. The data can be extracted to give depths relative to MSL. Over the Orkneys the spatial resolution is approximately 60m x 100m. As with the SHOM data the WGS84 spherical CRS is used to reference the data, QGIS was used to transform the coordinate system for mapping to the model.

Guillou & Thiébot [16] showed that including spatially varying bottom friction in regional models improved model accuracy and reduced tuning requirements. For both models the EMODnet EUSM2019 substrate class data covering the European shelf were used to generate maps of the bottom friction coefficient. This was achieved by mapping the substrate class data to C_{100} values taken from the literature. The C_{100} values were mapped onto the model nodes and converted to the required friction coefficient values. The mapping from substrate data onto the model nodes was done in QGIS, and the generated shape file with the friction coefficients was used to define the OpenTELEMAC bottom friction map in BlueKenue. Bottom friction values for the Manning, Chezy and Nikuradse friction models were calculated.

5.3.3 Open Boundary Forcing

OpenTELEMAC supports the Oregon State University (OSU) OTIS tidal solution based on the TPXO global tidal model data. The TPXO model assimilates available satellite altimetry data to constrain the

model tides to the observational state. There are a variety of solutions with different resolutions and spatial coverage. The FES2014 tidal harmonic atlas is a more up to date archive but is not currently supported directly in OpenTELEMAC. The data need to be extracted into a suitable harmonic constituent file, and the OpenTELEMAC code modified to read this file.

It was decided that the OSU tidal atlas was sufficient for the purposes of the work in D2.2. The AO2011 atlas was used for the Fromveur model. This atlas covers the Atlantic Ocean including the European Shelf waters. The ES2008 atlas was used for the Orkneys model. This atlas covers the Northern section of the European Shelf and is at higher spatial resolution compared with the AO2011 atlas. The ES2008 data do not cover the Fromveur Strait region.

Only the impact on mesh definition on the core hydrodynamic response is being investigated through the current set of models, for this reason the surface forcing by winds have not been included, and for reasons discussed earlier the wave-current interactions have not been modelled.

5.4 Model Numerical Setup

The user defines all of the model run options in a steering file which is passed to the OpenTELEMAC run script. For both models the same turbulence, wetting-drying, and numerical options were used. The values chosen have been found to produce the most reliable and stable solutions, allowing runs that cover long time periods to be produced. The key parameters used for model numerical options are collated in Table . The model by default uses a sigma layer scheme for the vertical model levels, which distributes the layer thicknesses from the bed to the sea surface according to a given functional form. As the surface elevation varies with time, the layer thicknesses also vary with time as the number of layers remains constant. Special rules are applied to cells that can dry out. The wetting/drying process is controlled by parameters in the steering file.

5.5 Model Runs

Each model construct has to be spun-up to allow any start-up transients to decay away. It was found that this could take between 6 to 12 hours of model time. To ensure there are no transients in the model data extracted, all models are spun-up for 24 hours. To simplify data management and limit data file sizes, models are run on a daily cycle using the model restart functionality in OpenTELEMAC; the final step of each daily run is stored as the restart point for the next daily run. For a given model run the only fields that change in the steering file are the input and output file names, all other parameters remain the same. The steering file is a simple text file, so running sequential days for a given construct was controlled by a script that created a new steering file for each day run. This allowed a set of days to be run as a single job on the server. This script could be modified to add more days to the end of a sequence simply by identifying the starting day for the new data.

The various model constructs were run for periods of time that overlap with available *in-situ* site data to allow a given construct to be validated, and to allow the quality of the *in-situ* ADCP data to be assessed. This second case is an import point which will be discussed in the following sub-section. Given the size of the model constructs it is not possible to store the output for every model time step. A set of 2-D and 3-D model fields were captured at 5 minute intervals. This interval was chosen to match the nominal time-windowing used to post-process the in-situ data for parameter extraction and subsequent integration with the database being constructed for RealTide D2.3. The fields stored are listed in Table . The 2-D data are store as functions of the timestamp T and the model node number N, and the 3-D data are stored as functions of the timestamp T, the model layer L. and the model node number N. The node locations and element sets (i.e. the nodes that define each triangle) are stored with the 2-D output, these are used to reconstruct full 2-D and 3-D maps of the fields.

Table 5-2: OpenTELEMAC numerical setup parameter values

Condition	Setting
NON-HYDROSTATIC VERSION	YES
HYDROSTATIC INCONSISTENCY FILTER	YES
CORIOLIS	YES
FREE SURFACE GRADIENT COMPATIBILITY	0.5
TIDAL FLATS	YES
BYPASS VOID VOLUMES	YES
OPTION FOR THE TREATMENT OF TIDAL FLATS	Corrected free-surface gradient
TREATMENT OF NEGATIVE DEPTHS	Flux control
OPTION FOR LIQUID BOUNDARIES	Thompson characteristics
LAW OF BOTTOM FRICTION	Nikuradse Formula
FRICTION COEFFICIENT FOR THE BOTTOM	From Geometry File
LAW OF FRICTION ON LATERAL BOUNDARIES	Nikuradse Formula
FRICTION COEFFICIENT FOR LATERAL SOLID BOUNDARIES	0.01
HORIZONTAL TURBULENCE MODEL	Smagorinski
TURBULENCE REGIME FOR LATERAL SOLID BOUNDARIES	Rough
VERTICAL TURBULENCE MODEL	Mixing Length
MIXING LENGTH MODEL	Prandtl
DAMPING FUNCTION	Munk and Anderson
SCHEME FOR ADVECTION OF VELOCITIES	Characteristics
MAXIMUM NUMBER OF ITERATIONS FOR ADVECTION SCHEMES	3500
TREATMENT OF FLUXES AT THE BOUNDARIES	Priority to prescribed values
MAXIMUM NUMBER OF ITERATIONS FOR DIFFUSION OF VELOCITIES	3500
ACCURACY FOR DIFFUSION OF VELOCITIES	1.E-8
PRECONDITIONING FOR DIFFUSION OF VELOCITIES	Diagonal
ACCURACY FOR PROPAGATION	1.E-8
MAXIMUM NUMBER OF ITERATIONS FOR PROPAGATION	1500
PRECONDITIONING FOR PROPAGATION	Diagonal
SOLVER FOR PROPAGATION	Conjugate residual
INITIAL GUESS FOR DEPTH	$\partial h = \partial h_n$
MAXIMUM NUMBER OF ITERATIONS FOR PPE	1500
ACCURACY FOR PPE	1.E-8
PRECONDITIONING FOR PPE	Direct solver on vertical
SOLVER FOR PPE	Conjugate gradient
IMPLICITATION FOR DEPTH	1.
IMPLICITATION FOR VELOCITIES	1.
IMPLICITATION FOR DIFFUSION	1.
MASS-LUMPING FOR DEPTH	1.
MASS-LUMPING FOR VELOCITIES	1.
MASS-LUMPING FOR DIFFUSION	1.

Table 5-3: Model fields stored for each run

Field Type	Model Variable	Description
2-D	U(T,N)	Depth-averaged eastward component of velocity
	V(T,N)	Depth-averaged northward component of velocity
	H(T,N)	Total water depth (bathymetry + surface elevation)
	S(T,N)	Surface elevation
	B(T,N)	Bathymetry (or mean water depth)
	W(T,N)	Bottom friction
3-D	Z(T,L,N)	Sigma layer positions
	U(T,L,N)	Eastward component of velocity
	V(T,L,N)	Northward component of velocity
	W(T,L,N)	Upward component of velocity.

The Iroise Sea models were run to coincide with legacy *in-situ* data provided by Sabella early in the project. These were ROWE RTI data that Sabella were not able to interrogate. We developed extraction software for these data as part of the post-processing work of this work package. These *in-situ* data run from the 08/10/2016 to 29/11/2016. The four versions of the model have been run for 14 days covering the 14/10/2016 to 27/10/2016, giving a single spring-neap tidal cycle. The run statistics are given in Table . All four models were run with a 5 second time step to ensure both model convergence for all constructs and consistency in run conditions out with the mesh construction.

Table 5-4: Iroise Sea model run information

Model	Time Step	N Days	N Layers	Average Run Time per Day	2-D File Size (GB)	3-D File Size (GB)	Data Volume (GB)
MODEL_A	5	14	11	00:27:49	0.3	2.3	39.2
MODEL_B	5	14	11	00:31:29	0.4	2.6	44.4
MODEL_C	5	14	11	04:00:49	1.2	9.2	156.3
MODEL_D	5	14	11	10:06:48	3.2	23.5	400.7

The Orkney models were run to cover some or all of the ReDAPT deployment period of the two ADPC's (TD7_01 & TD7_02) deployed either side of the DeepGen IV turbine. This period was chosen as these data are situated in ambient flow and highlighted significant differences in the vertical profiles of the horizontal velocities between the two locations, which are approximately 80m apart. The purpose of these two model constructs (medium and very high resolution) is to determine possible reasons for the observed variations in flow structures. The medium resolution model will be used to map statistical features of the flow across the site.

The medium resolution model was run for 90 days. The model was with a 10 second time step to allow the 90 days to be run in a reasonable time, while ensuring an acceptable level of model convergence. The size of the very high-resolution model construct could only be run for a limited number of days. A time step of 2 seconds was required for convergence and numerical stability leading to long computational times on the available 48 cores. This model is at the limit of the server capabilities. The density of the model nodes leads to very high data volumes being generated for the 5 minute sub-sampling. This the very high-resolution model was run for 14 days, covering a spring-neap cycle. A separate short run of the very high-resolution model was carried out to collect for every time step into hourly files. This was run for 14 hours covering a tidal cycle. These high-frequency data can be used to investigate the impacts of sub-sampling the model to instantaneous 5 minute output.

Table 5-5: Orkneys model run information

Model	Time Step (s)	N Days	N Layers	Average Run Time per Day	2-D File Size (GB)	3-D File Size (GB)	Data Volume (GB)
ORK_BASE	10	90	15	01:15:32	1.0	10.3	680.0
FOW_HiRes (daily)	2	14	15	29:48:00	2.1	20.9	321.2
FOW_HiRes (hourly)	2	0.5	15	00:27:49	5.2	51.7	796.5

5.6 Model Convergence, Calibration and Validation

There are three stages to the process of optimizing a numerical simulation: (1) convergence of the solution, (2) calibration of the controlling parameters, and (3) validation of the final output. The purpose of the convergence test is to determine the largest time step that can be used that produces results that lies within some predefine tolerance. Calibration is a process of modifying model input parameters and boundary conditions to move the solution closer to observed values. Validation is a statistical comparison of the final model version against observations. The validation observations should be independent of the calibration observations, ideally both in time and space. This last requirement is not always possible.

5.6.1 Convergence

Convergence is determined by running the model for a fixed length of time beyond the spin-up period for a range of different time steps, then comparing changes in model field predictions in the key region of interest. For convergence the amount the predicted fields change should reduce as the time step size decreases, to a point where the variation is considered negligible. Convergence testing is applied to the region(s) of interest(s) within in the model domain, e.g. for the Iroise Sea model the center of the Fromveur Straits is the region of interest, and for the Orkneys model it is the EMEC tidal energy test site in the Falls of Warness.

Changing the time step will change the system response across the entire domain, so a set of integrated parameters that characterize the dynamics should be used to test convergence. Given we are interested in the available energy at a given site, a measure of volume flux is an obvious choice of metric. A transect across the region of interest perpendicular to the dominant flow direction can be used to calculate the total volume flux passing through a cross-section of the strait or channel. The transect area will vary over a tidal cycle as the tide rises and falls, the mean of the transect area over a tidal cycle is another suitable metric.

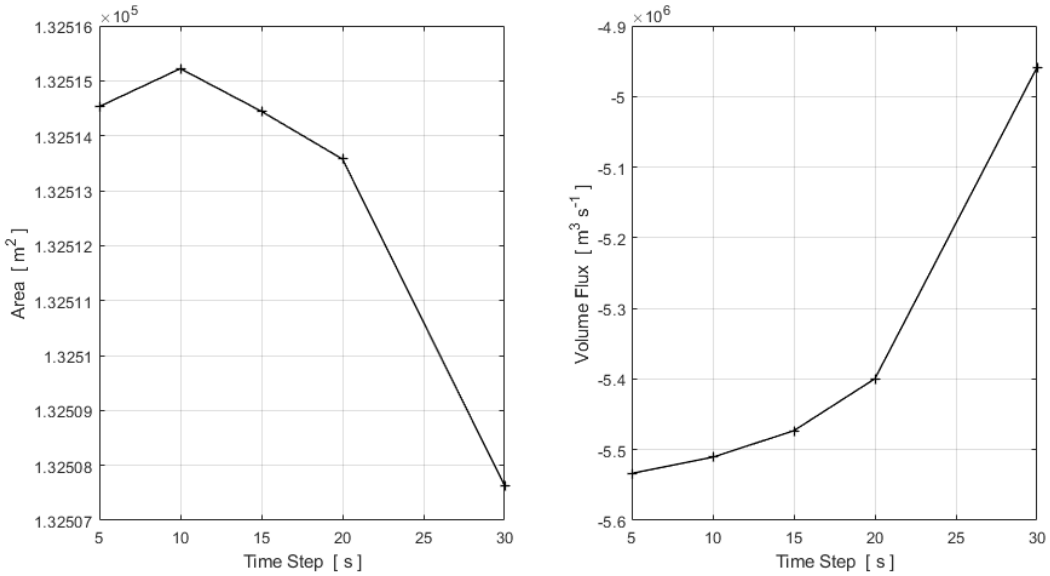

Figure 5-10: Result of convergence test applied to Iroise Sea MODEL_B construct

This process was applied to the various Iroise Sea model constructs. Figure 5-10 shows the results for the MODEL_B construct for the time steps 5s, 10s, 15s, 20s, and 30s. These data show that the variation in both the total volume flux and the mean cross-sectional area of the transect begin to plateau after the time step falls below 10s. Similar results were found for the other constructs, however it was found that the high-resolution model became unstable after a longer period run for a time step of 10s. It was decided that a 5s time step would be used for all Iroise Sea models to allow controlled inter-comparisons of the results. The convergence test was also applied to the Orkneys model. For the ORK_BASE model similar results were found. It was decided that a time step of 10s would be used for this construct as the intent was to generate a 90-day dataset. The high resolution FOW_HiRes model was numerically unstable for time steps greater than 5s; a time step of 2s was chosen for the 14-day run of this construct to produce the best possible results within the constraints of the computing facility.

5.6.2 Calibration

Model calibration is the process of modifying the model boundary conditions to improve agreement with observed states [80]. This is often required when the model construct provides a poor representation of the physical state. The parameters most commonly modified when calibrating hydrodynamic tidal models are the bottom friction, mean water depth, and the amplitude and phase of the open boundary forcing. All of these modifications are artificial and they are based on the assumption that the *in-situ* measurements are correct. The effect of modifying the bottom friction is to either remove (increasing friction) or add (decreasing friction) linear momentum to the flow. The consequence is a change in the vertical shear profile of velocity. In high-energy tidal straits this will modify other fluid processes in a non-linear manner. Altering the water depth adds mass to the system and will modify the hydraulic response to the tidal forcing. This will change the spatial variation in surface gradients that result from flow blockage by obstacles such as islands. A local correction may have significant impacts elsewhere in the model domain. Modifications to the tidal forcing amplitudes and phase is complicated as there is a non-linear relationship between the tidal harmonics.

The aim of the models constructed for this analysis was to get them as accurate as possible without applying calibrations. This is achieved by using the best available boundary conditions (bathymetry and tidal forcing), incorporating spatially varying bottom friction, and using a well-defined coastline. The

model is only ever going to be an approximation to the real-world state. What is more important is the quantification of the difference between the model and the observations, acknowledging the observations have inherent uncertainties. This approach also allows the impact of the mesh construction in the absence of artificial modifications to be determined. Therefore, none of the models present have been *calibrated*, i.e. none of the boundary parameters have been artificially modified.

5.6.3 Validation

There are two key fields that can be validated in a hydrodynamic tidal model. These are the surface elevation variation in time and space due to the open boundary tidal forcing, and the 3-D velocity flow structures that result from the tidal forcing. Data available for the validation of the predicted surface elevation are tide gauge data, pressure sensor data, and satellite altimetry data. Data available for validation of the 3-D velocity predictions are limited to *in-situ* velocity profile time records. The *in-situ* velocity data can come from either fixed moorings of vessel-base moving surveys.

Tide gauge data are the least appropriate for surface elevation validation as these are predominantly collected very close to the shore, where the models are limited by the resolution of the mesh and underlying bathymetry data, while the tide gauge data are strongly affected by local weather events and small-scale structures. Pressure sensor data collected from seabed moorings provide better quality data (dependent on the distance of the mooring from the shore) as they less affected by near-shore processes, but they are limited by the deployment length and only provide information for a single point in the model domain. Satellite altimetry data give the best temporal and spatial resolution but are limited to locations that are greater than 10km from land.

The CTOH along-track sea level altimetry data are available as the X-TRACK SLA archive on the AVISO data service. The X-TRACK data are regional altimetry product derived from Topex, Jason 1 & 2, GeoSat, ERS2 and ENVISAT data. Optimal corrections in coastal areas are applied as described by Birol et al. [81]. The data provide the tidal harmonics at the along-track sample locations for the various satellites used to derive the data. There is a track that runs through the Fromveur Strait; these data have been used to validate the model prediction of the surface elevation.

A harmonic reduction of the surface elevation data is applied to time series extracted from the model at the X-TRACK data locations. The length of the model time-series is too short to resolve all harmonics provided in the X-TRACK record. The length of the model time series also limits how accurately the phase of the harmonics are predicted, this is because the tidal fitting process distributes as much of the energy in the signal as possible into the available harmonics. The energy from harmonics that are close together in frequency and cannot be resolved, is placed in the dominant frequency, the resulting phase will be some form of average of the unresolved and resolved harmonics. The expectation is that the amplitude of the dominant tidal harmonics will be correct, but the phase will be significantly different for the higher-frequency constituents.

Figure 5-11 show the comparisons for the amplitudes of the first six dominant constituents resolved by the model data. The x-axis is the along-track location number in increasing order from west to east. The discontinuity between 19 and 20 is due to the Fromveur Strait where there is no validation returned from the satellite altimetry. The effect of the Strait on the altimetry data can be seen in the error bars of the M4, MS4 and N2 data at the western end of the Strait (location 19). The harmonic reduction software used to reduce the model data return errors for the estimate constituent data. It can be seen that for the dominant constituents the error bars all overlap, so within the constraints of the limited model time series length, the model is predicting the tidal elevation to a reliable level.

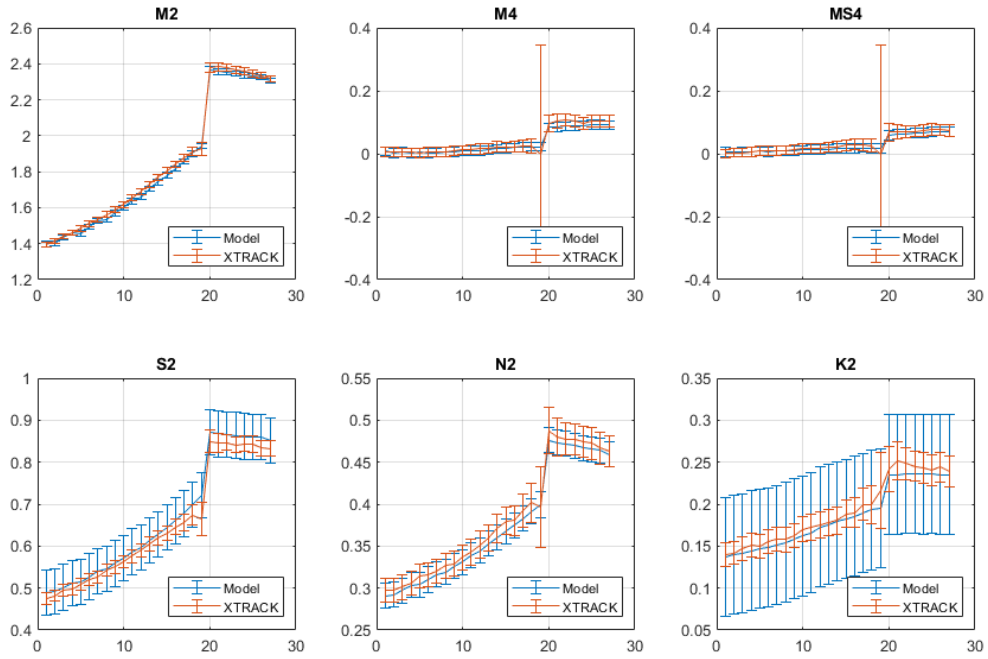

Figure 5-11: Iroise Sea MODEL_B surface elevation validation against X-TRACK altimetry data, comparison of the first six dominant constituents resolved.

Figure 5-12 shows the difference between the predicted and observed phase angles for the first six dominant constituents resolved from the model data. The M2 tidal constituent is the most dominant of all and has a very small phase bias (between +/- 0.6 degrees, this corresponds to +/- 2.5 minutes in time), but as expected the phase difference for the other constituents are large. Based from the value for the M2 tide phase difference, the models reliably predicting the phase of the key lunar tide.

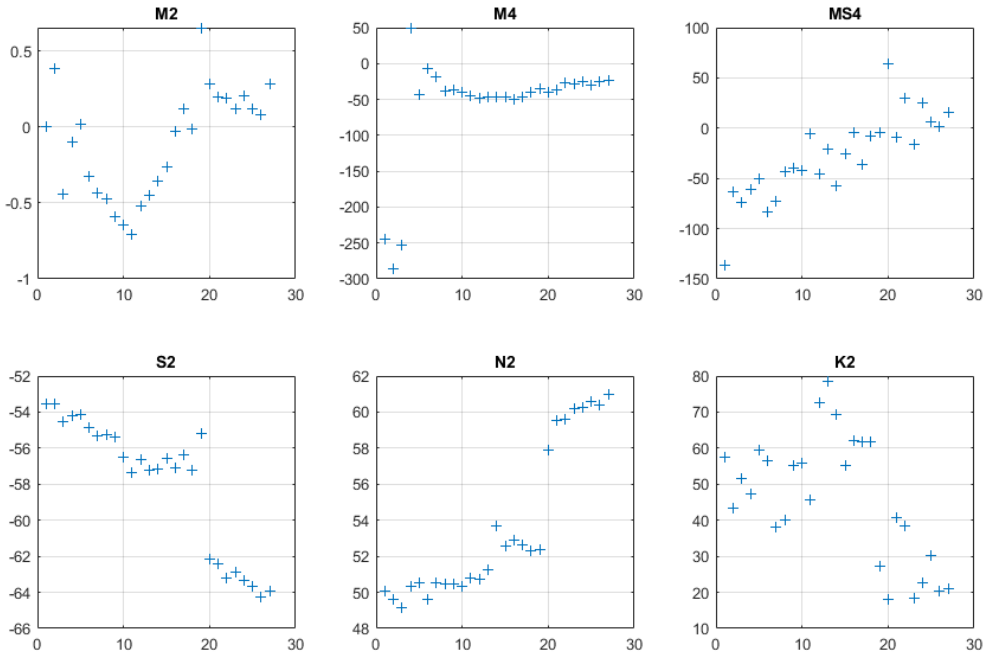

Figure 5-12: Iroise Sea MODEL_B surface elevation validation against X-TRACK altimetry data, phase angle differences for the first six dominant constituents resolve.

Validation against *in-situ* velocity data is more complicated as these data inherently contain signals from all physical processes that affected the site where and when the data were collected, while the model is only predicting the 3-D flow field formed in response to tidal forcing and the flow interaction with the resolved topographic features. ADCP's are typically used to collect velocity data at the locations of interest (as per the IEC guidance). These instruments are designed to operate in waters where there is little or no horizontal velocity gradient, i.e. ADCP's are not optimally designed to operate in high-energy tidal flow locations. This is a fundamental limitation base on the beam geometry of these instruments. Any horizontal velocity gradient across the ADCP beam spread cannot be resolved, so it is distributed between the estimated horizontal and vertical velocity components in the plane of a given beam pair. This leads to an inherent bias in the velocity magnitude and direction which varies with flow speed and with distance from the ADCP transducer head. Ideally the model constructs should be validated against measurements made in open water away from strong shear flows. For tidal developers these data are generally not available.

To date there is no adequate measure of the uncertainty in the ADCP velocity data due to the presence of strong velocity gradients. Without this measure of uncertainty, it is not clear how to interpret bias between the modelled and observed velocity data collected at high-energy tidal sites. A further issue to be considered is whether the ADCP data were collected in the presence or absence of a TEC and/or its support infrastructure. The IEC guidance recommends collecting data upstream and downstream of TEC's. At these locations the instruments will be measuring the TEC and/or support structure wake on one half of the tide. Therefore, data collected in these conditions only provide reliable information for half of a tidal cycle. This is the case with the small set of available *in-situ* data for Fromveur Strait. The uncertainty in the model estimates of the velocity data is not easily defined, limiting how well the validation process can be defined.

The key purpose of the models developed is to determine the impact of model construct on the estimation of the available power, and to better map spatial variability. To assess the model performance, a set of classification metrics are used that capture the principle long-term features of the flow. It is assumed that if these metrics are well matched then the model will provide a reliable estimate of the available power. These metrics will be calculated for a typical hub-height to simplify the processing of long time series data and the issues associated with the time varying sigma-layer depths for the model. These metrics are calculated from the model at the location of the validation data set.

The key long-term features of the flow at a location are:

- Peak flood and ebb flow directions
- Difference in the flood-ebb direction (directional asymmetry)
- Percentage of time in flood and ebb (temporal asymmetry)
- Mean and maximum flood and ebb flow speeds (tidal flow asymmetry)
- Total power
- Total stream-wise power

The height above bed chosen for model validation is 20m. The metric values for the Fromveur Strait models are presented as differenced from or ratio to the *in-situ* measured values, this has been done as these data are commercially sensitive. The data are presented in Table 5-6.

Table 5-6: Fromveur Strait model flow validation metrics (flood cases highlighted)

	MODEL A	MODEL B	MODEL C	MODEL D
$\Delta\theta_{flood}^{peak}$	1.4°	1.2°	1.2°	1.2°
$\Delta\theta_{ebb}^{peak}$	3.5°	3.7°	3.7°	3.7°
$\Delta\theta_{diff}^{peak}$	2.0°	2.4°	2.3°	2.4°
Ratio Max. Flood Speed	1.00	1.03	1.03	1.05
Ratio Mean Flood Speed	1.06	1.06	1.06	1.06
Ratio Max. Ebb Speed	1.05	1.08	1.13	1.11
Ratio Mean Ebb Speed	1.12	1.18	1.18	1.24
Ratio P_{flood}	1.2	1.3	1.3	1.3
Ratio P_{ebb}	1.7	1.8	1.8	1.9
$\Delta(\% \left\|\theta_{flood} - \theta_{flood}^{peak}\right\| < 5°)$	13.4%	7.0%	-0.4%	0.0%
$\Delta(\% \left\|\theta_{ebb} - \theta_{ebb}^{peak}\right\| < 5°)$	13.9%	10.4%	7.8%	10.4%

In general, the model predictions for the flood tide are closer to the observations than the ebb tide; this is expected as the instrument is in the wake of the TEC during the ebb tide so the flows are both slowed and the direction may be altered. We will only discuss the flood tide data, given the *in-situ* ebb tide data are not representative of the free stream flow. All models predicted very similar peak flood directions, with a constant bias between 1.2° and 1.4°. This could easily be due to compass error in the *in-situ* data, the compass error is typically of the order ±2°. The models over-predict the maximum flood speed by up to 5% and the mean flood speed by up to 6%. This translates into a 20% to 30% over estimation in the available power. It was found that the model predicted the neap tide magnitudes very well, but over-predicted the spring tides. During the spring tides the peak flows of the *in-situ* data where clipped, suggesting the presence of other physical processes, *e.g.* surface waves and swell, or wind driven blockage. This reinforces the problem posed by trying to "calibrate" a model to fit observations when the model does not include all physical drivers. The last metric is the percentage of flow that is within ±5° of the peak direction. This gives an indication of how much of the non-tidal processes that result from flow interaction are being captured by the model. What we find is that MODEL A does not reproduce as much of the directional variability as observer (i.e. 13.4% more time is spent aligned with the peak flow), as the model complexity increases the difference reduces, to the point where MODEL D is producing the same percentage as the *in situ* data.

Based on the above analysis, the set of Iroise Sea models are considered to be suitable for studying the impact of model mesh design on energy predictions. The analysis has highlighted that more work is required to determine how best to use *in situ* data collected in high-energy tidal site for model calibration and validation exercises.

6 FLOW CLASSIFICATION METRICS

The observed flow at a given location and depth in a tidal site is affected by the tidal forcing, hydraulic adjustments due to the presence of obstacles to the flow, local weather events, and remotely generated storm swell. These processes operate over a range of time scales, and a wide range of frequencies. In response to the various forcing processes a variety of different fluid structures are formed which also vary over a range of time scales and frequencies. To adequately classify the flow at a given point in the fluid domain we need a set of metrics that capture this range of processes and fluid response.

At the most fundamental level the observed flow is driven by the gravitational tidal forcing, this is the dominant force acting on the fluid. In the absence of obstacles, weather, *etc.*, the flow at a point in the fluid would be rectilinear with a dominant flow direction, and the magnitude of the flood and ebb flow would be the same. The presence of obstacle such as islands, channels, etc., produce blockages to the flow that the fluid must go around. These processes produce an asymmetry in the dominant flow

direction between the flood and ebb tides. Hydraulic heads are formed as a result of flow blockage caused by obstacles which result in persistent mean residual flows that are required to balance the flow dynamics. This dynamic readjustment leads to an asymmetry in the maximum flow speed between the flood and ebb tides.

The fluid is viscous so any gradient in the fluid velocity will produce a shear force which is resisted by the internal fluid friction that results from the viscosity. This leads to the generation of fluid rotation or vorticity. An accelerating flow with a velocity gradient will generate rotation which tends to form into coherent rotational structures, or eddies. Eddies extract linear moment from the flow and store the energy as rotational momentum. These structures are called the energy containing eddies formed by an enstrophy cascade. The laws of thermodynamics require this energy to be dissipated, this is achieved through fluid friction which creates an ever diminishing scale of eddies within the macro-scale structures, which eventually lead to dissipation of energy as heat once the molecular scales are reached. These smaller scale structures are the fluid turbulence, and the turbulence cascade to dissipation is defined by Kolmogorov's law. The energy-containing eddies propagate at speeds slower than the flow from which they extract energy, they can also be trapped by obstacles through a balance with the hydraulic head. The presence of these coherent structures will impact the flow locally and will operate at frequencies different to the tidal frequencies.

Based on the above descriptions there are two distinct parts to flow classification. The first is the description of the long term mean response to the tidal forcing and its interaction with local topography, the second is a spectral decomposition which will highlight the presence or absence of various physical processes. It is through the application of this flow classification process to both the *in situ* and model data that an alternate method of model validation can be applied. In essence if the model has comparable flow magnitudes and directions, has similar structural variations and contains energy in the frequencies of the non-tidal fluid response, then the model is performing as required. The formalization of this validation process will be carried out under a recently funded project.

The *in-situ* data provide limited information on the horizontal spatial variability of the flow, this is generally due to the high cost of multiple distributed instrument deployments, and the difficulties associated with moving vessel surveys in these very high flow regions. Regional scale hydrodynamic tidal models provide a more cost-effective method of addressing horizontal spatial variability. The descriptive metrics developed can be spatially mapped from the model to help classify the entire site. These maps will assist both the developers and people making site measurements.

6.1 Flow Classification – Descriptive

The most relevant information for tidal developers is what is the available energy at the TEC hub-height, and how does this vary with time. The descriptive flow classification aims to capture all of the relevant information in the form of a set of diagrams. The features of the hub-height flow that need to be quantified are:

- The flow speed range and flood/ebb asymmetry
- The peak flow directions and a measure of linearity
- The mean residual flow magnitude and direction
- The frequency of occurrence of flow speeds
- The frequency of occurrence of flow directions and the spread around the peak directions

These data then need to be related back to the operating limitations of the TEC, i.e.

- TEC cut-in speed
- TEC rated speed
- TEC cut-out speed
- TEC orientation (for models that are fixed) and the difference to peak flow directions

Lastly the IEC IEC TS 62600:200 [21] gives recommendations on the flow speed limits, based on the cut-in and rated speeds, used to generate a power curves. This information helps to determine whether the data from a given location is suitable for generating the power curve.

The data processing steps required to collect the required descriptive information are as follows:

1. Extract the hub-height velocity time series from the data records and average to a suitable time window if required.
2. Flag poor quality data using the QC flags – only use data the meet the required QC level.
3. Convert Cartesian velocity components into polar components, i.e. calculate the magnitude and direction of the flow for each time step.
4. Sort the data into flood and ebb sets and store the data indices
5. Determine the peak flow direction for each tide phase (flood/ebb).
6. Calculate flow speed statistics for each tide phase.
7. Calculate flow direction statistics for each tide phase.
8. Plot the data as magnitude as a function of direction along with the auxiliary TEC and IEC data.

Three separate figures are generated: (1) the descriptive flow classification diagram, (2) histograms of the binned speed data for each tide phase, and (3) histograms of the direction difference from the peak direction for each tide phase.

Data from the ReDAPT ADCPTD7_02 deployment have been used to demonstrate the method. These data are collected from a location beside the DeepGen IV turbine, so are not affected by machine wake. Figure 6-1 show the constructed flow classification diagram. The scatter plot is displayed as a colourized probability density plot, to give an indication of the amount of time the flow is in a given direction and speed bin. Vertical lines indicating the peak flow directions, and horizontal lines showing the TEC cut-in and rated speeds and the IEC power curve lower and upper speed limits are overlaid. The directions are given in mathematical convention, i.e. they measure anti-clockwise from the x-axis, but people working in the marine sector generally give directions as compass bearings from North, the four quadrant bearings have been marked on the corresponding vertical lines the and the bearing value for the peak flow directions are given.

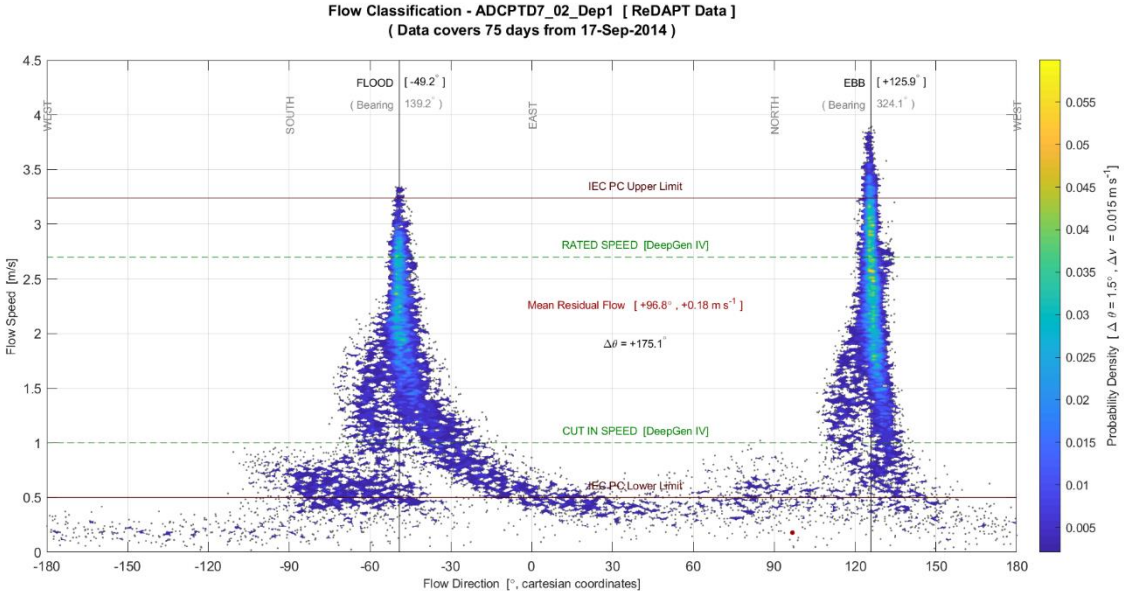

Figure 6-1: Flow classification diagram for the ReDAPT ADCPTD7_02_Dep1 data set.

The interpretation of this diagram is as follows:

- There is a significant asymmetry between the flood and ebb flow magnitudes, the ebb is stronger than the flood.
- The difference between the flood and ebb directions is 173.0°, this means there is a 7° offset from pure rectilinear flow (for rectilinear flow Δθ = 180°).
- There are periods of significant negative divergence (up to -30°) from the peak directions for speeds between the cut-in speed and 2.0 m/s on both phases of the tide. On the flood there are periods of significant divergence from the peak direction for speeds below 1.5 m/s. The frequency of occurrence is low compared with the peak directions, suggesting the only occur on particular tides (e.g. large spring or low neap tides).
- The rated speed is exceeded on both tides, so the TEC should reach optimal power on both phases of the tide.
- The ebb tide frequently reaches the IEC power curve upper limit speed, whereas the flood tide rarely reaches this level, suggesting that only the ebb tide should be used for determining the power curve.

To better understand the power production potential of the location, a breakdown of the flow speed into frequency of occurrence in speed bins is required. Figure 6-2 shows histograms of the velocity magnitude data sorted into 0.1 m/s speed bins for each phase of the tide, and the figure titles give the percentage of time spent in each tide phase. The cut-in and rated speeds are shown, along with the percentage of time spent below cut-in speed, between cut-in and rated speed and greater than rated speed. These data give an indication of the dominate flow speeds, and how much time the TEC is operating in flow speeds greater than the rated speed. Above the rated speed the TEC needs to control its power output to the optimal level, this either achieved by pitch controlling the blades or by gearbox and braking controls. The more time spent above the rated speed the greater the level of fatigue on the speed controllers and the loading on the turbine blades and support structures. These have implications for the fatigue life of the machine.

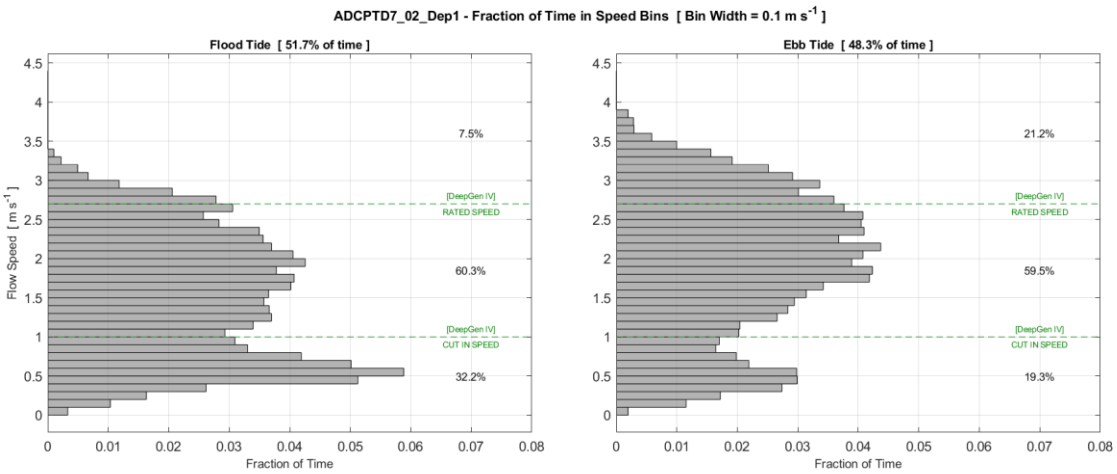

Figure 6-2: Breakdown of time spent in tide phases and speed bins for the ReDAPT ADCPTD7_02 dataset.

The interpretation for this site is as follows:

- The flood tide phase is longer than the ebb tide phase
- The most common speed above the TEC cut-in speed is approximately 2.0 m/s on both phases of the tide, but the histogram for the ebb tide is skewed towards the higher speeds.
- During the flood tide the speed is between the cut-in and rated speeds 60.2% of the time, compared with 58.2 percent for the ebb tide.

- During the flood tide the speed only exceeds the rated speed 6.1% of the time compared with 19.6 percent of the time for the ebb tide.

The frequency of occurrence of flow away from the peak direction has implications for both control and efficiency of the TEC. For systems that have yaw control, the power production can be optimized by pointing into the flow direction, but the rate at which this can be done is limited, so it is more likely the TEC will be aligned along the peak flow direction for each tidal phase. There will still potentially be some impact of flow directional variation on the efficiency. In contrast, a TEC that is static, will always be operating inefficiently, so some compromise between TEC alignment and optimal power generation needs to be determined. The divergence of the flow away from the peak direction is indicative of large-scale structures passing the location. These structures are less likely to occur during peak flow, when the dynamics are essentially stable. They are more likely to impact weaker flows, which may have an impact on turbine cut-in timing. The shape of the histogram of directional spread is indicative of the level of non-tidal dynamics. Turbines will operate more efficiently at locations where the histograms are narrow with the greatest percentage of flow along the peak flood and ebb directions.

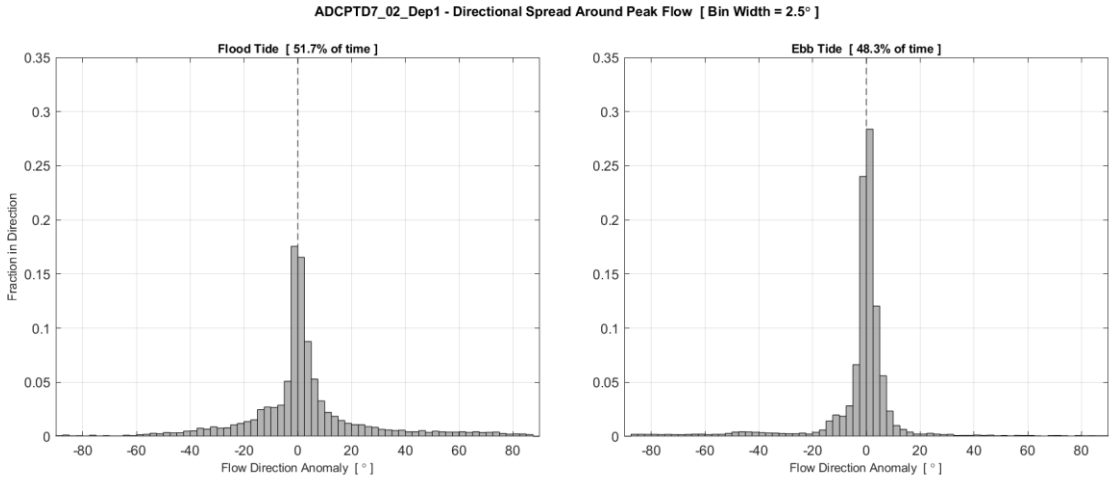

Figure 6-3: Directional spread histograms for the ReDAPT ADCPTD7_02 dataset.

6.2 Flow Classification – Spectral

Surface elevation and velocity measurements provide time-domain signals for a given location. Time-domain signals can be decomposed spectrally, showing the energy peaks associated with specific physical processes. The frequencies resolved depend on the sampling rate and length of the time series. The time series can be described as follows:

$$h(x,y,t) = h_{tide}(x,y,t) + h_{atm}(x,y,t) + h_{wave}(x,y,t) + h_{dyn}$$

and

$$v_i(x,y,z,t) = v_{i,tide}(x,y,z,t) + v_{i,wave}(x,y,z,t) + v_{i,dyn}(x,y,z,t) + v_{i,turb}(x,y,z,t)$$

where $h(x,y,t)$ is a time series of surface elevation at spatial location (x,y) and $v_i(x,y,z,t)$ is the time series of the i^{th} velocity component at the spatial location (x,y,z). The dominant signal at tidal sites is that due to the gravitational tidal forcing, the surface elevation can be affected by atmospheric pressure variations and local winds, surface gravity waves (either remotely generated swell or local wind waves) alter the surface elevation and impart velocity structure down through the water column, the interaction of the tidal flow with local topography generates flow-separation structures that in turn have a dynamic surface expression, finally the fluid has an inherent shear due to viscosity which works to dissipate the energy through the generation of turbulent structures on length scales down to

molecular scales. All of the processes have defined frequencies where they operate, so can be resolved spectrally. The signals that can be used to classify the flow across a site are the tide, dynamic response and turbulence. The atmospheric and wave processes are better represented by statistical information. Spectral analysis and appropriate filtering can be used to separate the classes of signal.

The surface elevation data are pre-filtered by applying a 5 minute averaging to sub-sample the data, this effectively removes (or reduces) the signal associated with waves. The large-scale dynamical processes operate on periods of minutes to days. The dominated energy in the surface elevation signal is in the tidal forcing frequencies and their associated harmonics. These are well known and can be removed using off-the-shelf tidal reduction software (e.g. t-tide, U_tide) to reconstruct the signal due to tidal forcing frequencies. Subtracting the reconstructed tide leaves the non-tidal signal due to atmospheric forcing and the dynamical response to flow blockage and flow separation processes. The atmospheric processes operate on time periods typically greater than 12 hours. A lowpass filter can be applied to extract the signal associated with atmospheric processes. Subtracting the atmospheric signal from the non-tidal signal leaves the dynamic response signal. Figure 6-4 shows the deconstruction process. The top panel show the tidal reduction, the second panel shows the atmospheric signal, and the final panel shows the remaining dynamical response signal. The dynamical response signal that can be used to provide a spectral classification for the location.

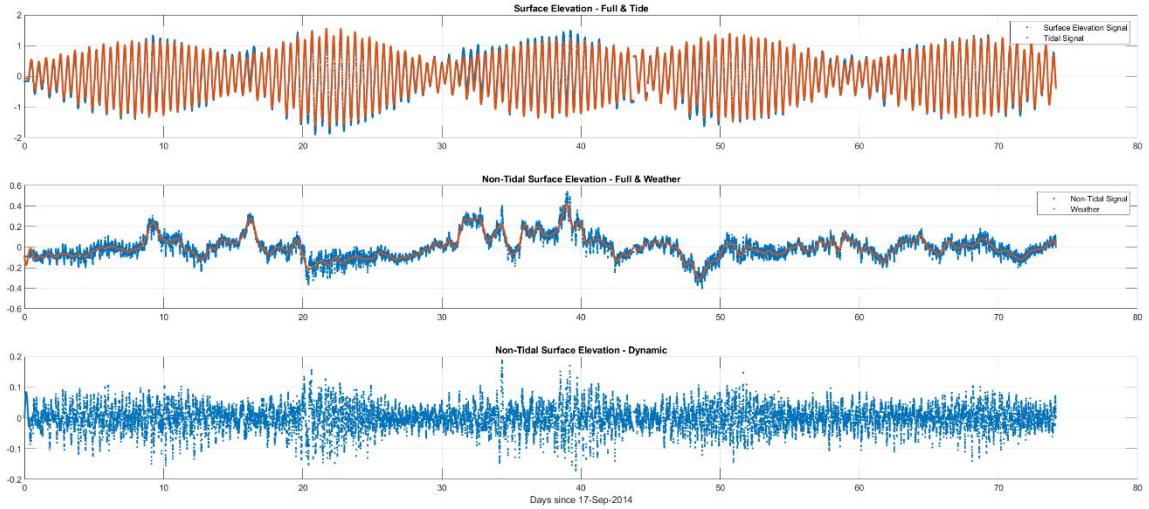

Figure 6-4: Decomposition of surface elevation data for ReDAPT ADCPTD7_02 dataset.

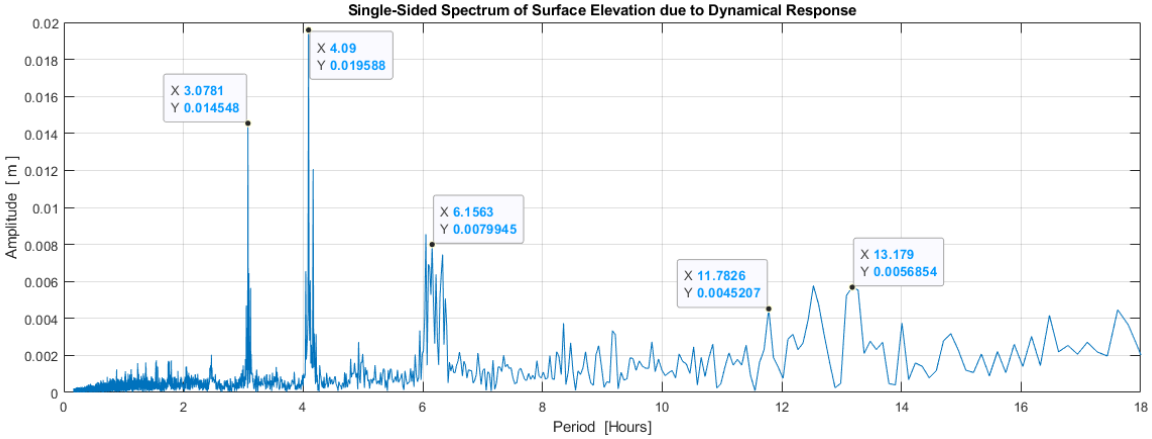

Figure 6-5: Frequency spectrum of the non-tidal dynamical response of the surface elevation from the ReDAPT ADCPTD7_02 dataset.

Figure 6-5 show the frequency spectrum for the non-tidal dynamical response of the surface elevation from the ADCPTD&_02 dataset. The dominant peaks are tagged with the period (x) and amplitude (y). The two peaks around 3.1 and 4.1 hours are close to the M6 and M8 tidal periods, these maybe been residual M6 and M8 signal that has been poorly resolved due to signal noise, or they may be due to dynamical processes at frequencies close to these tidal periods, but just below. There is a broad peak around 6.2 hours (M4 tidal period), the broadening is indicative of non-tidal response around this period which may be associated with the passage of large-scale eddies which are generated by the flow but propagate at a slower speed as the extract energy from the accelerating flow. There are two peaks either side of the 12.4 peak (M2 tidal period) at 11.8 hours and 13.2 hours, these are most likely due to large-area dynamical readjustments of the surface due to flow blockage by the islands and channel constrictions. Further work is required to attribute these non-tidal signals to physical processes.

A similar process can be applied to the time series data for the velocity components. Figure 6-6 shows the spectra for the non-tidal dynamical response of the eastward and northward velocity components at hub-height for the DeepGen IV tidal turbine. The velocity signals have peaks at similar frequencies to the surface elevation indicating a dynamical link between the flow and the surface elevation variations as expected. There are similar peaks near the M6 and M8 tidal harmonics, and there is a residual M2 signal.

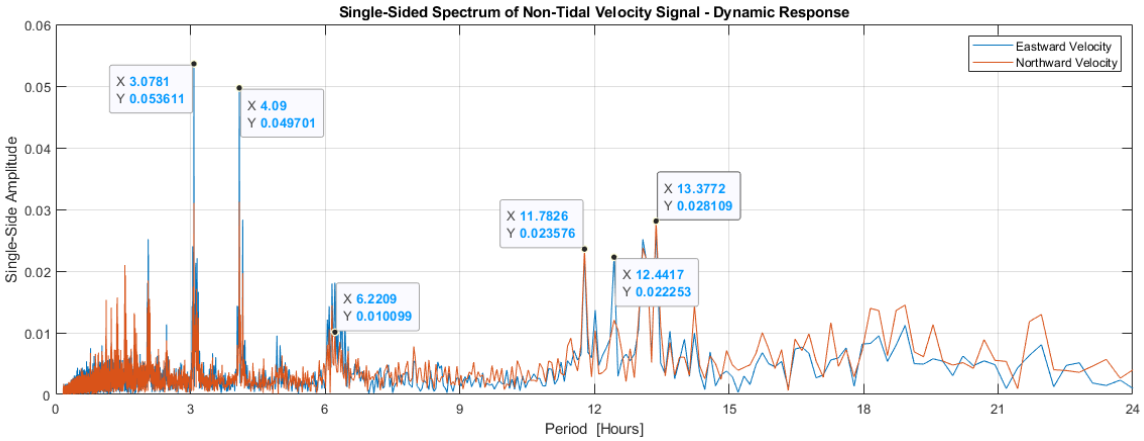

Figure 6-6: Frequency spectrum of the non-tidal dynamical response of the velocity components from the ReDAPT ADCPTD7_02 dataset.

6.3 Model – Data Comparison

The above process of flow classification can be applied to model prediction data. Comparisons with the *in-situ* data will indicate how well the model is reproducing the flow structures. Data extracted at the location of the ReDAPT ADCPTD7_02_Dep1 deployment from the ORK_BASE 90 day model run are used for this comparison. Time series of velocity data are extracted at the DeepGen IV hub-height. The model data extraction process takes the vertical profile data from the corner nodes of the triangular mesh element that the location of interest lies within and interpolates the data onto the location using the Barycentric weighting method. The hub-height data are then extracted by interpolating the location profile onto the required height above the seabed. This has to be done for each time step separately because the layer thickness (or z-level heights) vary with every time step. The data have been sub-set to match the time-period covered by the *in-situ* data.

Figure , Figure 6-10, and Figure 6-11 are the model analysis corresponding to the in situ data shown in Figure 6-1, Figure 6-2, and Figure 6-3. Broadly speaking, the model is reproducing the observed flow

structures, speed distributions and directional spread. This suggest that the model is capturing the key dynamics.

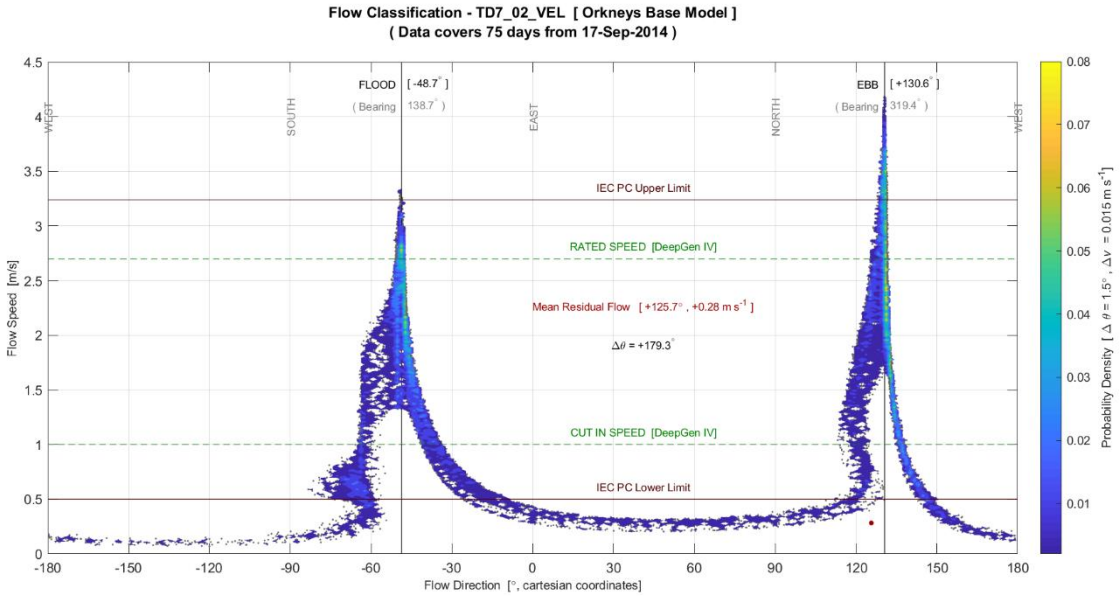

Figure 6-7: Flow classification diagram for the ORK_BASE model at the ReDAPT ADCPTD7_02_Dep1 site.

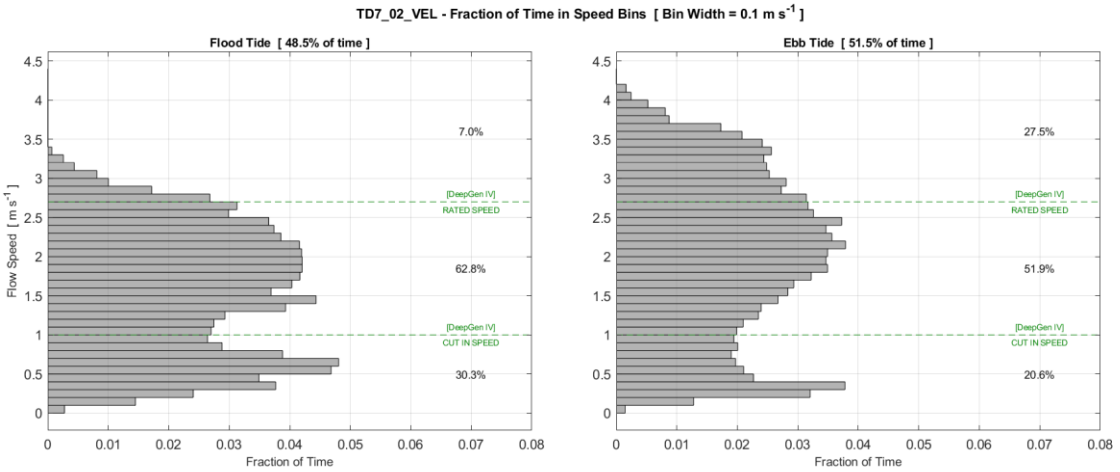

Figure 6-8: Breakdown of time spent in tide phases and speed bins for the ORK_BASE model at the ReDAPT ADCPTD7_02_Dep1 site.

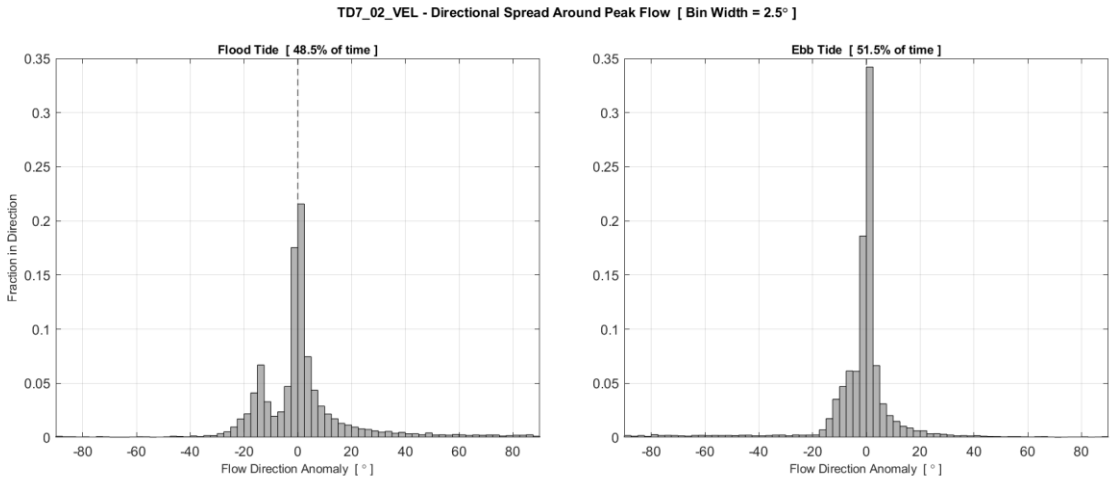

Figure 6-9: Directional spread histograms for the ORK_BASE model at the ReDAPT ADCPTD7_02_Dep1 site.

Figure 6-10 shows the decomposition of the modelled surface elevation. There is no atmospheric signal as the model does not include surface forcing by winds or variable atmospheric pressure. The remaining dynamical signal is not as variable as the observed data, but shows the same neap-spring related variations. Figure 6-11 shows the spectrum for the modelled surface elevation dynamical response. This produces peaks at the same frequencies as those seen for the observed data, but they show some defined structure to these peaks, suggesting that those near the tidal frequencies are likely to be due to dynamical processes that occur close to but not the same as the tidal forcing.

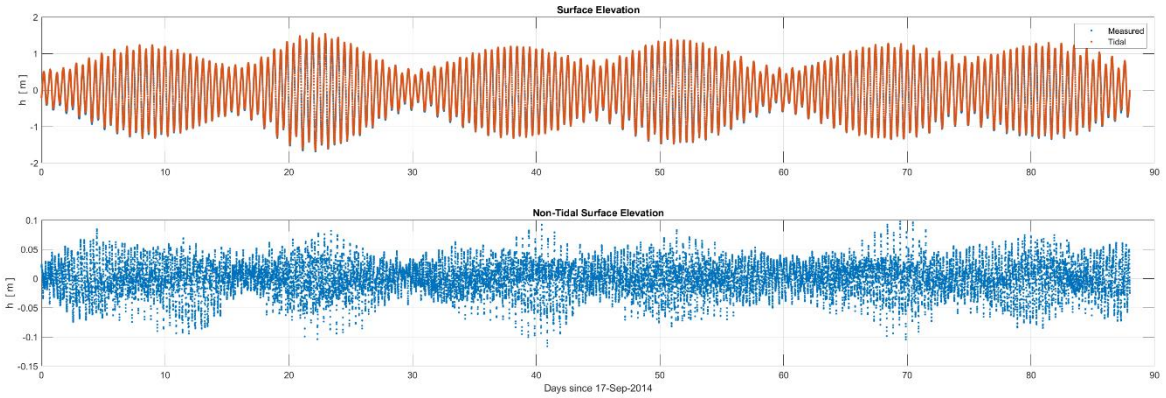

Figure 6-10: Harmonic reduction of ORK_BASE model surface elevation at the ReDAPT ADCPTD7_02_Dep1 site.

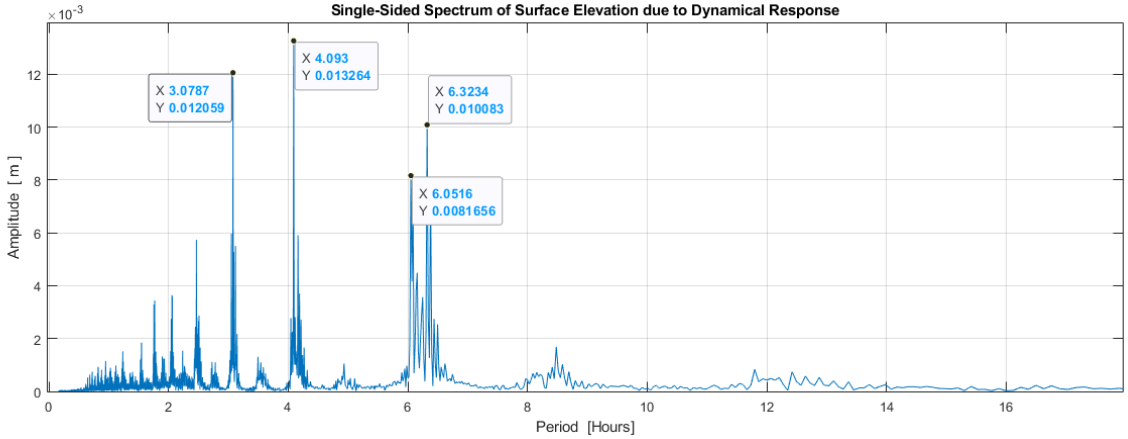

Figure 6-11: Spectral analysis of non-tidal surface elevation for the ORK_BASE model at the ReDAPT ADCPTD7_02_Dep1 site.

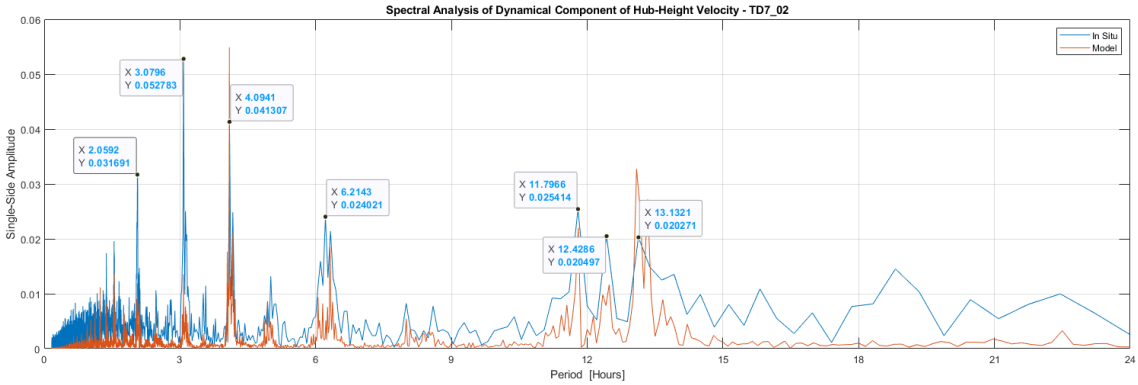

Figure 6-12: Comparison of modelled and observed hub-height velocity spectra at the ReDAPT ADCPTD7_02_Dep1 site.

Further support to the argument that the model is reproducing the key dynamics is given by the spectral comparison of the hub-height dynamical response velocity shown in Figure 6-12. The same peaks are reproduced, with the observations being more diffuse and the presence of energy for longer periods (i.e. lower frequencies). Overall, this presents a different approach to possible model validation methods, which will be followed up in the recently funded FASTWATER project.

6.4 Spatial Mapping of Flow Characteristics

The key feature of the model data is the provision of spatial variation information. The mapping of key classification features can aid the decision-making processes for site development and location of site measurements. Figure 6-13 shows the mappings of the spatial variation in four possible metrics, (a) peak flood flow speed, (b) peak ebb flow speed, (c) the difference between the peak ebb and flood flow speeds, and (d) the difference between the peak flood and ebb flow direction.

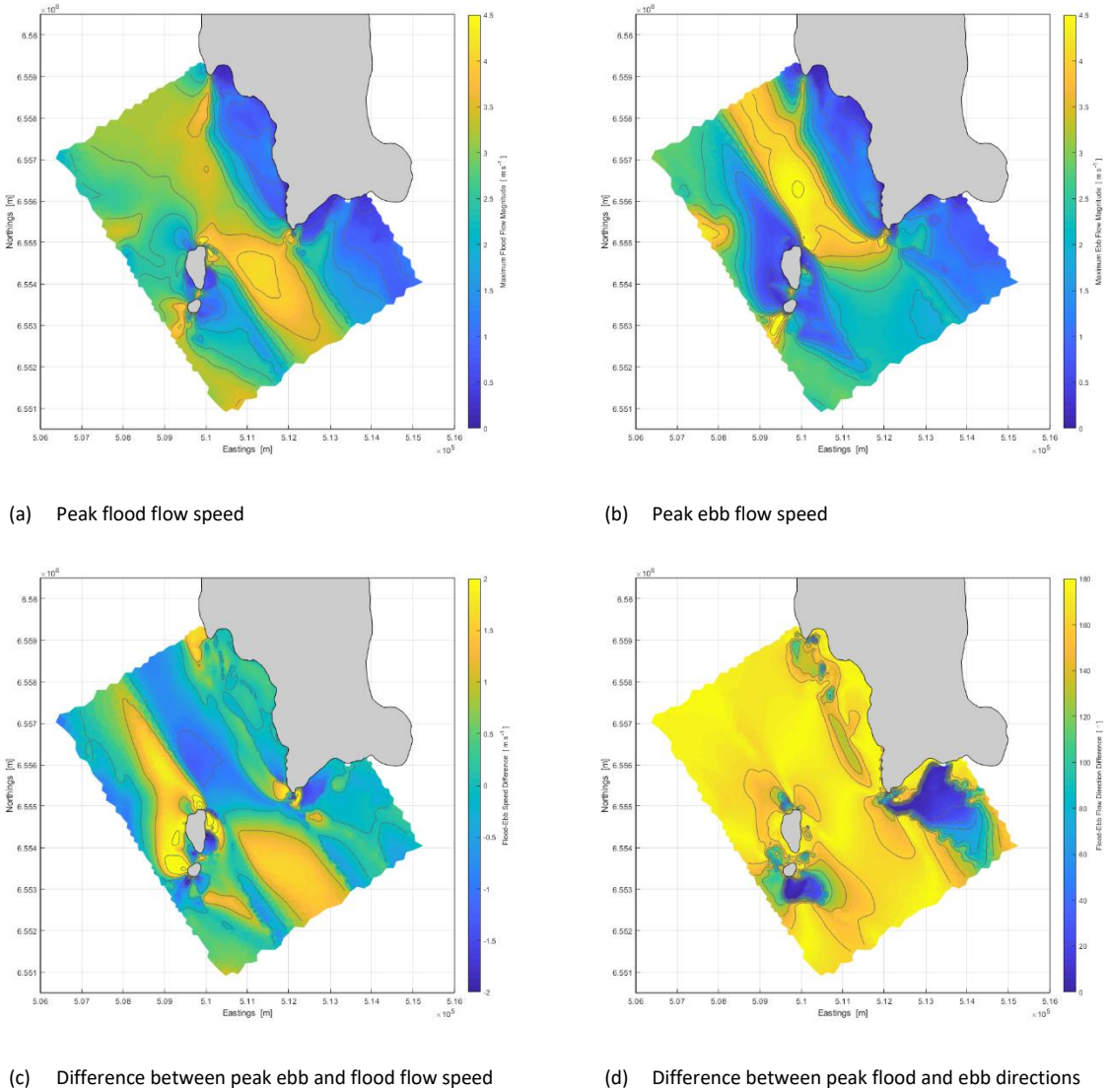

(a) Peak flood flow speed

(b) Peak ebb flow speed

(c) Difference between peak ebb and flood flow speed

(d) Difference between peak flood and ebb directions

Figure 6-13: Spatial mapping of flow classification metrics from the ORK_BASE model data.

Panels (a) and (b) show the variation in flood-ebb flow asymmetry, while the difference shown in (c) identifies where the ebb and flood flow speeds are the same (where the difference is approximately

zero). This information has implication on turbine siting for optimal power production, and where to site generators with different rated speeds for optimal yield and minimal loading. The peak flow directional difference shown in panel (d) indicates where best to place fixed turbines (*e.g.* TEC without yaw capability), *i.e.* where the directional difference is close to zero, and where to place yaw-enabled turbines. Combinations of the mapping information will help design array layout for optimal yield across a site. There are many other metrics that could be mapped, those shown are indicative of the potential end-use of this type of information breakdown.

7 SENSITIVITY ANALYSIS

The key parameter values extracted from the *in-situ* measurements and model predictions to meet the sectors end-use requirements may be sensitive to the generation methods used. In this section the sensitivity of parameters to methods will be summarized. A standard approach taken to estimate long-term yield is the take a times series of data from a tidal site that is at least 30 days long and perform a tidal reduction, then use the resolved harmonics to predict values out to one year. As has been shown in the flow classification, there is often energy in non-tidal signals within high-energy tidal sites that results from the interactions of the flow with the local topography. The impact of tidal reduction needs to be quantified.

The purpose of the multiple Iroise Sea model constructs was to determine what impact, if any, the extent of the fine resolution mesh has on the estimation of available power. A low-resolution mesh cannot support surface gradients less than twice the mesh resolution, this has the effect of diffusing coherent eddies smaller that the mesh resolution, which in turns stops large far field structures forming. The structures potentially increase the Island blockage effect, and the removal of eddy structures will lead to an increase in the linear momentum of the flow, *i.e.* the flow speed. If the associated changes are significant then they may have an impact on estimated available power. The sensitivity of the dynamics to mesh construct.

7.1 Impact of Tidal Reduction

The effect of applying a tidal reduction to the velocity data is demonstrated in the flow classification diagram for the tidal reduction of the ReDAPT ADCPTD7_02_Dep1 hub-height data shown in Figure 7-1. The effects of the eddies have been removed, but there is still an underlying divergence in the flow direction away from the peak above the DeepGen IV cut-in speed. Table 7-1 summarises the impact of calculating flow classification metrics from the tidal reduced signal. The ReDAPT ADCPTD7_02_Dep1 DeepGen IV hub-height data were used for this comparison. The variations in peak flow directions and directional asymmetry are negligible. The largest impact was on the ebb tide directional spread; this half of the tide has the most variation in flow direction. The available streamwise power is the metric most relevant to developers, tidal reduction leads to an under-estimate of available power.

Table 7-1: Impact of tidal reduction on flow metrics for the hub-height ADCPTD7_02_Dep1 data.

Metric	Full Data	Tidal Reduction	Difference	% Impact
θ_{flood}	-49.2°	-49.3°	+0.1°	+0.03 %
θ_{ebb}	125.9°	126.0°	+0.1°	+0.03 %
$\theta_{flood} - \theta_{ebb}$	175.1°	175.3°	+0.2°	+0.06 %
$\lvert\Delta\theta_{flood}\rvert < 5°$	48.0 %	45.6 %	-2.4 %	-1.3 %
$\lvert\Delta\theta_{ebb}\rvert < 5°$	71.1 %	62.3 %	-8.8 %	-4.8 %
Power (full)	7889 kW hr	7737 kW hr	-152 kW hr	-1.2 %
Power (stream)	7836 kW hr	7699 kW hr	-137 kW hr	-1.7 %

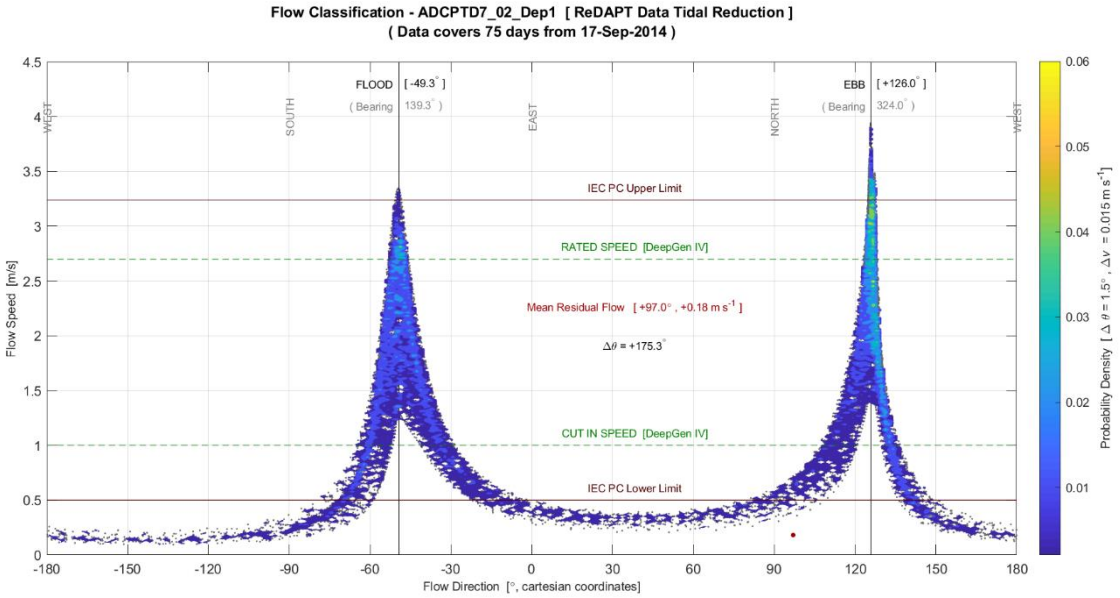

Figure 7-1: Flow classification diagram for the tidal reduction of the ReDAPT ADCPTD7_02 data set

Similar patterns of tidal reduction impact were observed for the Fromveur Strait data, suggesting that estimating available power based on a tidal reduction of the velocity data will lead to an under-estimate of available power. Economically for a developer this potentially has a positive impact.

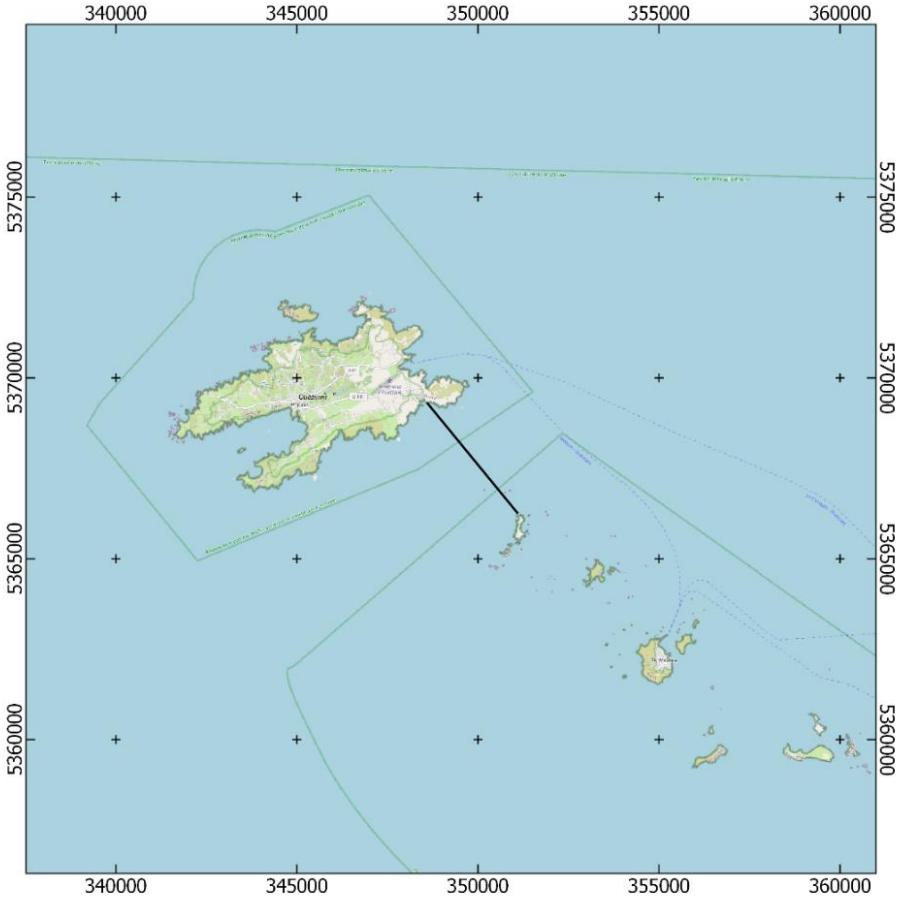

Figure 7-2: Fromveur Strait transect used to determine impact of model mesh construct on dynamics.

Table 7-2: Iroise Sea model construct inter-comparison metrics.

Metric	MODEL A	MODEL B	MODEL C
Mean X-section Area	+0.4 %	-0.1 %	-0.05 %
Flood Vol. Flux (+ve)	+7.2 %	+4.2%	+3.9%
Flood Vol. Flux (-ve)	-9.7 %	-8.4 %	-7.8%
Ebb Vol. Flux (+ve)	+1.0 %	+1.4 %	+1.6 %
Ebb Vol. Flux (-ve)	+0.8 %	+4.0 %	+1.0 %
Power	-7.7 %	+1.4 %	+2.6 %

7.2 Impact of Model Construct

The hypothesis being tested with the multiple model mesh constructs was that in regions like Fromveur Strait, where there are large-scale persistent coherent flow structures formed by the forcing of the flow through a strait, diffusion of these structures by the mesh resolution will modify the dynamics in and around the Strait. The main dynamics that would be modified are the volume flux through an across-channel transect across the Strait, changes in recirculation levels in the Strait, and changes in the available power at a given location. The across-channel transect used is shown in Figure 7-2. The volume flux through the across-channel transect was separated into the ebb and flood tides, and further separated into positive and negative fluxes to indicate changes in recirculation. The total cross-sectional area was calculated to determine if there is a dynamical shift in the hydraulic balance. The available energy at the mid-point of the across-channel transect and 20m above the bed was calculated for each construct. These data are commercially sensitive, so the results are presented as percentage differences compared with MODEL D predictions; MODEL D is assumed to be the most representative of the real dynamical variations.

The results of the inter-comparison are summarized in Table 7-2. The variation in mean cross-sectional area is small but indicative of a hydraulic adjustment in mean along-transect surface elevation. The variations in the positive and negative volume flux for each tide, indicate a change in the level of recirculate flow, which will be due to changes in the secondary circulation rates and levels of horizontal vorticity due to shear flow structures. The power estimate is the key metric for developers, this shows that the simplest model (MODEL A) under-predicts the available power by 7.7%, both MODEL B and MODEL C over-predict the available power. This suggest that if a regional model is used to predict power at a specific location, then the extent of the high-resolution mesh needs to capture far-field processes. A paper investigating the full spatial variability in dynamical response, and the implications for site yield predictions is currently in preparation.

8 OUTPUTS

8.1 Key Outputs

Multiple outputs have been generated via the designed holistic approach to data capture and data provision through the activities of work-package 2. This approach is visually summarised in
Figure 8-1. Many others outputs have been identified as either important work for the future, or are being continued in whole or in part in new and aligned research projects, as well as part of ongoing internal research.

The key outputs of RealTide work-package 2, categorised into the five themes listed below are described in Table 8-1.

1. **Data Analyses**
2. **Regional Modelling**
3. **Data Tools**
4. **Sensor Systems**
5. **Database and Data Access**

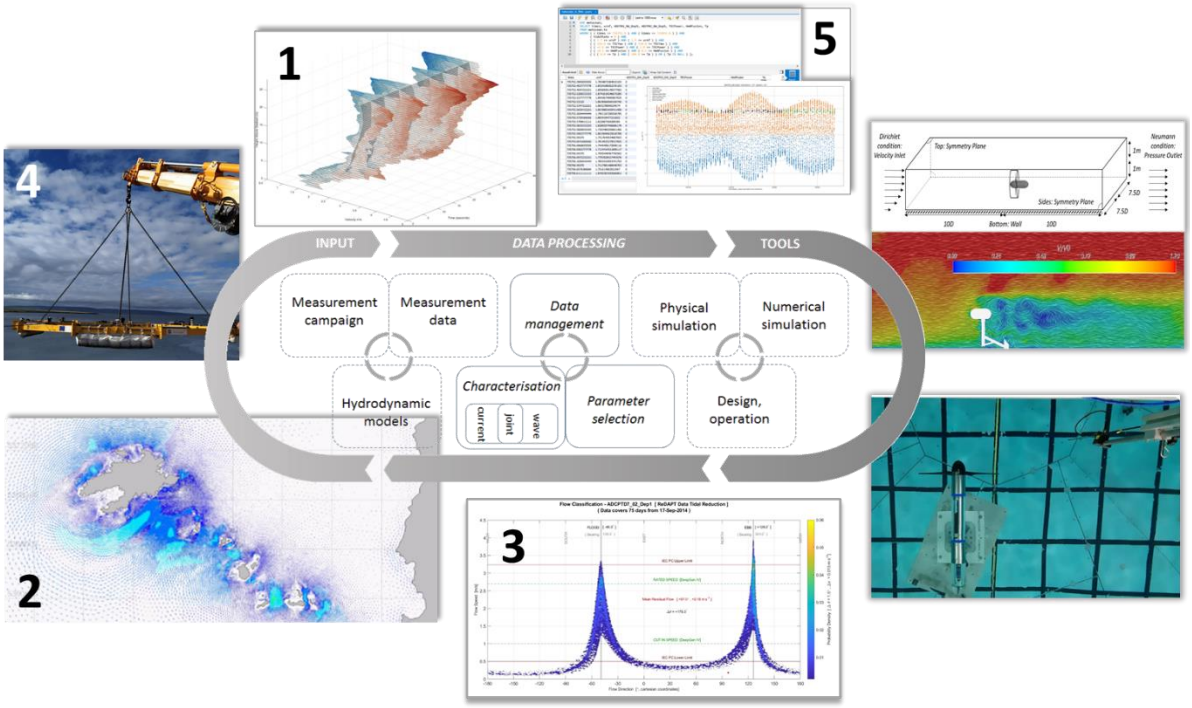

Figure 8-1. The RealTide Holistic Approach. Clockwise from bottom left: RealTide developed 3D models of a commercial tidal energy site; Field work completed in France and the UK, Captured data processed and visualised - showing strong influence of ocean waves; screenshot of the WP2 Database architecture; outputs of WP3's CFD modelling using WP2 inputs, FloWave tests of an instrumented scale TEC and proximal and essential flow-measuring sensor [17]; and site characterisation techniques (central image courtesy of [18]).

Table 8-1. Summary of WP2 Outputs

DATA ANALYSES	
Flow Conditions	Output flow conditions to inform the CFD activities of WP3
Wave-Current Conditions	Output to Tank-Testing activities of WP3
Wave-Current Conditions	Provided datasets on multiple flow conditions, legacy tank-test data and knowledge transfer to enable the rapid development of a project BEMT tool
Spatial Variation Studies	Delivered via re-processing two previously unavailable datasets covering 70 days+ of contemporaneous measurement allowing studies of spatial variation at TEC-relevant scales.
Power Performance Studies	Delivered via re-processing two previously unavailable datasets covering 40 days of contemporaneous measurement allowing study of power performance assessment methodologies

REGIONAL MODELLING	
- Design	Methodology developed to capture key flow features of tidal energy sites using open modelling tools that can be replicated at other sites.
- Configuration	Demonstrated the importance of key model design steps to tidal energy applications.
- Run Control	Methods for automating the execution of multiple single day runs as a batch developed.
- Runs	Demonstrated and quantified the importance of model design
- Interrogation	Methodology developed for extracting data and computing advanced metrics from large volume model output.
- Visualisation	Methods for animating time series of 2-D model data extracts developed.

DATA TOOLS	
- Handling	Data extraction tool for datasets in a legacy file format for one manufacturer
- Handling	Time-series extraction from a prescribed hub-height from a 4D vector field -> 2D vector field
- Processing	Pre-processing for key parameters e.g., tidal direction and peak-flows etc.
- Processing	Tidal reduction using surface elevation or velocities
- Processing	Spectral analysis of non-tidal component of modelled and measured signals
- Processing	Pressure to 1D wave spectra
- Processing	Beam-wise acoustic Doppler Profiler turbulence processing toolset
- Visualisation	Model output visualization tools including the visualization of flow rotation.
-Quality Control	A QC process has been developed to fit the co-developed data processes that is scale-able, transparent and readily upgradeable. . It is anticipated that updated QC-flags will be readily and transparently added to the datasets held in the RealTide Database. These have been tested through related staff and Masters and PhD student project work.

SENSOR SYSTEMS	
-Component-level	Demonstrated & Implemented: embedded computing solutions for subsea use, arrays of motion-sensors for system pose measurement, multi-voltage, multi-redundancy power handling for TEC and autonomous systems
-Sub-System-Level	Demonstrated actuated C-ADP, Demonstrated a subsea low power IEEE1538 timing network, Demonstrated a smart-fusing system. Developed software control and processing algorithms for the development and operation of C-ADP sensor platforms.
-Hard Wired	Fully implemented wired solution for flexible operation of seabed sensor packages
-Autonomous	Fully implemented an autonomous control system which preliminary analysis suggests operated multiple sensors and auxiliary systems as intended with no user intervention
-Remote Systems	Demonstrated a configurable power and comms system that was accessible either by user or autonomous controller.
-Battery Systems	Developed smart (motion sensing) modular and low-cost pressure vessels for coastal-region sensing applications
-TEC Installed	Multiple fully integrated systems retrofitted to TEC designed, implemented and proven functional
-Seabed Installed	Multiple high quality data sets produced that exceeded project needs at multiple sites (France and UK). Developed novel advanced turbulence sensor system across 3 phases (laboratory, field-trial, full-scale prototype deployment).

DATABASE AND DATA ACCESS	
-Database Design	Design of stable and scale-able database for WP2 internally tested using experience and datasets generated in WP2. This will be made available to the public by end of 2021. www.tidalenergydata.org
-Database Design	Transferred knowledge, methodology and implementation from WP2 to WP1, in assisting BV with Reliability Database.
-Backend Extraction	File handling, data extraction and standardisation
-User Interface	Front end web-app
	DATABASE In-Situ Data
-Public Website	A public website has been setup to aid immediate to long-term impact from RealTide: www.tidalenergydata.org
-Data Set 1*	Open data (reprocessed & updated) - instrument located 3D/5D upstream of TEC
-Data Set 2*	Open data (reprocessed & updated) - instrument located 2D to port/starboard of TEC
-Data Set 3*	Open data (Sep. 2021) – 5-Beam ADCP in 35m for 40 days in important location
	DATABASE - Simulated Data
-Physical Models	Expanded database scope by incorporating tank-test and numerical simulation data to allow cross-benchmarking of reliability-focused engineering tools Data handling routines have been developed to convert tests completed at FloWave into Database-ready formats
-Regional Models	Data handling routines have been developed to convert data extracts from the 3-D regional models into Database-ready formats

*Data sets – together with version-controlled meta-data and user manuals are in the process of being archived permanently in the UEDIN Datashare service, where permanent DOIs will be generated. DOIs and public access will be available by end of November 2021 for Data Sets 1-2 and end of December 2021 for Data Set 3.

The extent to which the RealTide measurement campaign and data-provisioning activities of WP2 fit the identified data requirements of project partners and in many cases the wider tidal energy sector (as introduced in Table 2-3) is summarised below in Table 8-2.

Table 8-2. RealTide Data Requirements: Reflection on Requirements.

Requirement	Notes on multiple analyses of RealTide processed datasets
VELOCITY PROFILE	
Turbulence Power Spectrum	Processing shows that spectral fits of power spectral density plots are highly sensitive to the presence or lack of non-tidal components.
Turbulence Intensity	Wave-current decoupling is required for much of the periods of the data analysed under RealTide – which covered winter months where waves were almost ever-present in cases and close to dominant in some. Other non-tidal components also increase uncertainty in TI estimates.
Turbulence Length Scales	Re-processing of ReDAPT TEC-mounted sensors (which will be published on the RealTide website) may offer more stable estimates of length-scale.
Reynold's Stress Tensor	The results of the C-ADP MkIII deployment are required to undertake advanced studies on this, however, internal analysis will be conducted on the 5-Beam datasets collected. C-ADP laboratory test data may also offer insights.
Turbulence Anisotropy	Work is underway via re-analysis and new processing of Fall of Warness TEC-mounted data. It was hoped that D10 TEC acquired data would assist with this work but insufficient data was retrieved due to the unplanned removal of the D10 TEC.
Coherency	The measurement campaign was designed to enable future assessments of this property of the flow. This analysis may be able to be conducted in the future based on datasets made public.
WAVES	
Surface Elevation	Surface elevations recovered by the Fromveur winter campaign of 2019 are excellent. Storms can be readily observed in the pressure records. Signal quality is very high. In addition, during periods of very high wave echo-location can be used to track the surface.
2D Wave Spectra for TEC and instrument locations. *Wave Statistics*	Re: 2D - The D10-TEC-installed RDI Workhorse sentinel was configured to operate in waves mode and would have made use of RDI's proprietary wave processing software – which would have allowed some trialing of array-based in-house scripts. The data was unavailable due to D10 unavailability. Re: 1D Stats: These have been extracted through a pressure-to-wave processer (see Outputs).
WIND SPEED	Readily available
SURFACE PRESSURE	Readily available
TEC STATUS	
Type A: Basic Operational System State of Machine	N/A for D10 TEC Available and re-processed for Fall of Warness studies via DeepGEN IV.
Type B: Electro-Mechanical System State of Machine	N/A for D10 TEC May be available as data is currently being recovered from fragmented dataset which contains detailed electro-mechanical high-frequency data of the DeepGEN IV.

8.2 Outputs – Dissemination and Further Information

The following outputs have resulted from activities conducted in whole or in part from RealTide WP2. Multiple follow-on publications are in preparation.

Ingram, David M., Sellar, Brian G. Sellar, Old, Chris, Davey, Tom, Gabl, Roman, Jordan, Laura-Beth, Nourisson, Ophelie, and Paboeuf, Stephane. 2021. *"Experimental measurement of the loads on tidal turbines using conditions derived from field measurements ".* The 14th European Wave and Tidal Energy Conference (*EWTEC 2021*).

Dorward, Mairi, Brian Sellar, Chris Old, and Philipp R. Thies. 2019. "Currents, Waves and Turbulence Measurement: A View from Multiple Industrial-Academic Projects in Tidal Stream Energy." In *Institute of Electrical and Electronics Engineers (IEEE)*. https://doi.org/doi:10.1109/CWTM43797.2019.8955294.

Harding, Samuel, Brian G. Sellar, and Mairi Dorward. 2019. "Implications of Asymmetric Beam Geometry for Convergent Acoustic Doppler Profilers." In *In IEEE/OES Twelfth Current, Waves and Turbulence Measurement (CWTM 2019)*. https://doi.org/10.1109/ CWTM43797.2019.8955290.

Harding, Samuel, Mairi Dorward, Brian Sellar, and Marshall Richmond. 2021. "Field Validation of an Actuated Convergent-Beam Acoustic Doppler Profiler for High Resolution Flow Mapping." *Measurement Science and Technology* 32 (4). https://doi.org/10.1088/1361-6501/abd5ef.

Jourdain de Thieulloy, Marilou, Mairi Dorward, Chris Old, Roman Gabl, Thomas Davey, David M. Ingram, and Brian G. Sellar. 2020. "On the Use of a Single Beam Acoustic Current Profiler for Multi-Point Velocity Measurement in a Wave and Current Basin." *Sensors (Switzerland)* 20 (14): 1–21. https://doi.org/10.3390/s20143881.

Jourdain de Thieulloy, Marilou, Mairi Dorward, Chris Old, Roman Gabl, Thomas Davey, David M. Ingram, and Brian G. Sellar. 2020. "Single-Beam Acoustic Doppler Profiler and Co-Located Acoustic Doppler Velocimeter Flow Velocity Data." *Data* 5 (3): 1–11. https://doi.org/ 10.3390/data5030061.

Gaurier, Benoît, Stephanie Ordonez-Sanchez, Jean Valéry Facq, Grégory Germain, Cameron Johnstone, Rodrigo Martinez, Francesco Salvatore, et al. 2020. "MaRINET2 Tidal Energy Round Robin Tests-Performance Comparison of a Horizontal Axis Turbine Subjected to Combined Wave and Current Conditions." *Journal of Marine Science and Engineering* 8 (6). https://doi.org/10.3390/JMSE8060463.

RealTide. 2018. "Technical Report (Internal): Deliverable 1.5 - Increased Reliability of Tidal Rotors (RLT-WP1-5-PDL-000-01)."

RealTide. 2018. "Technical Report: Deliverable 3.4 - Inter-Comparison of BEMT, Blade-Resolved CFD, and BEMT-CFD Hybrid Models of Scale Turbines (RLT-WP3-4-PDL-000-01)." https://realtide.eu/realtide-project-deliverables.

RealTide. 2019. "Technical Report: Deliverable 2.1 - Deployment and Instrument Specification for Advanced Flow Characterisation (RLT-WP2-1-PDL-000-03)." https://realtide.eu/realtide-project-deliverables.

RealTide. 2021. "Technical Report: Deliverable 3.5 - Synthetic Load Spectra and Time Series of Tidal Turbines (RLT-WP3-5-PDL-001-02)." https://realtide.eu/realtide-project-deliverables.

RealTide. 2021. "Technical Report: Deliverable 2.3 - Environmental Conditions Database: Collation, Demonstration and Dissemination (RLT-WP2-3-PDL-001-03)." https://realtide.eu /realtide-project-deliverables.

9 LESSONS LEARNED, RECOMMENDATIONS AND NEXT STEPS

9.1 Lessons Learned

Lessons learned are summarised below across the five activity themes as those presented in Section 8 and Table 8-1, namely: Data Analysis, Regional Modelling, Data Tools, Sensors and Sensor Systems, and Database and Data Access.

1) DATA ANALYSES

1.1 When capturing and comparing model and in-situ results, e.g., for model calibration / validation the specific the final use-case of the analysis should be considered, where anticipated turbine geometry and location in the water column will play a significant role in the interpretation of the results. For example, large differences in velocity agreement at the seabed may or may not be relevant to exploiting the model data at a particular hub-height.

1.2 Drivers of large flow variation at the European Marine Energy Centre: Evidence from previous major tidal energy projects suggested that spatial variation levels in constricted channels would present major uncertainties in energy yield (and device loading). This insight has been investigated, substantiated and partially quantified within RealTide.

1.3 Analysis of data sets at three separate locations and three water depths approximately 35 m, 45 m, 55 m show significant and varied wave activity (in time, space and phasing with the tidal currents) that at times extends significant influence to the seabed. The acquired data suggests a complex response of the wave field to the wider channel dynamics.

1.4 The inclusion of non-tidal components e.g., waves and large eddies in measurements strongly affects turbulence analysis, including estimates of Turbulence Intensity and in spectral analyses.

1.5 Signal detrending: Methods developed in RealTide have demonstrated that the deconstruction of measured or predicted time series of data base on physical processes, such as tidal signal, weather, and dynamic response, is a more effective method of pre-processing the data prior to the extraction of key parameters.

2) REGIONAL MODELLING

2.1 The RealTide approach and analyses asked questions on the interpretation of IEC guidance on model development provided to developers. The guidelines acknowledged that large-scale flow structures need to be considered, but do not provide any further detail. There are recommended mesh resolutions within the region of interest depending on the end-use of the model data, but no discussion of the extent this region should cover. It was decided that this was a fundamental and highest-priority question that needed to be addressed before advancing to the full wave modelling. The subsequent analyses on this aspect affected time and resource constraints which meant that proposed wave modelling work could not be addressed in the project time frame.

2.2 Open source 3D non-hydrostatic models – if properly configured – can capture both the tidal *and* crucially non-tidal response over a large area.

2.3 *DATA ANALYSES & REGIONAL MODELLING:* Model validation against in situ data collected in high-energy tidal sites remains a challenge. This is related to the interpretation and processing of the *in situ* data, which have unresolved uncertainties and contain signals from processes not included in the models. Models should not be “tuned” to match data from a single location. Maps of spatial

variability in key flow metrics can be used to identify sites where model validation data should be collected, in particular away from upstream obstacles that will modify the flow, and away from areas with strongly varying horizontal velocity gradients.

2.4 Spatially varying bottom friction should be included in the domain definition for accuracy and stability.

2.5 For tidal energy applications model mesh resolution needs to be able to represent key far-field large-scale flow structures.

2.6 3-D non-hydrostatic models are required to capture the complex flow structures, such as coherent eddies and secondary circulations, and to accurately estimate available power for a range of turbine designs and installation methods and locations.

2.7 Model validation against data from high-energy tidal sites required new methodologies.

2.8 Executing two-way wave-current modelling under the open-source methodology is difficult and computationally expensive and requires further development work to bridge the expertise gap and to reduce barriers to exploitation of these tools by tidal energy developers.

2.9 Workstation-class (as of 2021 e.g., 32-core machines) computing is sufficient to make valuable inroads into developing useful fit-for-purpose models for tidal energy applications. Extending the modelling to wave-current two-way coupled capable modelling requires increased computational power.

3) DATA TOOLS

3.1 Lack of transparent and user-friendly tools / limited uptake of tools that are available hinders post-processing of data and is a barrier to researcher and developer participation.

3.2 There is a need for robust and systematic QC procedures tailored for high-energy tidal channels.

3.3 The prevalence of non-tidal processes integrated in site measurements reduces the reliability of

3.4 Turbulence Intensity estimates and necessitates standardized post-processing.

3.5 There is a lack of robust, open and verified algorithms for the extraction of 3D wave information from ADCPs.

4) SENSORS AND SENSOR SYSTEMS

4.1 Further work is required on the quantification of the consequences and increase in uncertainty of sampling flow-fields using D-ADP devices in extremely high energy sites where levels of spatial variation of flow scales comparable to the acoustic beam separation distances in horizontal and vertical directions is large and temporally varying.

4.2 TEC-installed pressure gauges should be available to resource characterisation efforts due to their ability to provide online and improved 1D wave spectra over seabed-located gauges.

4.3 Latest generation of 5-Beam ADCPs offer significant advantages over previous 4-Beam generation in terms of data storage, diagnostics, sampling rate and direct capture of vertical processes.

4.4 For cabled solutions hybrid and robustly switchable power systems incorporating battery back-up power are implementable using small low-power components and are valuable investment.

4.5 Turbine retrofitting of sensors and auxiliary systems remains a high cost and high risk activity but with benefits in terms of data capture that merit the effort/investment.

4.6 Systems developed for multi-type deployment and retrieval – and diver intervention – proved worth the design and engineering cost with sensor packages deployed using various techniques depending on equipment / vessel availability.

4.7 Cabling and connectors represent a significant proportion of system cost.

4.8 Low-cost pressure vessels can be designed and implemented but further (low-cost) systematic testing is required to enable reliable roll out where their use is mission-critical.

4.9 Accurate IEEE 1588 Precision Time Protocol timing networks can be achieved sub-sea via low cost embedded systems.

4.10 It is challenging and time consuming – but not impossible – to execute interfaced engineering works remotely where travel restrictions are in place with sufficient levels of time and *enthusiasm*.

4.11 Prototype complex subsea autonomous systems are high risk

5) DATABASE AND DATA ACCESS

5.1 Provisioning external public access to the internal systems of an organisation comes with technical and security risks. Long-term a pooled and dedicated service provider should be engaged with. A system can be developed more readily where a barrier is implemented between the user-interface and the file store and back-end data processing. This has been implemented in RealTide.

5.2 Re-analysis legacy data is time consuming. It is much better to capture the data correct "first time around" including all necessary meta-data. Working to tight and dynamic schedules puts pressure on this element of data campaigns – but time should be made in the plan for this – even at the cost of not pursuing arising opportunities.

5.3 Designing data campaigns with the final database of data in mind leads to the establishment of good practice.

See RealTide Deliverable D2.3 for further information on the Database and Data-Access implementation of RealTide work-package 2.

9.2 Recommendations

The following recommendations, whilst not exhaustive, follow from the collation of Lessons Learned (see previous Section) and are formed as a result of implementing the measurement and modelling campaigns of the RealTide project.

Fit-for-purpose tidal energy modelling: The creation of the model domain construct is the most important process in regional modelling. Taking the time to define a properly constructed model domain, using the most up to date data, an appropriately defined coastline, and consideration taken of far field processes, significantly improves model accuracy (limiting the requirement for calibration) and model stability (reducing the time spent getting the model to run for extended time windows). When comparing model and in-situ results, e.g., for model calibration / validation the specific the final use-case of the analysis should be considered, where turbine geometry and location in the water column will play a significant role in interpretation results. For example, large differences in velocity agreement at the seabed may or may not be relevant to exploiting the model data at a particular hub-height. In order to capture the intra-channel dynamics, extra-channel dynamics must also be resolved, thus careful consideration of mesh resolution and extent is essential. Further work on how model performance is assessed given the high levels of spatial variation in tidal energy sites and the limitations of current sensing techniques including sparsity of data. Model setup should feature 3D non-hydrostatic schemes and take advantage of high resolution information on bathymetry, topology and variable bottom friction as these play a strong role in model performance for tidal energy applications.

Integrated sensing for tidal energy: Retrofitting of extensive sensor systems to Tidal Turbines is a viable endeavour and can make use of commercially available auxiliary equipment (comms, power, mechanical). Indeed it should be pursued since it potentially offers the best access to mid-depth flow mapping currently available, however, extensive testing is required that is difficult to prioritise during prototype maintenance and or commissioning. Wherever possible these activities should be considered at the machine design stage to avoid many of the challenges of retrofitting. Where measurement systems are interfaced – e.g., between tidal turbines and sensor-packages redundancies should be implemented to allow full or partial operation when the interface fails. An example is in the stand-alone seabed deployments in the Fromveur Strait that collected multiple months of data despite the unavailability of the turbine. Since we are not yet at the stage of being able to exploit autonomous and intelligent distributed sensing for ORE applications it is highly advantageous to implement remote access to designed and deployed sensor packages. This is worth the significant cost and staff resource effort as this capability enables online data streaming, system monitoring and where required human intervention to improve data quality.

The data chain: Data collection should be conducted with strict adherence to quality assurance standards (as described in D2.1) to ensure collected data meets requirements of the end-use case, is traceable, captures all relevant meta-data and is readily database-able. In the data sets analysed within RealTide across multiple high-energy sites, non-tidal dynamics including eddies and ocean surface gravity waves are a near-constant feature. Data processing standards needs to accommodate these features. Data Processing (QC). Information derived from datasets is highly sensitive to instrument noise, and artefacts of implementation. Therefore data provenance is important and robust quality assurance and quality control methods are required. Whilst existing guidance represent a good starting point, further focus on tidal-channel specific methods would be useful to reduce uncertainty in derived parameters. Data accessibility is a barrier to data exploitation by the tidal energy sector as a whole, therefore data collection and post-processing methods need to be targeted towards allowing integration with intelligent data service systems e.g., the database methodology developed in WP2

(see D2.3). And in relation to the previous point, data access is made easier if data collection adheres to good standards.

Open source tools: The generation of data sets within WP2 were generated using, wherever possible, an open-source and open data approach. Open source software and datasets show promise for developing better engineering tools for tidal energy applications and increasing accessibility and potentially wider uptake by the sector. This is reflected in recent industrial activities outside of tidal energy. Application of open source software (including for any planning, design and operations activities) should consider the requirements of the OpenChain standard (ISO 5230) for open source software compliance, as this recent standard has been adopted by third-party certification bodies, such as Bureau Veritas [82]. This should address some of the complex issues relating to acceptance and integration of open source software in industry; however, widespread acknowledgment and integration of this standard will take time. Institutional recognition and awareness of ISO 5230 is a key step for the progression of the tidal sector.

9.3 Next Steps

RealTide outputs will be further explored and progressed in multiple areas as part of internal research and ongoing collaborative projects. These include data archival and publishing activities to increase impact of the acquired datasets, from RealTide and previous and affiliated projects, together with post-processing tools to help extract meaningful information from large complex datasets. The modeling work continues in internal projects as well as new funded projects with the overarching aim of removing barriers to model use; for making informed techno-economic decisions in tidal energy.

Data archival and publishing: It is planned to re-analyze, QC, convert, archive and publish all UEDIN-held site measurement datasets in addition to those already in the RealTide D2.3 demonstrator. The RealTide data infrastructure (Database, Tools, Website) will be augmented and exploited under follow-on projects including the SuperGEN ORE Hub funded FASTWATER project. Identified tank-test results – those that will aid development of engineering tools for tidal energy applications by e.g., allowing benchmarking of new software - will be prepared and transferred to the database. These datasets comprise measurements of scale model forces and surrounding wave-current conditions. In addition to the tests conducted at FloWave under RealTide related testing conducted under pervious EPSRC, UK SuperGen Marine programmes will also be consolidated, processed, archived and uploaded to the Database. Already identified CFD and BEMT will be prepared and transferred to the database. Permissions, where required, have already been granted.

Data post-processing: Efforts will continue via internal research and through collaborations established during RealTide. For example analyses will continue in partnership with the team behind the MONITOR project where data sharing between RealTide and MONITOR has already led to a joint workshop at an international conference. Efforts will seek to extract further site parameters including turbulence metrics and wave statistics – which will be captured in academic publications as well, as being archived and published to the database.

Efforts will continue on Data QC processes as the consolidated database forms a unique basis to develop and assess robust thresholds that are valid at multiple sites: currently derived outputs are sensitive to data pre-processing. Sensitivity analysis is underway on the performance of tidal energy models against key metrics such as uncertainty in power production and energy yield. Specific processing tasks have been identified in relation to the long-duration (220 days) Fromveur Strait dataset including advanced tidal harmonic reductions and wave-current analysis (including the trialing of recently developed algorithms by academia). RealTide reanalysis on DeepGEN IV mounted instruments (multiple single-beam acoustic Doppler profilers which were operated near hub-height) is

ongoing as is the re-analyses of prior datasets relating to the assessment of tidal turbine power performance.

Further data capture campaigns: In parallel to processing any retrieved data from the C-ADP MkIII prototype which was successfully recovered at the end of the RealTide project, opportunities are being explored to exploit progress made on hardware and software related to advanced sensing. This includes exploring options to redeploy and to reconfigure seabed and TEC-mounted measurement systems – based on lessons learned in RealTide - to continue progress in providing better and fit-for-purpose site characterisation.

Advanced open modelling: In separate work further model methodological development will be conducted exploiting the RealTide winter 2019 Fromveur Strait datasets. This will be used directly in an ongoing research project and will assist the tidal turbine developer in their technology programme. In the UK FASTWATER project the RealTide modelling methodology will be exploited, standardized and made more accessible to the wider community. These stable and flow-capturing base models can form the platform for wave-current coupling – which will be carried out around Q2 2022. Academic publications are in preparation on the lessons-learned around modelling methodology for tidal energy applications.

Long-term legacy: Experience from similar industrial-academic research programmes shows that if the acquired project data and knowledge can be curated appropriately, new research and industrial opportunities and routes to impact will arise. By widening participation in the analyses of the captured data further gains should be made in improving reliability and lowering cost of the tidal energy sector. RealTide, by implementing an integrated and sustainable data management plan, and resulting data platform via www.tidalenergydata.org, improves the chances of these works generating long term impacts for the sector.

APPENDIX A – INTERNATIONAL SITE CHARACTERISATION

Table 0-1 lists some notable site characterisation works conducted internationally.

Table 0-1: ADV and ADCP deployment: selected examples for tidal stream energy

Deployment Location & Reference	Summary	Stated Relevance of Result
Cordova Channel, Vancouver Island, USA [83, 84]	Deployment of an RDI Workhorse (600 kHz) and subsequent data processing to obtain velocity profiling in a turbulent environment. Uncertainty depends on turbulence characteristics, not the instrument, therefore need rapid sampling (and recording) to resolve velocity fluctuations.	Overview of measurement principles of an ADCP, and the data processing to enable velocity profiling in a turbulent environment divergent beam ADCP only obtain mean velocity vectors (unlike instantaneous measurement from current meter).
Puget Sound, WA, USA [85]	Bottom mounted RDI Workhorse ADCP and tripod mounted Nortek Vector ADV time series data analysed to obtain statistical measures of fluctuations in both the magnitude and direction of the tidal currents.	Estimate performance and fatigue of tidal turbines given that turbulence can't be modelled at all relevant scales.
Sound of Islay, UK [86]	Tri-beam Nortek Vector ADV deployed 5 m above seabed for 15 days to quantify the structure of the flow in an energetic tidal channel with mean flows of 2.5 m/s.	Understanding turbulence in tidal stream boundary layers enhances confidence in the predictions of yield and load for devices operating in unsteady flow environments.
Puget Sound, WA, USA [87]	Acoustic profilers including RDI Workhorse (300 kHz) and Nortek Continental (470 kHz), deployed at 8 locations for between 1 month and a year to characterise variation in the tidal resource over different spatial and temporal scales	Finite-record length observations of tidal currents can be used to estimate device performance, but not loadings. Variation in tidal resource occurs over length scales of less than 100 m.
Inner Sound (Pentland Firth), UK [88]	Vessel transect surveys conducted with 300-kHz Teledyne RDI Workhorse Sentinel and hydrodynamic model used to interpolate measured data.	Fine scale velocity variations found to result from tidal flow interaction with land and islands. Complexity and variability in tidal stream not captured by model, influencing site selection.
Roosevelt Island, New York, USA [89]	Two months of Sontek 10 MHz ADVs measurements at design hub height of the Verdant Power Gen5 hydrokinetic turbine (4.25 m above seabed).	Theoretical force and power densities derived from current measurements influenced by time window used to average the current speed. Discrepancy in theoretical power density from current speed measurements & from national records highlights importance of site-specific measurement campaigns.

Deployment Location & Reference	Summary	Stated Relevance of Result
Strangford Lough, Northern Ireland [90]	Nortek Aquadopp Acoustic Doppler Profile mounted on same vessel as tidal turbine, simplifying quantification of inflow velocities.	Simultaneous collection of velocity measurements and turbine data (e.g. power, thrust and pitch) produced loading and system efficiency estimations.
Puget Sound, WA, USA [91]	Nortek Vector ADV data used to characterise turbulent flow using metrics such as turbulence intensity, structure functions, probability density functions, intermittency, coherent turbulence kinetic energy, anisotropy invariants.	Description of energetic tidal channels using higher order statistics reveals additional insights into the turbulent environment. More realistic modelling of the performance and loading of turbines in realistic ocean environments.
West Anglesey Demo. Zone, Wales, UK [92]	Teledyne 600 kHz used to characterise vertical structure of flow and profile extrapolated via 3D ROMS tidal model. Identified spatial and temporal variability in velocity profile.	Realistic characterisation of the velocity profile required, affects cyclic loading on turbine blades.
West Anglesey Demo. Zone, Wales, UK [47, 93]	RDI Sentinel V and model simulation comparison of turbulence demonstrated the significant influence of waves on turbulence.	Using models to predict turbulence aids targeting of measurement campaigns (spatially and temporally) and provides input conditions for physical modelling.
Puget Sound, WA, USA [94, 95]	Dynamic motion characterisation of a variety of instrumentation platforms deployed to acquire turbulence measurements mid-water column. Platforms hosted Nortek Vector ADV.	If ADV deployed via tethered instrumentation platform, motion induced velocities can contaminate velocity signal. Motion correction of measured velocity signals via IMU.
Puget Sound, WA, USA [96]	Fixed Nortek Signature1000 AD2CP & Teledyne RDI Sentinel V50 deployed; Nortek Vector ADV mounted on mooring.	Use of 5 beam acoustic profilers to assess higher order turbulence Parameters.
Falls of Warness, Orkney, UK [69]	Seabed-mounted RDI ADCP and remotely operated Nortek s-ADP on the front, top and rear of a tidal turbine. Tidal flow velocities and associated turbulence reported in the absence of waves.	Industry standard flow characterisation metrics rely on u. Determination of u is sensitive to spatial averaging, duration of data acquisition and data processing of e.g. wave influences.
Alderney Race, Raz Blanchard, France [66]	Interpolation separated the spatial and temporal variation in the flow measured by a towed 600 kHz Teledyne RDIWorkHorse Sentinel ADCP.	Constraining model simulations with measured velocity increases the accuracy of tidal stream resource assessment.

APPENDIX B – HYDRODYNAMIC MODEL INPUT SOURCES

Modelling work in RealTide required data for modelling, operation, calibration and validation. Within the work-package multiple relevant data sources have been identified and are listed in Table 0-1.

Table 0-1: Hydrodynamic model input sources

Data Source	Summary	URL Link	Note on License/Restrictions
CANDHIS	Kereon (02919) Wave buoy measurements between 02/10/12 and 17/04/14 H_{mo}, wave rose, $H_{\max}$, $H_{1/3}$, T_p, T_{02} Nearest real time: Les Pierres Noires (02911) Measurement from 15/10/2005 to today	http://candhis.cetmef.developpement-durable.gouv.fr/	Open access Details of restriction
IFREMER (IOWAGA)	Wave forcings at open boundary	ftp://ftp.ifremer.fr/ifremer/ww3/HINDCAST/	Open access
MARC	MARS 2D Model on a 250 m regular grid (depth averaged - Forecast - 15 min timestep) MARS 3D Model on a 2500m regular grid (Forecast - 1 hour timestep; no.levels, tbc) 5-yr MARS3D hindcast on 500 m grid	http://marc.ifremer.fr/en/results/currents	FTP access to be applied for Access to 5yr hindcast is to be confirmed
HOMERE	23 year long database derived from application of the WaveWatch III model [97]	http://marc.ifremer.fr/en/produits/hindcast_sea_states_homere	FTP access to be applied for
SHOM	High resolution digital terrain model of the marine current turbine farm area Large scale map of the surface sediment types Four-layer, 3D ocean current chart, with 15 minute resolution (the data from a current profiler located in the area is also supplied)	https://data.shom.fr/	Open access
EMODNet portals	Bathymetry Wave buoy Surface currents from HF radar Seabed substrate maps And multiple other sets	http://portal.emodnet-bathymetry.eu/ http://www.emodnet-physics.eu/Map/ https://www.emodnet-seabedhabitats.eu/	Open access
CMEMS	Bathymetry Wave Buoy Met Buoy Drifters HF Radar CTD	https://marine.copernicus.eu/access-data http://www.marineinsitu.eu/dashboard/	Open access

APPENDIX C – GLOSSARY OF TERMS: IN-SITU SENSING

The table below provides the reader with some introductory and summarised explanation of terms and principles of operation related to in-situ sensing via acoustic Doppler Profilometry.

Table 0-1: Acoustic velocimetry: principles of operation and their implications (After RDI, 2011; ISO/TR 24578, 2012; Nortek, 2017; [18]).

Principle	Definition	Application
Doppler effect	Change in wave frequency when a wave source moves with respect to an "observer", or when the "observer" moves relative to the wave source.	Doppler effect utilised by acoustic velocimeters. A frequency change & a phase shift occur between transmitted acoustic pulses & the reflection of these pulses from particles in the water. The particles are assumed to be moving, on average, at the velocity of the water. Magnitude of Doppler effect proportional to velocity.
Signal processing method	**Pulse incoherent (Narrowband)** Measures Doppler shift of single, relatively long pulse of sound. **Pulse to pulse coherent** Measures phase shift ($\Delta \varphi$) between two short successive pulses. **Broad spectrum (Broadband)** Measures phase shift ($\Delta \varphi$) between two successive pulses.	**Pulse incoherent (Narrowband)** Instruments have a longer measurement range; Highest noise levels; Rapid processing of the (relatively) simple signal. **Pulse to pulse coherent** Instruments have small measurement cell sizes (1 cm); Lowest noise levels; Limited maximum velocity which can be measured; Limited measurement range. **Broad spectrum (Broadband)** Both pulses within profiling range at the same time, each being a pseudo-random code within the waveform. Several independent samples obtained per ping. Measurement range and noise level lies between that of narrowband and pulse to pulse coherent instruments; Longer processing time of more complex signal.
Acoustic beam & side lobes	A single acoustic beam measures a single velocity component that is parallel to beam, i.e. the along beam radial velocity. Each acoustic beam has a main lobe plus side lobes, acoustic energy "leaking" from main lobe.	To resolve the 3 components of velocity, data is required from a minimum of 3 non co-planar beams pointed in different angular directions relative to the profiler's principal axis. Additional beams allow error estimation. Velocity perpendicular to the beam can't be measured. Interference occurs when side lobes are reflected off a boundary more strongly than the main lobe is reflected by particles, thereby contaminating the returned signal.
Beam angle	The angle between the instrument vertical and the beam. Beam angle relative to instrument is fixed in standard instruments	In a diverging acoustic instrument, optimal beam angle is 20 - 30 degrees from vertical. To correct for instrument orientation, heading is measured by fluxgate or gyro compass. Pitch & roll is measured by an inclinometer or vertical gyro.

Co-ordinate transform	Direct measurement of along beam velocity with application of trigonometric relations to transform into Cartesian co-ordinates (x,y,z) & subsequently earth coordinates (E,N,U).	A transformation matrix converts from beam to Cartesian coordinates, relying on the assumption of horizontal flow homogeneity between beams. The transformation matrix is fixed in industry standard instruments.
Chirp	A frequency modulated pulse shown as an acoustic sine wave. Multiple chirps form the transmit pulse.	Chirp length controls the velocity range which can be measured by an instrument.
Ping	A transmit pulse consisting of a series of chirps.	The more pings within an averaging period, the lower the measurement uncertainty.
Transmit frequency	The acoustic frequency of a transmit pulse.	The higher the transmit (carrier) frequency, the lower an instrument's measurement range and the smaller the minimum size of a measurement cell.
Measurement profile	Measurements are returned from a range of locations through the water column.	Range-gating of the back-scattered signal against time i.e. the returned signal is divided up and processed separately.
Correlation	Statistical measure of similarity between received signals over time, measured in percent.	Quality indicator of velocity data, lying between 0 – 100 % & decreasing with range from instrument. Typically, correlation < 50 % indicative of low-quality data.
Amplitude (Echo intensity)	Strength of return signal in decibels. Attenuation depends on sound absorption; beam spreading; transmitted power; back-scattering in water.	Amplitude typically decreases with range from the instrument to a minimum which represents the limit at which measurements can be obtained. The Signal to Noise ratio is the strength of the acoustic signal relative to the background noise level
Nyquist frequency	The highest frequency that can be accurately sampled with a given sample rate.	Signals containing frequencies above the Nyquist frequency are subject to aliasing (high frequency signals appear as low frequency signals). Sample rates are required that are at least double the frequency of the signal of interest in order to resolve it without ambiguity
Doppler noise	Standard error resulting from estimation of the doppler shift of finite length acoustic pulses. Assumed to be random and non-biased.	Noise depends on the signal processing method, sample rate and bin size (via pulse length). The longer the averaging period, the better the estimate of mean velocity (lower noise) but lower temporal resolution of measurement. Balance velocity precision with noise minimisation.